MODELLING AND CONTROL OF MICRO-COMBINED HEAT AND POWER (CHP) TO OPTIMISE ENERGY CONVERSION AND SUPPORT POWER DISTRIBUTION NETWORKS

SAMIR KARMACHARYA

PhD

2013

MODELLING AND CONTROL OF MICRO-COMBINED HEAT AND POWER (CHP) TO OPTIMISE ENERGY CONVERSION AND SUPPORT POWER DISTRIBUTION NETWORKS

SAMIR KARMACHARYA

A thesis submitted in partial fulfilment
of the requirements of the
University of Northumbria at Newcastle
for the degree of
Doctor of Philosophy

Research Undertaken in the
Faculty of Engineering and Environment and in collaboration with
National Renewable Research Centre (Narec)

October 2013

ABSTRACT

Climate change and continuously increasing energy prices have driven the need for low carbon and renewable energy technologies from different sectors, including the domestic sector, by installing higher energy efficiency technologies. One of these technologies is the Stirling engine based micro-combined heat and power (CHP) which has the potential to achieve lower overall carbon emissions by generating both heat and electricity locally. Its successful implementation to meet the energy demands (thermal and electrical) throughout the year depends on several factors such as the size and type of building and demand profiles. In addition, the deployment of large number of micro-CHPs may have significant impact on the performance of the power distribution networks.

In this research, a dynamic model of a domestic-scale natural gas fired Stirling Engine based micro-CHP unit (including start-up and shut-down characteristics) is developed using experimental data of a 6 kW (heat output) and 1 kW (electrical output) laboratory prototype. A dynamic thermal model of a house along with its heating system is also developed. Domestic renewable energy sources such as photovoltaic (PV) and micro-wind turbine are also considered. The integrated energy model has been applied to two typical UK houses: semi-detached and detached. The model was simulated for a typical winter and summer week as well as for the whole year. Results for the two cases show that the electrical contribution of a Stirling engine type micro-CHP heavily depends on the thermal demand of the building and that up to 19% of the locally-generated electricity is exported whilst meeting a similar percentage of the overall annual electricity demand.

A fuzzy logic controller for micro-CHP is proposed with the aim of managing the energy generated by micro-CHP and supporting the distribution network. Two different scenarios based on network health are considered. For the network operating under healthy condition: feed-in-tariff and electricity trading cases were considered. When considering feed-in-tariff, the micro-CHP with controller showed the annual operating cost and carbon savings when compared to conventional boiler or a micro-CHP without a controller. In the case of electricity trading scenario, the annual operating cost saving was much less than the feed-in-tariff scenario. For the scenario where the network is close to voltage statutory limits the response of the fuzzy logic controller is shown to support the grid.

LIST OF CONTENTS

LIST OF FIGURES

LIST OF TABLES

ACKNOWLEDGEMENTS

I wish to express my sincere thanks and gratitude to my supervision team, Professor Ghanim Putrus, Professor Chris Underwood and Professor Khamid Mahkamov for their great support and guidance to make the project a success. I appreciate their idea for allowing me to create my own academic interest. I wish to express my profound thanks to Dr. Steve McDonald at NaREC, Blyth, UK for his guidance and advice for my project as the industrial supervisor.

I would like to thank Northumbria University and NaREC, Blyth, UK for the financial support they provided during the project.

I would like to give great appreciation and thanks to my colleagues at the Power and Wind Energy Research group, Northumbria University for their kind help in doing this project. Also, I would like to thank all administrative staff at the Faculty of Engineering and Environment for their support and all others who directly or indirectly helped me doing this research project.

I am very grateful to my parents, Mr Daya Man Karmacharya and Mrs. Usha Karmacharya, my brother, sister for their continuous support. I am very grateful to my beloved wife, Sarina, and son who are giving me never ending support by sacrificing a lot of things in their life.

DECLARATION

I declare that the work contained in this thesis has not been submitted for any award and that it is all my own work. I also confirm that this work fully acknowledges opinions, ideas and contributions from the work of others. The work was done in collaboration with National Renewable Energy Centre, Blyth.

I declare that the Word Count of this Thesis is 36,771 words.

Name: Samir Karmacharya

Signature:

Date:

NOMENCLATURE

$\varepsilon(s)$	Uniformly distributed error
τ	Time constant (sec)
ρ	Density of air (kg/m^3)
φ_m	Magnetic flux linkage (Wb)
λ	Tip speed ratio of wind rotor
ω	Rotational speed of the wind rotor (rad/s)
ω_s	Rotational speed of electric field of d.c. motor (rad/s)
a, a_1, a_2	Ideal factor of diode, diode 1 and diode 2 respectively
c_p	Specific heat capacity of water (J/g˚C)
C	Total thermal capacity (J /kgK)
C_i	Internal thermal capacity (J /kgK)
C_o	Outer thermal capacity (J /kgK)
C_P	Power coefficient of wind rotor
C_t	Torque coefficient of wind rotor
C_w	Overall thermal capacity of emitter (include the radiator material and water) (J/kgK)
D	Duty ratio of buck-boost converter
E_0	Generated EMF (V)
E_G	Energy band gap of semiconductor (1.12 eV)
G	Surface irradiance of the cell (W/m^2)
G_{STC}	Surface irradiance of the cell at STC (W/m^2)
G_{inh}	Inherent valve characteristics
G_{ins}	Installed valve characteristics
G_o	Valve let-by
$G(s)$	Transfer function to represent response in heat/power output
I	Output current from solar cell (A)
I_d	d.c. current (A)
I_{mp}	Output current from the solar cell during maximum power (A)

I_{o1}, I_{o2}	Reserve saturation current of diode 1 and diode 2 respectively (A)
I_B	Current flowing towards d.c. bus (A)
I_G	Current flowing from the PMG generator (A)
I_{PV}	Current generated by incident of sunlight (A)
I_{PV_STC}	Current generated by incident of sunlight at STC (A)
k	Boltzmann constant (1.3806503×10-23 J/K)
k'	Constant
K	Gain
K_I	Short-circuit current coefficient of the PV cell (%/°C)
K_e	Overall emission constant for the emitter
K_V	Open circuit voltage coefficient of the PV cell (%/°C)
L_{ph}	Phase Inductance ($L_a = L_b = L_c$) (mH)
m_w	Mass of water (kg)
n	Heat transfer index
N	Valve authority (fraction)
N_s	Number of cell connected in series
p	Number of pole pairs
P	Power captured by the wind rotor (W)
P_{max_C}	Maximum power calculated (W)
P_{max_E}	Maximum power from data sheet (W)
q	Electronic charge (= 1.60217646×10^{-19} C)
q_{rad}	Heat input by solar radiation (W)
q_p	Heat input by heating system (W)
R	Total thermal resistance (m^2/kW)
R_{dc}	Effective armature resistance (ohm)
R_i	Internal thermal resistance (m^2/kW)
R_m	Middle thermal resistance (m^2/kW)
R_o	Outer thermal resistance (m^2/kW)
R_{over}	Overlap resistance (ohm)
R_p	Shunt resistance of PV cell (ohm)

R_{p0}	Initial shunt resistance of PV cell (ohm)
R_{ph}	Phase resistances ($R_a = R_b = R_c$) (ohm)
R_r	Radius of the wind rotor (m)
R_s	Series resistance of PV cell (ohm)
R_{s0}	Initial series resistance of PV cell (ohm)
t_d	Time delay (S)
T	Temperature of p-n junction (K)
T_a	Aerodynamic torque (N.m)
T_e	Electromagnetic torque (N.m)
T_i	Internal air temperature (°C)
T_o	Outside air temperature (°C)
T_{off}	Off time of the duty cycle of buck-boost converter (S)
T_{on}	On time of the duty cycle of buck-boost converter (S)
T_{STC}	Temperature of p-n junction at STC (K)
T_{w1}	Temperature of water in zone 1 (°C)
T_{w2}	Temperature of water in zone 2 of emitter (°C)
T_{wi}	Temperature of water going into the emitter (°C)
T_{wr}	Temperature of water coming out of emitter (°C)
T_{z1}	Temperature of zone 1 (°C)
T_{z2}	Temperature of zone 2 (°C)
T_{z3}	Temperature of zone 3 (°C)
u	Stem position (fraction)
V_d	Output d.c. voltage (V)
V_{mp}	Voltage across PV cell during the maximum power (V)
V_B	Voltage at the DC bus (V)
V_G	Voltage at the generator side of PMG (V)
V_{OC_STC}	Open circuit voltage of PV cell at STC (V)
V_{T1}, V_{T1}	Thermal voltage of diode 1 and diode 2
x_i, x_m, x_o	Ratio of total thermal resistance (fraction)
y_i, y_m, y_o	Ratio of total thermal capacitance (fraction)

ABBREVIATION

AC	Alternating Current
ASHRAE	American Society of Heating Refrigeration and Air-Conditioning Engineers
BESTest	Building Energy Simulation Test
CHP	Combined Heat and Power
CPF	Carbon Price Floor
DC	Direct Current
DG	Distributed Generation
DHW	Domestic Hot Water
DNO	Distribution Network Operator
ECBCS	Energy Conservation in Building & Community Systems
EPS	Emissions Performance Standards
FIT	Feed-in-Tariff
IC	Internal Combustion
IEA	International Energy Agency
IWEC	International Weather form Energy Calculations
micro-CHP	Micro-Combined Heat and Power
MPP	Maximum Power Point
MPPT	Maximum Power Point Tracking
OLTC	On load Tap Changing
PEMFC	Polymer Electrolyte Membrane Fuel Cell
PCC	Point of Common Coupling
PMG	Permanent Magnet Generator
PV	Photovoltaic
RHI	Renewable Heat Incentive
SOFC	Solid Oxide Fuel Cell
STC	Standard Test Condition
WECS	Wind Energy Conversion System

Chapter 1 Introduction

1.1 Background

Climate change, insecurity of the supply of energy and reduction in fossil fuels resources are leading to continuous increase in energy prices and the desire of countries to be energy self-sufficient. Different climatic agreements made in Kyoto, Bali and Copenhagen reflect human realisation about the threat of climate change and its impact on humanitarian crisis and global ecology. The UK government (through the European Union) has set legally binding carbon emission reduction targets of at least 80% lower than the 1990 baseline by 2050 and has introduced carbon budgets to meet these targets through the climate change Act 2008. To meet these targets carbon emissions are to be decreased from different sectors including domestic sector by increasing the thermal insulation and using higher energy efficiency technologies. The UK government has lowered VAT for households installing energy saving material and technologies and set out the targets for households to reduce carbon emissions by 60% by 2050 [1].

Existing centralised thermal power stations not only produce electricity but they also produce large amounts of heat in the process of power generation, which is simply wasted to the environment. The size and location of centralised plants prevent the use of this heat for building and industry. In the UK, building heating is usually on-site and gas boilers fired by natural gas are common, with an average efficiency of 80% [2].

A distributed system of heat and electricity generation in individual houses or buildings could offer significant advantages over the traditional systems. This concept is known as

'Combined Heat and Power (CHP)' which is widely used in energy intensive industries where both electricity and heat generated are fully used to reduce the cost of fuel. This technology is based on utilizing waste heat in order to significantly increase the total efficiency of the CHP system to over 80% compared to an efficiency of 30-35% in conventional electricity generation system, resulting in significant reduction of operation costs and carbon dioxide emissions.

Small scale version of such technology, suitable for dwellings or small buildings, is referred as micro-CHP. Micro-CHP is a growing technology in Europe due to its advantages such as higher energy efficiency, low emissions, increased energy security, lower transmission losses etc. There are many technologies of micro-CHP based on the energy conversion method: Stirling engine, internal combustion engine, fuel cell, organic Rankine cycle and micro gas turbine. Out of these, the internal combustion engine is commercially available, the Stirling engine is close to market availability and fuel cells are in prototype stage. Research has shown that the Stirling engine based micro-CHP provides economical and emission benefits when compared to a condensing boiler in domestic scenario [3]. Much of the progress concerning the behaviour of micro-CHP plant in domestic applications has focused on comparing the seasonal economics of alternative module types [4-6] and on the measurement of the individual and comparative performances of these systems [7, 8]. Stirling engine based micro-CHP is considered as best current option for a range of domestic operating scenarios when compared to other micro-CHP technologies [5].

Control of a micro-CHP in a single dwelling is a challenge as the thermal demand and electrical demand does not coincide. Peacock and Newborough [9] have stated that annual

heat to power ratio in a UK single house varies from approximately 2:1 to 8:1 approximately and this ratio is not always constant over the operation of the micro-CHP. As a result, micro-CHP systems must be connected to the electrical distribution network or storage devices (for both thermal and electrical storage).

In the future, residential combined heat and power units at the domestic user level are expected to be installed on a large scale along with other distributed generators such as photovoltaics (PV) and micro wind turbines. These will have significant impact on the low voltage power network performance, the generation methods, transportation and supply of electricity. At least 20% of domestic heating systems are expected to be replaced by micro-CHP in future and this rollout of micro-CHP technology on such a scale will change the way electricity networks have to be controlled [10, 11].

Even though there are benefits of micro-CHP, there are still challenges which needs to be addressed such as

- Integrating these units into an unfamiliar application in which both thermal demand and power demand vary throughout the season often with a significant random component,
- Wide ranges of electrical and fuel tariff possibilities,
- Possible existence of other competing embedded renewable energy supply technologies and the way micro-CHP response to the change in power distribution network parameters such as voltage, dynamic pricing or frequency.

Among the issues mentioned above, fulfilling the energy demand (electrical and thermal) of the building and responding to the change in voltage (or frequency) of supply power in order

to reduce strain on the power network and thus avoid black out would be the most important issues. These issues need to be addressed before the full potential of micro-CHP systems within the building can be realised. Reducing strain in the power distribution network refers to supply of power from micro-CHP when the grid voltage decreases and is close to lower limit or drop in frequency and switching 'off' of the micro-CHP system when the grid voltage increases (and is close to the upper limit) or a rise in frequency. Changes in power distribution network can be communicated through smart meters, which will replace the gas and electricity meters in the houses by 2020. So this research focuses on these issues by trying to optimise the benefit of micro-CHP system not only from the user's point of view (energy efficiency) but also from the power distribution network operator's (DNO) point of view (network support).

To address the above issues, a fuzzy logic controller has been developed which will respond based on space heating requirement, hot water demand and voltage of the supply power. Here, voltage is taken as a reference to support the grid. However, other reference signals such as dynamic pricing or supply frequency could be taken to support the grid and reduce the stress on the power supply infrastructure. Dynamic pricing (also known as real-time pricing) refers to time based pricing where electricity price may change as often as hourly.

1.2 Research Aims and Objectives

This research aims to develop a controller for micro-CHP which would optimise the energy efficiency on the basis of dwelling energy demand as well as to support the power distribution network depending upon the signal received from the DNO via smart meter. The proposed control strategy will enable the micro-CHP to:

- Communicate with the DNO via the smart meter.
- Consider energy demands (both heat and power) of the dwelling and manage energy produced by micro-CHP.
- Consider other local renewable energy sources.

On the basis of these factors, an appropriate control strategy based on fuzzy logic is to be developed.

The objectives of the research may be summarized as follow:

- Develop a dynamic simulation model of a typical house in the UK, to analysis the thermal and electrical demands.
- Develop a model of micro-CHP incorporating start-up and shut down characteristic.
- Analyse the performance of the micro-CHP for typical electrical load profile and heat demand in the dwelling.
- Investigate the possibility of integrating the operation of the micro-CHP with other renewable energy sources such as micro PV and wind turbines.
- Develop a smart controller which would manage the energy available in the dwelling and support the power distribution network.

The conceptual arrangement of the residential micro-CHP system with the proposed controller is shown in Figure 1.1. The renewable energy sources, shown in Figure 1.1 only contribute in the electrical energy flow as micro-CHP does.

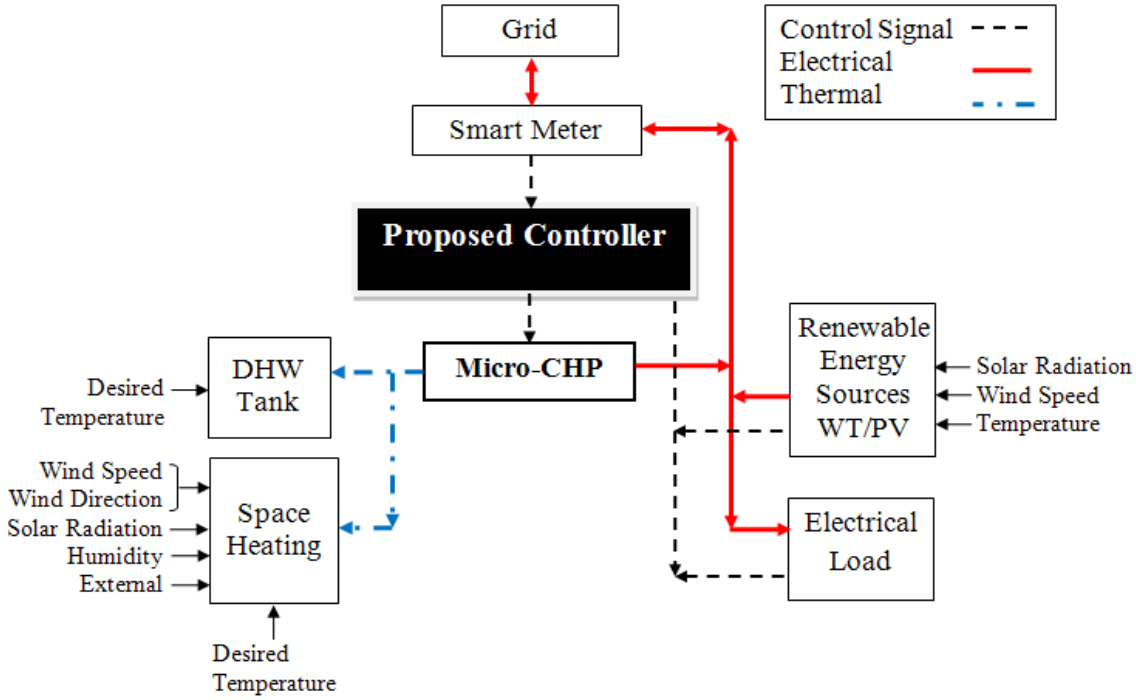

Figure 1.1 Micro-CHP system with proposed controller

1.3 Original Contribution

- Development of generic model of a typical house with its heating system in the UK incorporating a micro-CHP, which enables dynamic analysis of the thermal and electrical requirements of the house.
- Dynamic model of a Stirling engine based micro-CHP featuring its start-up and shut down of thermal and electrical characteristics.
- The proposed model is of first kind which involves micro-CHP coupled to heating system of a house that is fully dynamic, allowing to deal with spikes of load demands (i.e. hot water and electrical demands) as well as being able to interact with energy storage systems.

- Design of a controller for Stirling engine based micro-CHP which would manage the available energy conversion in the building and support the distribution power network.

As shown in the literature review, described in the following section, no previous work has been carried out on the dynamic modelling of this combination of system components.

1.4Overview of the Thesis

This thesis is structured as follows:

In chapter two, the energy used within the building and the means of reducing the energy is discussed. A literature review is presented on the performance of micro-CHP, modelling of micro-CHP with energy demands within the building and strategies used to operate micro-CHP to fulfil the energy need of the dwelling.

Chapter three describes energy generation systems and energy storage systems for domestic applications. Characteristics of different distributed generation technologies (such as micro-CHP, PV, wind turbine) that are usually used in dwellings and considered in this work are discussed. The advantages of these technologies and their impact on the grid such as voltage rise, increase in fault level, etc, are also presented in this chapter.

Chapter four presents a dynamic thermal model of the building envelop, dynamic modelling of the heating system within a building and solar radiation model (solar gain model). These models are put together and presented as a case study for a two storey 3-bedroom house in

the city of Newcastle. The results obtained from the case study are then compared with the results obtained from another reference program with identical inputs.

The developed mathematical models of different distributed generators considered in this work are presented in chapter five along with a model of a typical UK power distribution network. These models are implemented in Matlab/Simulink and the results obtained are presented in this chapter.

Chapter six analyses the results obtained when all the above mentioned models are put together in two case study houses with different design, construction and energy demands.

Chapter seven describes the development of the proposed controller for micro-CHP. It presents the inputs considered and discusses the fuzzy logic controller and the results obtained.

In the last chapter, chapter eight, the results have been further discussed and conclusions have drawn from the thesis and the steps identified for the required further studies in the field are described.

Chapter 2 Literature Review

2.1 Introduction

This chapter summarises the background research that has been conducted to extract the key points that outlines the trends of current research carried out in the field of technologies developed for energy use within the residential buildings.

2.2 Energy Use within a Dwelling

In 2011, the domestic sector consumed 1626.24 TJ (38,842 thousand tonnes of oil equivalent) which accounts 26% of total UK consumption of energy. Of all the energy consumed in the domestic sector, space heating accounted for 60%, water heating 18%, lighting and appliances 19% and cooking was responsible for 3% [12]. Energy demand in a house can be divided into two categories: thermal energy demand and electricity demand. Both energy demands vary significantly from one household to another due to different characteristics of each house and the occupants living in that house. Peacock and Newborough [13] found that for nine dwellings, the annual thermal demand varied from 9.3 to 27.2 MWh and the annual electrical power demand varies from 3.5 to 7.5 MWh resulting in annual heat to power ratios ranging from 1.5 to 5.7. These variations in energy demand depend on various factors such as geographical location, building design, occupancy patterns, economic status of the occupants and efficiency of the heating system. Therefore, determining the thermal and electrical demand of a residential building is important in order to maximise the energy conversion of the micro-CHP systems. The pattern of use of

electricity, space heating and hot water consumed over the course of time are critical when analysing micro-CHP system.

2.2.1 Thermal energy

The thermal demand of a house may be considered to consist of three components

I. Space heating: Space heating is provided by the central heating system and mainly depends on the season/weather, house design and occupancy pattern. It is usually supplied by a central heating system using a boiler. If all the occupants are not at home during the day, such as on weekdays the heating system is turned on only in the morning and evening. However for weekends, it may be turned on all day when the occupants are at home.

   The heating demand is a combination of comfort aspirations, economic circumstances and living habits. There are different factors which influence the space heating energy requirement which can be divided into five categories:

   - Physical characteristic of the house: U-values, thermal capacity, internal heat transfers, infiltration rate, etc.
   - External weather condition: temperature, solar radiation, wind speed, etc.
   - Physical characteristic of heating system: system efficiency, responding time according to heat requirement, controls, etc.
   - User requirement: temperature level in different parts of the house at different times of the day and times of the year, window opening, etc.
   - Internal heat gain due to the use of electrical equipment and from the occupants' behaviour.

II. Domestic hot water (DHW): The majority of hot water is required for one of the main activities: washing machine, shower, bath, washing dishes and hand and face washing. Other miscellaneous uses such as car washing are not daily and cannot be predicted. In general, the pattern of hot water used in a house is very irregular and the quantity varies widely for several different purposes. The common pattern of hot water use is in the morning and in the evening around the limited occupancy periods. DHW demand is mostly met by the central heating boiler but sometimes it can be supplied by electricity (immersion heater). However, hot water energy supply can be decoupled from the demand in most houses by means of a conventional hot water storage tank.

In the UK, on average 49 litres of hot water is used per person per day, with little variation [14]. Yao and Steemers [15] developed a simple method to generate domestic hot water load profiles based on the energy profile of each appliance such as dish washer, bath/shower, hand wash etc. A report published by the Energy Saving Trust [16], based on the hot water consumption data from 120 houses, indicates that the mean consumption per household is 122 litres/day, with a 95% confidence interval of ± 18 litres/day. The report revealed that the consumption is mainly influenced by the number of occupants (including children) not the geographical region or the boiler type. The report also mentions that some households heat water as and when it is required and the remainder generally heat between 8 a.m. and 10 a.m. in the morning and between 6 p.m. and 11 p.m. in the evening.

III. Cooking: Cooking which may be characterised as the requirement of small heat inputs at high temperature for relatively short durations. The fuel used for cooking may be gas, electricity, oil or solid fuel. Mostly gas is used for cooking, however if electricity is used for cooking, relatively large fluctuations in the electrical demand profile tend to occur during the peak periods. Heat produced during cooking contributes to the thermal gain in the house, though not significantly.

2.2.2 Electrical energy

Electrical demand in a house is dynamic and energy use varies dramatically with time of day and time of year. Electrical demand in a house depends on many factors such as social status of occupants, size of dwelling, number of occupant, time of day and year, geographical location and ownership of the appliances. It mainly depends on the behaviour of the occupants and their use of the appliances. The component of electrical consumption in a house may be classified in three categories: predictable, moderately predictable and unpredictable [17]. Energy consumed by appliances in a house when unoccupied or occupants are asleep are predictable such as a refrigerator, security lights, standby appliances. Moderately predictable energy consumption is related to the habitual behaviour patterns of the occupants such as watching TV, switching lights on/off and occupancy times/durations. However, washing clothes, ironing of clothes and other kitchen appliances are unpredictable energy consumptions.

Daily electrical demand data are available at half-hour intervals [18, 19] and averaged over a year [20]. Figure 2.1 compares the actual daily electricity demand of a house and annual averaged daily electricity demand of a house at an interval of 1 minute obtained from a

survey published in [21]. The actual electrical demand curve shows rapid variations and many higher peaks of short intervals whereas annual averaged daily load curve shows relatively slow steady rise and fall in electrical demand. The maximum and minimum load for actual demand is 11.43 kW and 0.164 kW respectively whereas for the annual averaged maximum and minimum load is 1.65 kW and 0.265 kW. Similarly using daily electricity demand at a time interval of 30 minutes tends to hide loads with short intervals and there are numbers of appliances which operate for short intervals in dwellings. This could lead to over/under estimates of the import and export of power and consequently affect the feasibility of installing on-site generation in the dwelling [22, 23]. Therefore, a proper representation of the actual electrical demand of a house requires actual (not averaged) and high temporal resolution data.

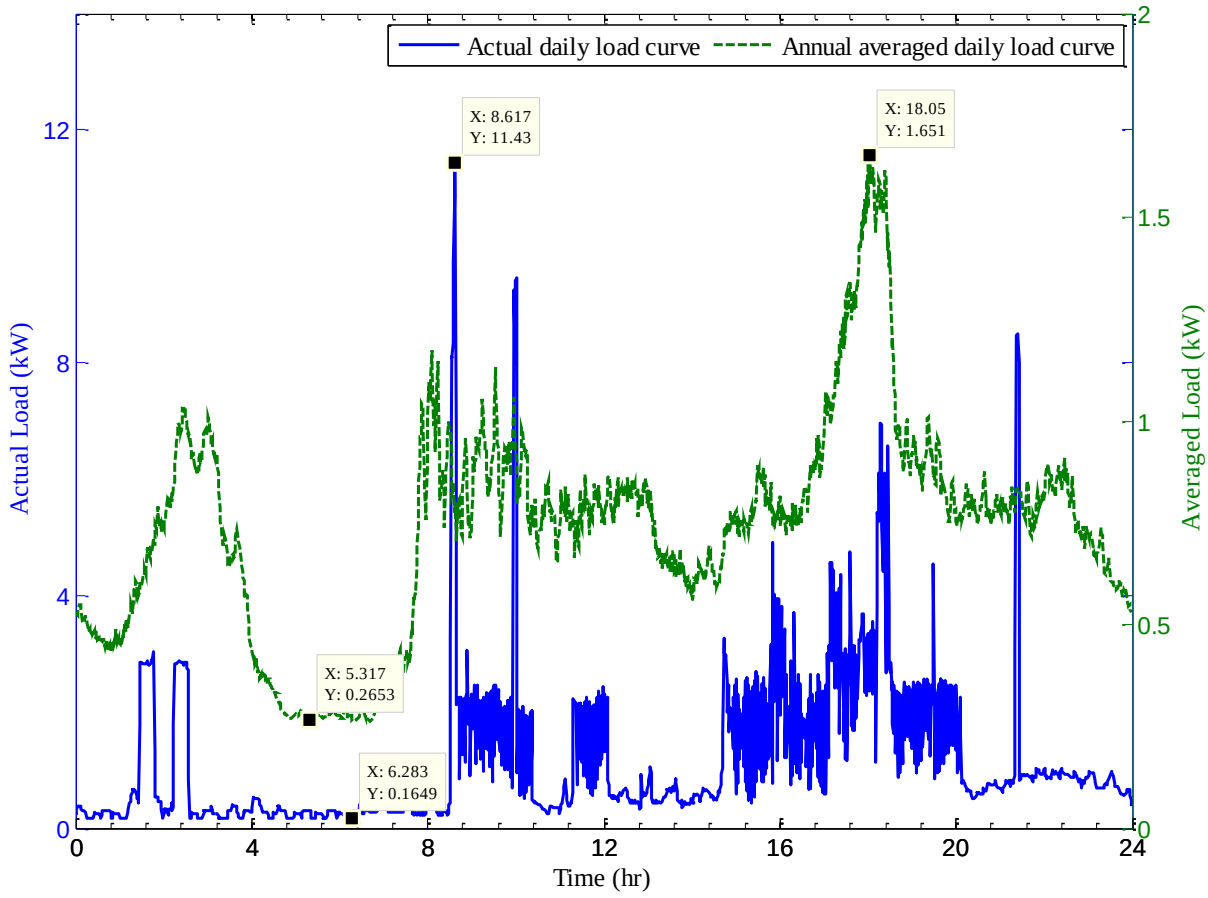

Figure 2.1 Comparison of the actual and annual averaged daily electricity demand at one minute resolution[21].

Widen and Wackelgard [24] developed a stochastic model that generates domestic electricity demand for an individual household on the basis of occupancy pattern. Similarly, Yao and Steemers [15] developed a simple method to predict the daily load profile which can be applied to individual houses and regional levels. Richardson, et al. [25] developed a domestic electricity use model which is based on a combination of patterns of active occupancy and daily activity profile. All these models are developed with a high resolution; i.e. they can generate electrical demand of a house at an interval of 1 min. The international research project conducted by the IEA Energy Conservation in Buildings & Community

Systems (IEA/ECBCS) [26] has published data sets referred as Annex 42 European Domestic Electrical Energy Consumption Profile based on actual data monitoring which took place between 2002 and 2005. The time interval for monitoring was 5 minutes.

Data sets of daily load (kW) at 1 minute intervals were obtained from UK Data Archive [21] for 22 dwelling in East Midlands of England between January 2008 and December 2009. Three different types of dwelling were included in the data set: detached, semi-detached and terraced with the number of occupants varying from 1 to 6. Along with these data sets, the electrical monitoring equipment available at Northumbria University were used to monitor domestic electrical demand in selected dwellings and these results were also used in this research.

2.3 Reduction of energy consumption

It is has been clear for many years that inefficient consumption of both thermal and electrical energy, derived from fossil fuel sources, has both environmental and economic effects. Thus there is a clear need to improve the energy efficiency of buildings. There are three general routes for reducing the energy consumption in the domestic sector and thereby reducing CO_2 emissions [17]:

I. Minimise the heating and cooling loads by replacing the existing housing stocks with low-energy building design (i.e. reducing the energy consumption at end-use).
II. Develop and install low energy using domestic equipment (e.g. appliances, lighting and IT) and
III. Promote and adapt ‘energy-conscious’ behaviour among the end users.

The rate of demolition, new build and refurbishment are very slow which will take decades to achieve nationally significant energy savings. Replacements of domestic appliances are relatively frequent but increasing the energy efficiency of those appliances and restocking is a slow process. The application of energy labels is increasing the awareness about the energy performance of the particular appliance but the behaviour to use the appliance efficiently is hard to develop. Research is therefore needed to develop new control strategies depending upon the demand and user behaviour.

Another option would be to integrate micro-generators such as micro-CHP systems, photovoltaics, micro-wind turbine etc. along with the storage systems if necessary to displace imported electricity from the grid and to store renewable energy generation for later use.

There are many types of micro-CHP systems: Stirling Engine, internal combustion engine, fuel cell, organic Rankine cycle and gas turbine [27]. Among these, the Stirling engine micro-CHP, internal combustion micro-CHP and fuel cell are suitable for use in single dwelling [28]. A detailed review of different residential micro-CHP can be found in [29]. Table 2-1 shows a comparison of three micro-CHP technologies suitable for residential buildings. Of these, the natural gas fired micro-CHP based on Stirling engine are considered to be most suitable for domestic installation due to its high overall efficiency, low noise level and less maintenance requirements.

Table 2-1 Comparison of different micro-CHP technologies [27, 30]

No.	Characteristics	Stirling Engine	IC Engine	Fuel Cell
1.	Noise level	Low	Relatively high	Lowest
2.	CO_2 Emission	Low	Low but increases with age	Low
3.	Other pollutants	Low	High	Lowest
4.	Overall efficiency	70-90%	85-90%	85-90%
5.	Electrical efficiency	≈ 20% (theoretical) 5-10% (practical)	20-25%	Up to 50% (theoretical)
6.	H:P ratio	12:1(approx.)	3:1(approx.)	1(approx.)
7.	Capital cost	High	Low	Relatively higher
8.	Maintenance required	Low	Frequently	Lowest
9.	Life time	Long	Long	Relatively short
10.	Fuel type	Natural gas or renewable fuels	Natural gas	Hydrogen or natural gas
11.	Start-up time	Quick	Quick	Relatively slow
12.	Load following capability	Good	Good	Relatively quick
13.	Market availability	Soon	Available	Not commercial yet

2.3.1 Performance of micro-generation systems for domestic buildings

Clearly, an integrated power generating system in a building has become an important feature in recent years. However to achieve the potential benefits of such systems they must be properly designed and controlled as an integrated part of a building.

Existing prototypes of micro-CHP systems have very low electrical efficiencies, as low as 2-3% even though overall efficiency is higher (Stirling engine based micro-CHP) [2], and some are yet to be practically proven even though it has high electrical efficiency (fuel cell

based micro-CHP) [31]. As such, it is essential to utilise the thermal output of micro-CHP systems to meet the heat demand of the dwelling otherwise using micro-CHP systems would not be more favourable (in terms of carbon saving) than the existing systems. However, a perfect exploitation of the energy from these technologies is not an easy task because of the mismatch between the electrical and thermal demands of dwellings which varies a lot throughout the year and varies from one dwelling to another considerably. Carbon savings can be significant when micro-CHP systems are installed in appropriate applications [2]. Carbon savings from Stirling engine micro-CHP systems are reported to be higher in the dwelling with higher heat demands [2].

Much of the progress concerning the behaviour of micro-CHP systems in domestic applications has focused on comparing the seasonal economics of alternative module types [4-6] and on the measurement of the individual and comparative performances of these systems [7, 14, 32]. Barbieri, Spina, and Venturini [5] evaluated the feasibility of five different micro-CHP systems technologies for two different single family dwellings and found that energy savings can be achieved and that correct sizing of the thermal storage capacity is crucial. Regarding economic feasibility, the study showed that at present these technologies are not very attractive and that micro-CHP systems based on Stirling engine is best in almost all scenarios. Peacock and Newborough [28] studied the Stirling engine (1 kW) and fuel cell (3 kW) modules using constant effective module data and one minute recording of domestic energy demand and concluded that 25% (using 1 kW SE system) and 46% (using 3 kW FC system) of annual electrical demand of single dwelling can be supplied by micro-CHP systems. However, Paepe, *et al.* [33] concluded that only 10-15% of the electricity generated by 5 different types of micro-CHP modules can be used within the

dwelling. The difference in electrical energy used in the house could be due to the energy demand considered for the dwelling as Peacock and Newborough considered monitored one minute data in the UK whereas Paepe, *et al.* considered hourly data generated by the building energy analysis software for the Belgium family house and other considered parameters such as the electrical efficiency of micro-CHP (15% by Peacock and Newborough and 12% by Peape *et al.*) Ren and Gao[26] analysed the performance of gas engine and fuel cell based micro-CHP with minimum-cost operation and minimum-emission operation modes for residential buildings in Japan. They concluded that fuel cell micro-CHP was better option from both economic and environmental aspect. TeymouriHamzehkolaei and Sattari [34] carried out a technical and economic feasibility study of Stirling engine based micro-CHP in different climate zones of Iran. Their analysis indicated that profitability of micro-CHP system is sensitive to energy prices as well as the operation time. The fuel cells for micro-CHP have been considered in several feasibility studies and broad assessments of micro-generation. Conroy et al. [35] performed the comparative energy, economic and environmental analysis of Stirling engine based micro-CHP and found that the annual saving of €180 with an simple payback period of 13.8 years could be achieved with CO_2 emissions decreased by 16.1%. Field trial carried out by Carbon Trust [2] came with conclusions that Stirling engine based micro-CHP performed better in the households with higher thermal demands and identified the key drivers of the performance of micro-CHP systems. Key driver include reducing installed cost, targeting appropriate applications, increasing electrical efficiency and optimising installation and controls.

The general impression is that fuel cells have great potential to reduce costs and environmental impacts in this sector, but the technology is still emerging from its infancy.

However, the immaturity of the technology hinders such studies, limiting both the accuracy and validity of their conclusions, and preventing a more thorough and integrated analysis from being undertaken. The most notable gaps in current understanding relate to the current and future price of fuel cell micro-CHP systems, and the efficiency and durability that can be achieved in real-world use.

Building mounted micro-wind turbines and photovoltaics have the potential to provide widely applicable carbon free electricity generation. Research into wind speed estimation for the urban environment has shown that street canyons affect urban wind flow, that wind speed up over the roof ridge is only evident for isolated single buildings, that the wind resource "seen" by a building mounted wind turbine is affected by positioning (height above roof ridge and position relative to the prevailing wind direction), that urban terrain roughness is high, and that adjacent buildings can cause wind shadow [36]. This multiplicity of factors makes it difficult to generalise a wind resource estimation methodology for the urban environment. Current methods of estimating the wind speed are reported to over predict by approximately 2 m/s [37]. Viability of micro-wind turbine varies for individual household taking into consideration of local climate condition and the surrounding. Micro-wind turbine, however, is far more complex and in comparison poorly understood. Li *et al.* [38] evaluated the economic viability of six micro wind turbine for Irish conditions and found that it was not economically viable to install micro-wind turbine if the wind speed of the location is lower than 5 m/s and it is more promising only when it is installed in location where wind speed is greater than 6 m/s and higher financial incentives are given for installation. Greening and Azapagic [39] evaluated the life cycle environment sustainability of micro wind turbine compared to PV and grid and the contribution micro-wind turbine can

have on the UK climate change targets. The result showed that the wind turbine was more environmentally sustainable, however the contribution to the UK's climate change targets was very little even for the most optimistic assumptions in terms of their market penetration. Paper presented by James *et al.* [40] based on UK micro-wind trial under taken by the Energy Saving Trust found that performance of urban and suburban micro-wind sites was poor with annual generation of less than 75 kWh/m^2 swept area, the majority of which were less than 25 kWh/m^2 and good rural sites had annual generation of between 100 and 280 kWh/m^2, far less than the nominal 360 kWh/m^2.

For grid connected residential PV system, Pillai *et al.* [41] found that for most locations in the UK, cost reduction is needed to achieve near-term financial benefits and it varies depending on the location of installation. It also concluded with the importance of location specific system planning and demand-generation matching through optimal sizing of the PV system and demand side management. Li *et al.* [42] have shown that the unclear economics of domestic solar PV systems for Irish condition is the biggest obstacle for expanding domestic solar PV system installation in Ireland.

2.4 Modelling of micro-CHP systems with energy demands

Modelling of micro-CHP systems has received reasonable attention, however most of them are related to the proton exchange membrane fuel cell [22, 43, 44] and the solid oxide fuel cell [45]. Along with that, some models applied to assess different technologies of micro-CHP systems in terms of cost and emissions could also be found in the literature [4, 46, 47]. A detailed semi-empirical dynamic model of a domestic-scale Stirling engine micro-CHP systems has been presented by Lombardi, Ugursal, and Morrison [48], which demonstrate

improvements over existing models as well as a reduction in the number of experimental parameters needed. However, no attention is given in this model to the balance of system components and sub-systems (i.e. building, heating, electrical connections etc.).

Very little work has been done on the dynamic simulation of these plants including the detailed dynamic response of the local heating and electrical demand environment. Dorer and Weber [49] used a simulation modelling approach to compare two types of fuel cells, internal combustion engine and Stirling engine based micro-CHP systems at domestic scale using the modular simulation program TRNSYS. Onovwiona, Ugursal, and Fung [50], proposed a simple empirical model to simulate the performance of internal combustion engine based micro-CHP systems in building-integrated application. However most of their simulations were conducted at time intervals of 15-minutes which is adequate for capturing daily and seasonal energy profiles and mean performances but can fail to capture many of the shorter term dynamics particularly in relation to local loading changes and electrical grid interaction.

2.5 Operating strategies for micro-CHP systems

An operating strategy describes the way of operating micro-CHP systems and controlling the flow of thermal and electrical energy from the system. The purpose of controlling the micro-CHP system is to achieve specific beneficial targets for the household and the distribution network such as to reduce operating cost, decrease carbon emission and reduce the stress on the distribution network. Many feasible micro-CHP systems control strategies are limited due to the operating constraints of the prime mover technology and balance of

plant. A field trial of micro-CHP systems [2] has indicated that one of the key drivers of the performance of micro-CHP systems is by optimising their installation and control.

Various control options can be found in the literature and these can be summarized into two main categories: conventional and non-conventional operating strategies. Conventional operating strategies are heat-led [4, 8, 9, 51, 52] and electricity-led operating strategies [4, 51]. In a heat-led operating strategy, micro-CHP systems are controlled based on heat demand in the building. This type of strategy is mostly prominent in Stirling engine based micro-CHP systems due to its high heat to power ratio. Internal combustion engine based micro-CHP systems are also suitable for heat-led operation. Similarly, in electricity-led operating strategies micro-CHP systems are controlled based on electrical demand in the building. Fuel cell micro-CHP systems are suitable to operate in this mode, due to its lowest heat to power ratio. The idea behind these conventional strategies is to fulfil heat or electricity demand only.

The main aim of non-conventional operating strategies is to search for the optimal or near-optimal working condition of the system at each time step which can be in terms of cost or carbon emissions or efficient energy use. Online linear programming [53] and fuzzy logic operating strategy [51] for micro-CHP systems have been presented in the literature as possible operating strategies for micro-CHP in terms of reduction in operating cost and carbon emissions as compared to conventional operating strategies. Arsalis, Nielsen, and Kær [43] have also proposed an improved control strategy based on a combination of heat-led and electricity-led operation, for better performance (higher efficiencies) for the Danish single-family dwellings on averaged load profile. However, these control strategies were all

proposed for fuel cell based micro-CHP systems taking into account domestic loads only. Operating control strategies for Stirling engine based micro-CHP systems have not been proposed yet. Along with that, supporting the grid in terms of voltage control due to the export of electricity from a high penetration of micro-CHP has also not been considered.

2.6Effects of micro-CHP systems on distribution networks

It is very difficult to predict the future penetration level of micro-CHP systems in the LV network. An estimate of the UK market potential for SE micro-CHP systems of 13.5 million units has been made [54], and if 1 kW size of micro-CHP system is assumed, this would represent 13.5 GW of installed capacity. However, the application of different sizes and types of micro-CHP, plus deployment of those independent of gas network may ultimately result in higher installed capacity within the electricity network. Installing this higher capacity in the LV network would affect the electricity distribution system in terms of power flow and its protection system. Different studies [18, 19, 55] have investigated the effect of mass deployment of micro-CHP system of 1.1 kW upon the LV network Barbier *et al.* [18] have shown that voltage control is the primary issue of concern when large amounts of micro-CHPs are connected to the LV network, with penetration levels over 40% having a detrimental impact on the LV network in the worst case scenario. Other issues that could arise due to the connection of large number of micro-CHPs are increase in fault level due to its contribution to the fault current, reverse power flow when penetration levels of micro-CHP reaches 100% and voltage unbalance when penetration level exceeds 150%. A 40% penetration of micro-CHP thus means that 40% of the total households considered have 1.1kW of micro-CHP installed. For penetration higher than 100%, it is assumed that the

"effective" size of the micro-CHP is increased proportionally. A 200% penetration of micro-CHP thus means that "effectively" 100% of the households have 2.2kW of micro-CHP installed.

Chapter 3 Distributed Generation & Storage Systems

3.1 Introduction

A large share of greenhouse gas emission (especially CO_2) is due to power generation. So, many new sustainable technologies for electricity generation are currently under development. Many of these technologies are designed for application at the distribution level of the power network. Such small-scale electricity generation systems are referred as distributed generation (DG). Distributed generation refers to power generators that produce power from a fraction of kilowatt (kW) to tens of megawatts (50 MW) and are generally connected to the grid at the distribution levels (below 33 kV) [18]. Photovoltaic systems, wind energy conversion systems (wind turbine), combined heat and power technologies, biomass, gas turbine and small hydroelectric generators are examples of distributed generation technologies. Distributed generation can be owned and operated by utilities or individual customers. Large DG units are typically controlled and communicate with DNO like central power generating stations do. However, neither network operators nor utilities typically monitor or control the operation of small DG units, especially those in residential applications.

3.2 Small Scale Distributed Generation

From a recently published UK White Paper [56], the UK government is committed to transform the UK's electricity system to ensure that the future of electricity supply is secure,

low-carbon and affordable. The aim is to provide flexible, smart and responsive electricity systems powered by a secure and diverse range of low-carbon electricity sources where demand management, storage and interconnection will help to keep the costs down. There are various types of power generating sources that could be installed in buildings and connect to the grid. Some of these technologies considered in this project are discussed below.

3.2.1 Micro-combined heat and power

The concept of combined heat and power (CHP) or cogeneration has been known for long time. Combined heat and power production is defined as "the process of producing both electricity and usable thermal energy (heat and/or cooling) at high efficiency and near the point of use" [57]. This definition incorporates three defining elements: simultaneous production of electricity and useable heat; performance of higher total efficiency compared to separate electricity and heat generation; and location of the CHP with regards to load (or point of use) and reduced transmission losses.

The discussion on micro-CHP has recently gained momentum. However, the technology of micro-cogeneration goes back to the 18^{th} and 19^{th} centuries with the development of steam and Stirling engines respectively. Advancement in the technology and trend toward smaller unit size power plants have led to boosted interest in micro-CHP with the expectation to meet partial or full electrical and heat demand for individual buildings. So, micro-CHP is defined based on small energy conversion units below 15 kW_{el} for individual building [58] in which heat produced is used for space heating and water heating and electricity produced is used within the building or exported to the grid. Opposed to that, the EU cogeneration

directive [59] has defined micro-CHP as a unit with a maximum capacity below 50 kWel. Pehnt *et al.* [58] have given sensible reasons for limiting up to 15 kWel as micro-CHP which are: these systems are used for single-family dwellings, apartment houses, small business etc. which can be distinguished from district heating systems and no additional heat distribution grid is required and the system be connected directly to the three-phase grid.

Micro-CHP is currently in focus for domestic application so they are also termed as 'domestic-CHP'. Different micro-CHP conversion technologies have been developed based on combustion and subsequent conversion of heat into mechanical energy, which then drives a generator for production of electricity such as Stirling engine, reciprocating engine, gas turbine etc. Alternatively, micro-CHP can be based on direct electrochemical conversion from chemical energy to electrical and heat energy such as in case of fuel cells.

Micro-CHP is operated in mainly two modes of operation: heat-led and power-led. Stirling engine and internal combustion engine based micro-CHP are suited to operate in heat-led mode, sized to meet the full heat demand of a house [27]. Whereas, fuel cell based micro-CHP has potential to operate in power-led mode sized to generate electricity constantly with the associated heat , providing small part of the overall heat demand, with a separate boiler providing the remaining heat [27]. Apart from these two modes, Newborough [8] has investigated six different modes of operation for micro-CHP taking into account the size of prime mover, length of operation per day and whether or not to charge an electricity storage bank. He did not attempt to minimize the cost of operation nor considered managing the thermal energy (assumed thermal load to be greater than micro-CHP output per day). However, these six modes of operation could be generally classified as heat-lead mode or

power-lead mode. Hawkes and Leach [4] looked into two main modes considering cost as main factor. He concluded that running heat-led mode may not provide the minimum cost of meeting energy demand but following heat and electricity load during winter months would provide least cost operation rather than using either heat-led or electricity-led as the only dispatch signal.

3.2.1.1 Stirling engine micro-CHP

Stirling engine micro-CHP is an emerging technology. It is an external combustion engine that utilizes heat from combustion to drive pistons. A working fluid, helium or nitrogen, expands and contracts within each cylinder by means of hot and cold heat exchanger, forcing the piston to move in and out. A transmission system converts the linear piston motion to rotation that drives an alternator. Heat is provided to the hot end of the cylinder by an external flame and cooling water removes heat from the cold piston end. The cooling water through the cold side of the piston in series with an exhaust gas heat exchanger provides the thermal output which can be used domestically. The engine and lubrication system are typically fully sealed and good designed, requiring less maintenance. Stirling engine micro-CHP can be divided into two types: crank-driven and free piston [29]. It can have many complex designs ranging from single cylinder free piston to four cylinder 'wobble' yoke. Most commonly, Stirling-cycle machine uses a piston cylinder in either an α or β configuration.

In an ideal Stirling-cycle engine the components of the machine interact to produce four separate thermodynamic processes. The processes are illustrated using a simplified β-

configured machine in Figure 3.1 and the pressure-volume and temperature-entropy diagrams are shown in Figure 3.2.

Process 1-2, Isothermal (constant temperature) expansion: the high-pressure working gas absorbs heat from the external source (via the heat absorbing heat-exchanger) and expands isothermally, thus doing work on the power-piston.

Process 2-3, Isochoric (constant volume) displacement: the displacer-piston transfers all the working gas isochorically through the regenerator to the cold end of the machine. Heat is absorbed from the gas as it passes through the regenerator, thus lowering the temperature of the gas to that of the cold space. As the temperature reduces, the gas pressure drops significantly.

Process 3-4, Isothermal compression: the power-piston does work on the gas and compresses it isothermally at cold end temperature, hence rejecting heat to the cold space (via the heat rejecting heat-exchanger). Because the gas is at low pressure, less work is required for compression than was obtained from the gas during expansion (in 1-2). The cycle therefore has a net work output.

Process 4-1, Isochoric displacement: the displacer-piston transfers all the working gas isochorically through the regenerator to the hot end of the machine. Heat is delivered to the gas as it passes through the regenerator, thus raising the temperature of the gas to that of the hot space. As the temperature rises, the gas pressure increases significantly, and the system returns to its initial conditions.

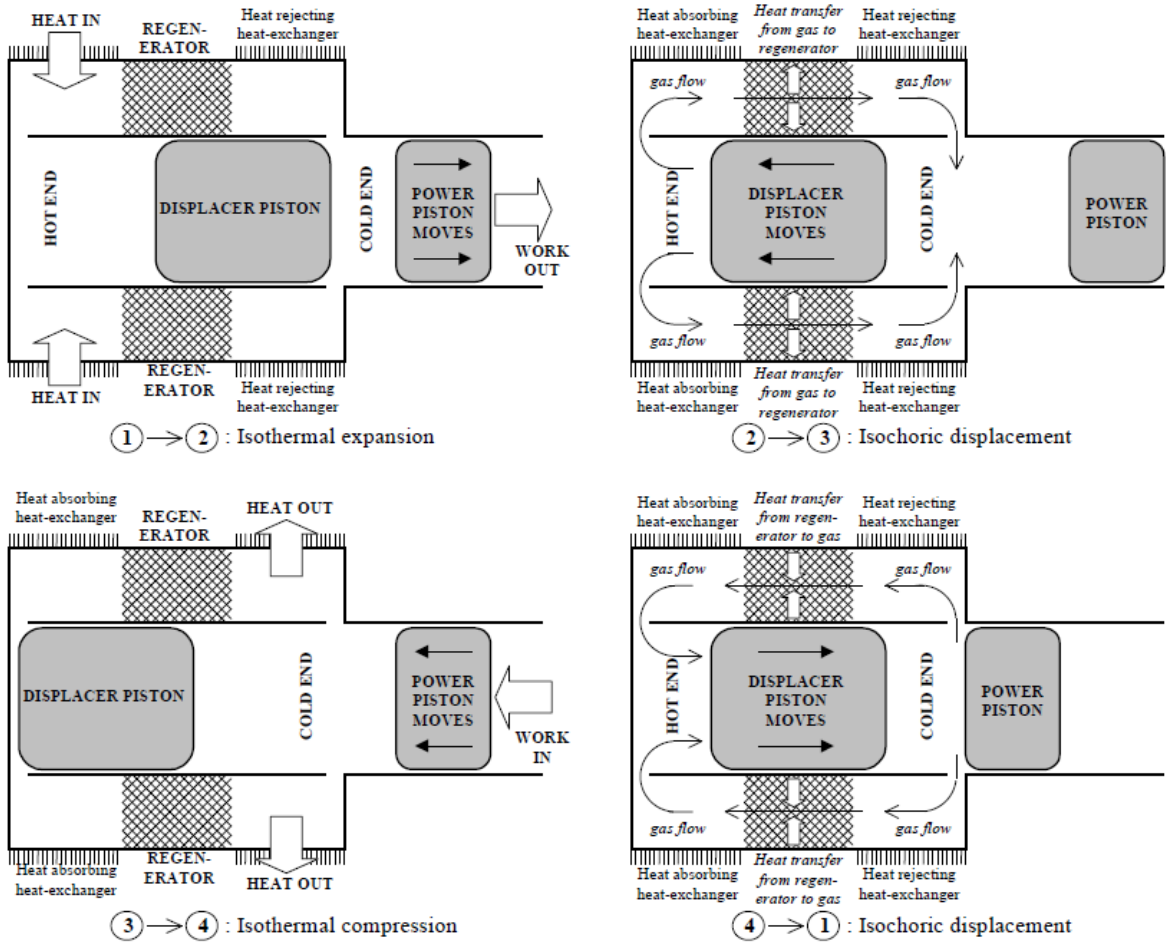

Figure 3.1 Thermodynamic processes in the ideal Stirling-cycle engine as shown on a simplified β-configuration machine.

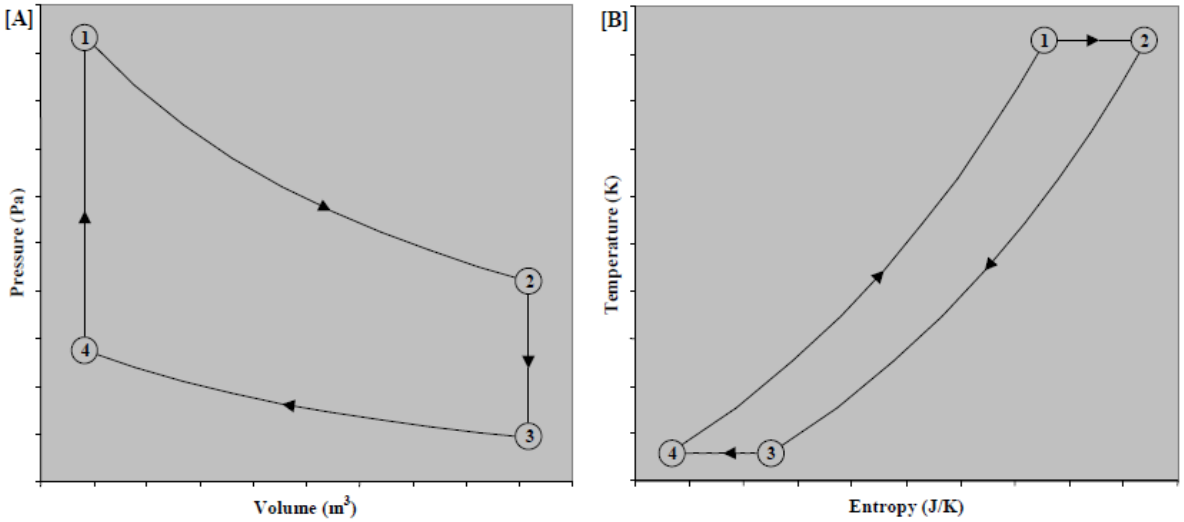

Figure 3.2 Thermodynamic processes in the ideal Stirling-cycle engine. (A) Pressure-volume diagram. (B) Temperature-entropy diagram.

The simplicity, potential long life with low levels of noise and small size makes Stirling engine micro-CHP suitable for individual domestic houses. In addition to the core engine, some manufacturers include an auxiliary burner to supply higher heat demands for a given electrical output. Stirling engine micro-CHP is more suited to operate in heat-led mode, as their heat-to-power ratio is higher than IC engines.

The Whispergen unit comprises a 1 kWel, 230 V, 4 pole AC induction generator which is driven via wobble yoke by an external combustion engine. Key components of Whispergen within the unit are shown in Figure 3.3 below. This unit forms the basis for the modelling of micro-CHP system which is discussed in section 5.2.

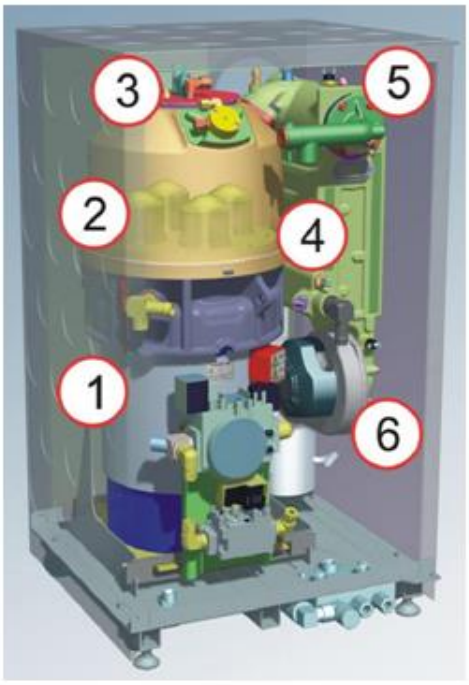

1. Electric generator produces electricity at 220- 240V
2. Stirling Engine produces the momentum necessary to operate the generator
3. Gas burner to give heat input the Stirling engine
4. Heat exchanger that recovers heat from the hot gases produced by the burner
5. Auxiliary burner to provide extra heat when there is more heat demand
6. Valve for exhaust gas that provides combustion gases to the burner and clears the waste gases into the atmosphere

Figure 3.3 Key components of Stirling engine based micro-CHP

The Whispergen operates by supply of natural gas into the main burner chamber where electronic ignition establishes the main burner flame. Heat energy within the main burner chamber is transferred across the heads of four pistons. Nitrogen gas, the operating fluid, is sealed inside the piston chamber and gets heated and produces movement and kinetic energy. The coolant at the bottom of the chamber extracts the heat from the working fluid thus giving another movement and kinetic energy. Combination of these two movements gives to and fro movement in the piston.

A regenerator in the middle of piston i.e. between the two heat exchange areas allows for transient storage of heat for increasing cycle efficiency.

Four pistons are positioned out of phase geometrically with respect to each other but are interconnected with each other by wobble yoke mechanism. The vertical movements of

pistons, acting simultaneously on the yoke, combine to produce rotary movement of the wobble yoke which enables rotary movement to take place between the rotor and stator of the generator, thereby generating electricity.

In addition to above, an auxiliary burner and heat exchanger is present in the Whispergen unit which has no direct impact upon the operation of the electrical generator. Control of auxiliary burner is done by automatic on/off switch in accordance with energy management software which monitors the absolute and rate of change of engine coolant temperature.

3.2.1.2 Internal combustion engine (IC engine) micro-CHP

Internal combustion engines based micro-CHP is the most mature technology of all the micro-CHP technologies. These systems are based on engine technology common in the automotive sector and can be classified into two categories based on ignition method: compression ignition (Diesel) engine and spark ignition (Otto) engines.

In the Otto engine, mixture of air and fuel is drawn into the cylinder through the intake valve and then adiabatic compression of the mixture takes place which increase the temperatue inside the cylinder. After compression ignition is caused by an externally supplied spark. The ignition adds heat to the working fluid at constant volume (isometric process) which increases pressure and exerts a force on the piston causing expansion/power stroke. This expansion of the working fluid takes place adiabatically and work is done by the system on the piston. The final stroke is the exhaust stroke where the gas is exhausted out of the piston. In Diesel engine, only the compression of air in the cylinder and the fuel is introduced into the cylinder towards the end of the compression stroke, thus the spontaneous ignition is caused by the high temperature of the compressed air.

For micro-CHP applications, typically spark ignition (Otto-cycle) engines are used with their heat recovery system producing up to 160°C hot water when using an exhaust gas heat recovery heat exchanger, though the engine wall cooling system must operate at much lower temperature (typically maximum 90°C).

IC engine micro-CHPs are suitable for medium and large applications such as schools, hospitals, hotels and industrial buildings due to their relatively large size and level of noise they produce during operation [27]. However, the benchmark test done at Reutlingen University with regards to the regulation of German environmental label [60], describes the noise and vibration level of SenerTech 'Dachs' and Ecopower by PowerPlus Technologies, which are IC engine based micro-CHP, with in the acceptable range for single or more family house application. Fuel used for IC engine micro-CHP is mainly natural gas, however other fuel based are also available. IC engine used as micro-CHP unit vary in size from 1-4 kW of electrical output.

3.2.1.3 Fuel cell

Fuel cell technology is based on the concept of direct electrochemical energy conversion, close to those of electrical battery. Fuel cells have the potential for both power generation and cogeneration applications. Because of the ability to produce electricity at relatively high efficiency compared to conventional power plants and significant reduction of greenhouse emission, fuel cell cogeneration based systems have perhaps the greatest potential in residential and small-scale commercial application. Figure 3.4 shows the typical breakdown of the overall efficiency of fuel cell based micro-CHP system.

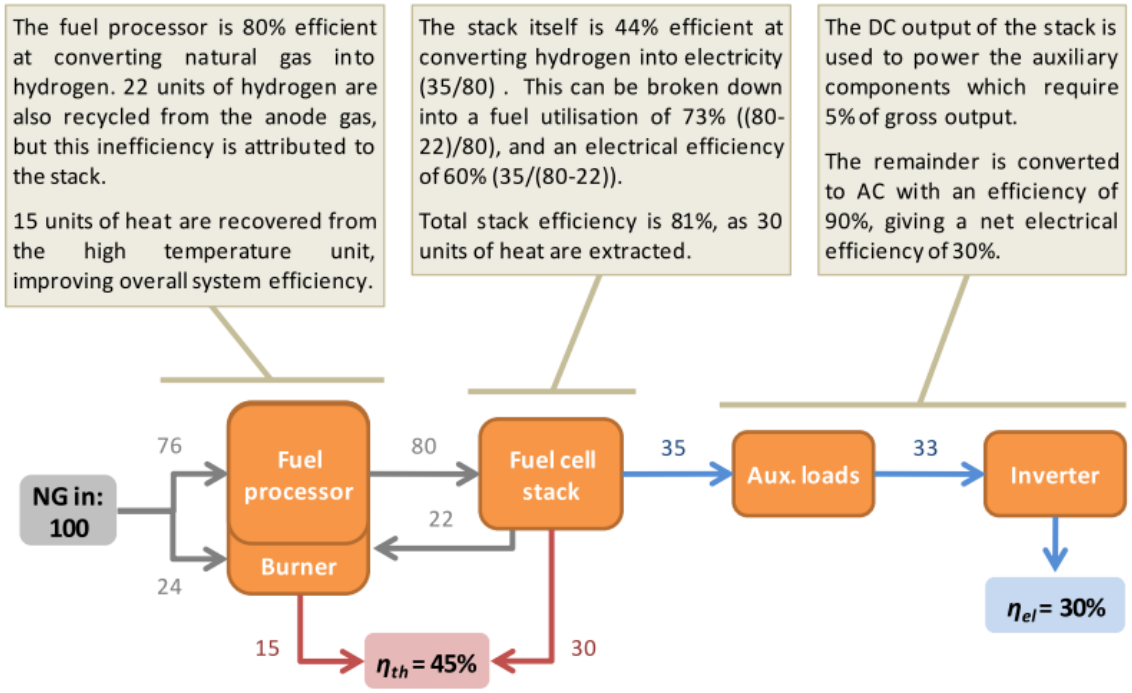

Figure 3.4 A typical breakdown of the overall efficiency of a fuel cell based micro-CHP system [61]

A fuel cell converts fuel and air directly into power and heat through a quiet, efficient, solid-state electro-chemical reaction. Several cells are connected in series to increase the voltage for efficient conversion to AC in a solid state inverter. Though fuel cells use hydrogen and, as yet, a hydrogen fuel infrastructure is lacking in most part of the worlds, hydrogen can be generated from natural gas in a reformer. It generates power significantly more efficiently than IC engines because they convert chemical energy directly to electrical current rather than via a mechanical intermediate phase. Fuel cells operate at high efficiency at part load and their efficiency is unaffected by size. Figure 3.5 shows the part load efficiency of fuel cell based micro-CHP system ENEFARM. Although many types of fuel cell exist, Solid Oxide Fuel Cell (SOFC) and Polymer Electrolyte Membrane Fuel Cell (PEMFC) are the

dominant types used for micro-CHP system [62]. SOFC and PEMFC have the advantage of reduced fuel consumption, better environmental impacts and good match for residential heat to power ratio [29].

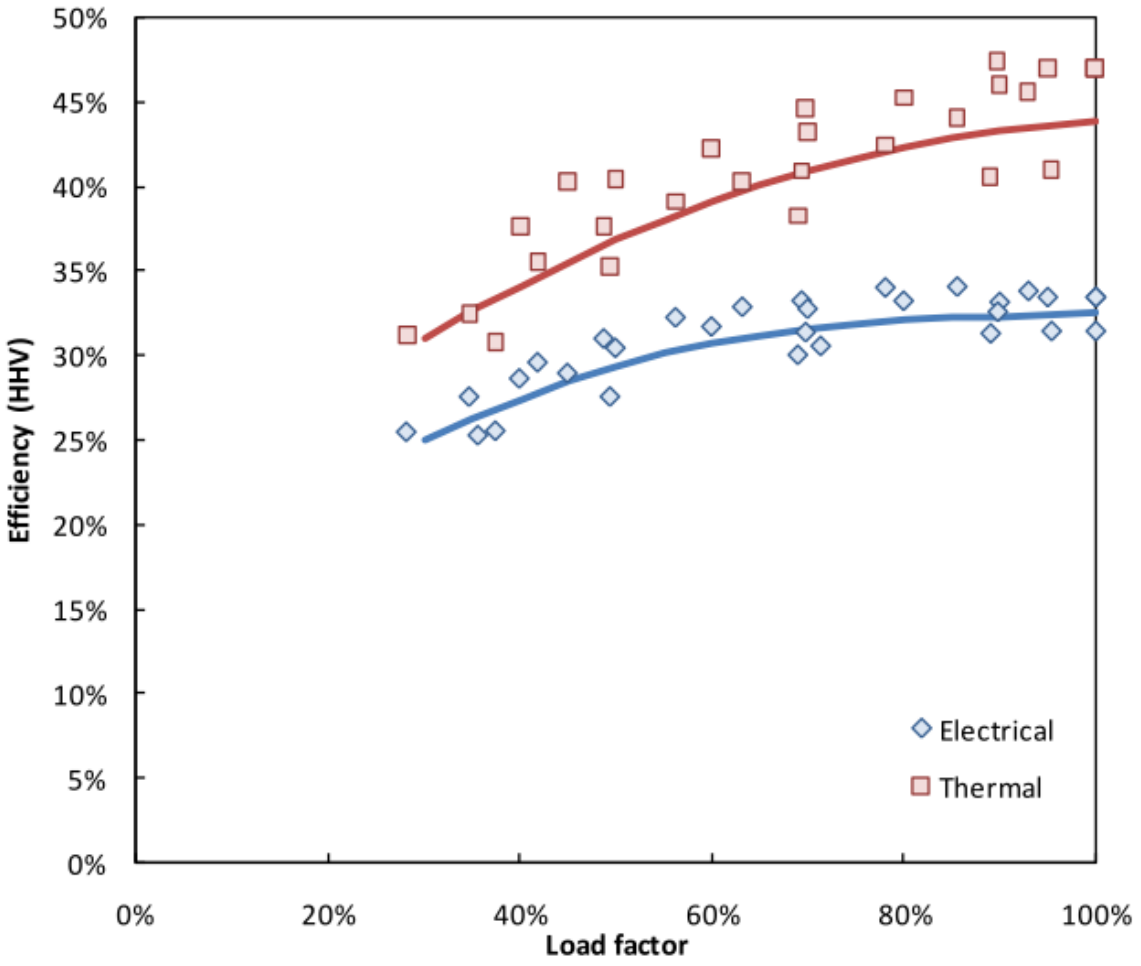

Figure 3.5 The part load efficiency for fuel cell based micro-CHP, ENEFARM [61]

Fuel cells currently available have complex designs and require careful control during start-up. This includes requiring all parts of the system to be raised to the correct operating temperature before generation can begin. Although fuel cell micro-CHP are less mature than

other technologies, if they can be optimized to offer sufficient performance and reliability with acceptable size and cost, they may have greatest potential [27].

3.2.2 Photovoltaic (PV)

Photovoltaic converts solar energy into electricity in an environmental friendly manner. Typical PV cells are made of semiconductor materials such as silicon which shares some of the properties of metals and some of those of an electrical insulator. Sunlight is composed of particles called photons, which radiate from the sun. As sunlight hits the silicon atom of the solar cells, they transfer their energy to free up electrons from atom. Freeing up electron is only half work of a solar cell: it needs to convert these electrons into an electric current. This is done by creating an electrical imbalance within the cell. Creating this imbalance is made possible by the internal organisation of silicon by creating two different types of silicon: p-type, which is missing electrons, leaving 'holes' in their place and n-type, which has spare electrons. When these two materials are placed side by side inside a solar cell, the spare electrons in n-type silicon jump over to fill the gaps in the p-type silicon. This means that the n-type silicon becomes positively charged and p-type silicon becomes negatively charged, creating an electric field across the cell. The insulating nature of the semiconductor ensures that this imbalance is maintained. As the photons frees the electrons from the silicon atoms, this field drives them along in an orderly manner, providing the electric current [63].

These PV cells are connected in series in order to obtain large output voltages and in parallel to obtain large output current. A set of connected cells form a panel. A PV array may be either a panel or a set of panels connected in series or parallel to form large PV systems. A typical I-V and P-V characteristic curve of a practical PV array and the three remarkable

points: short circuit current (0, Isc), maximum power point MPP (Vmp, Imp) and open circuit voltage (Voc, 0) are shown in Figure 3.6

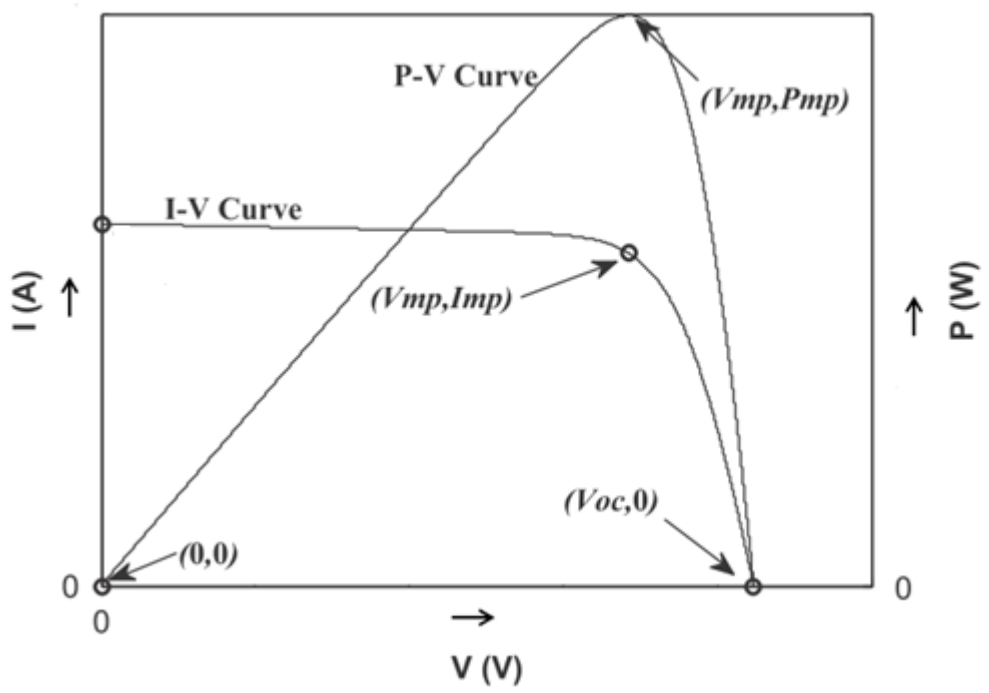

Figure 3.6 I-V and P-V characteristics curves of a typical PV array

The transformation of energy is carried out using PV modules or panels made up of solar PV cells. The major advantages of a PV system are: sustainable nature of solar energy as fuel, minimum environmental impact, long life with minimum maintenance, silent operation and, in the UK, tariff incentives which generate income due to the clean electricity generated – the feed-in-tariff. Though PV cells can be effectively used as a distributed energy resource, they suffer from the disadvantage of high installation cost and low energy efficiency. PV systems not only generate electricity during sunny days but also in cloudy condition (through at considerably reduced output). Electricity generated by PV is DC, therefore an inverter is connected to convert DC to AC at the specified frequency level.

There are mainly four types of PV cells, which are: monocrystalline silicon, multicrystalline silicon, thin-film silicon and hybrid. Monocrystalline cells are made from a single cylindrical crystal of silicon. The main advantage of monocrystalline cells is their higher efficiencies of about 15%, although the manufacturing process is complicated and expensive. Multicrystalline silicon cells, also sometimes known as polycrystalline cells, are made from cells cut from an ingot of melted and re-crystallised silicon. The ingots are then saw-cut into very thin wafers and assembled into complete cells; they are generally cheaper to produce than monocrystalline cells, due to the simpler manufacturing process, but they tend to be slightly less efficient, with average efficiencies of around 12%. Thin film solar cells or amorphous solar PV cells are made from a thin film of amorphous (non-crystalline) silicon. This can be placed on a wide range of different surfaces and, because the amorphous silicon layer is flexible, if placed on a flexible surface, then the whole solar PV cell can be flexible. These panels are the least expensive to produce but are also the least efficient (typical efficiency around 5%). Hybrid photovoltaic cells are classified as PV cells that use two different types of PV technology to produce a cell with best features of both technologies. The advantages of these types of cell are that they perform well at high temperatures and maintain higher efficiencies (17%) than conventional silicon PV cells. However, these cells come at a premium cost.

Based on application, PV systems can be either grid connected or stand-alone. Distributed generation falls into the grid connected PV system category. A grid connected PV system is made up of an array of panels mounted on rack-type supports or integrated into a building. Integration of PV modules in the building can be done on the roof or façade, most common being mounting in the roof.

The amount of electricity generated by a solar PV system can vary depending on orientation, wind speed, air temperature, spectral irradiance and various system losses. The performance of PV panels in rural areas varies with those in urban areas. In urban areas lower output may be experienced from PV modules due to the attenuation of solar radiation, mainly due to air pollution, lower wind speed and higher air temperature than in rural area. However, temperature of installed PV panels in the urban area are witnessed to be lower which leads to higher conversion as a result the reduced solar radiation does not have great impact on PV output [40]. Efficient power utilization depends not only on efficient generation in the cell but also on dynamic load matching in the external circuit. An increase in module temperature decreases the panel voltage and therefore reduces the power output.

Power produced from the modules can be maximised using a maximum power point tracker (MPPT). It is not a mechanical tracking system that physically moves the modules but it is a fully electronic system that varies the electrical operating point of the modules so that the modules are able to deliver maximum available power. There are many MPPT methods available in the literature and the comparison of these methods is given in paper [41]. Overall there is always one true maximum power point, except under partial shading conditions it is possible to have multiple local maxima. Most of the MPPT techniques respond to change in both temperature and irradiance but some are more useful if temperature is approximately constant. With numerous MPPT techniques having a range of strengths and weaknesses it is important to select the best technique based on implementation, sensor, multiple local maxima, cost and application.

Building-integrated PV systems can also contribute to the electrical demand of the house. A PV domestic field trial [42] monitored 474 individual PV systems installed in a wide variety of dwelling type (217) within the UK, showed that even fairly small sized PV systems of around 1.6 kWp can meet a significant fraction of the house demand. It was also shown that a majority of systems provide between 20% and 80% of the building demand with an average of 51%.

3.2.3 Small scale wind turbine system

Along with micro-CHP and PV, there is growing interest for small scale wind turbine systems in the domestic sector. Small scale wind turbines are a technology that could develop into a market-mature technology applicable for widespread adoption. A majority of small scale wind turbines are installed for educational reasons and there are presently very few in domestic buildings especially in urban areas.

Small scale wind turbine systems convert wind energy into electrical energy. They capture the kinetic energy of wind through rotor blades and transfer it to mechanical energy from which a generator converts the mechanical energy into electrical energy. In this process, aerodynamic power conversion losses are very high. According to Betz limit, the maximum theoretical wind power conversion efficiency of wind rotor is 59% [64]. However, due to losses in blade roughness, hub and tip losses the maximum efficiency of a wind rotor obtained in practice is around 45% [65]. In order to extract the maximum energy, the wind rotor is required to operate at a certain rotational speed for a particular wind speed. Due to continuous variation of wind speed and direction, changing of wind rotor rotational speed to follow the maximum power point becomes difficult, thus the efficiency decreases. The flow

of power conversion in wind energy conversion system is illustrated in Figure 3.7. Based on design, a wind turbine may be horizontal axis or vertical axis configuration. Most are installed predominantly on free-standing vertical pole in open and exposed locations. Some small scale wind turbine can be mounted on the roof of building.

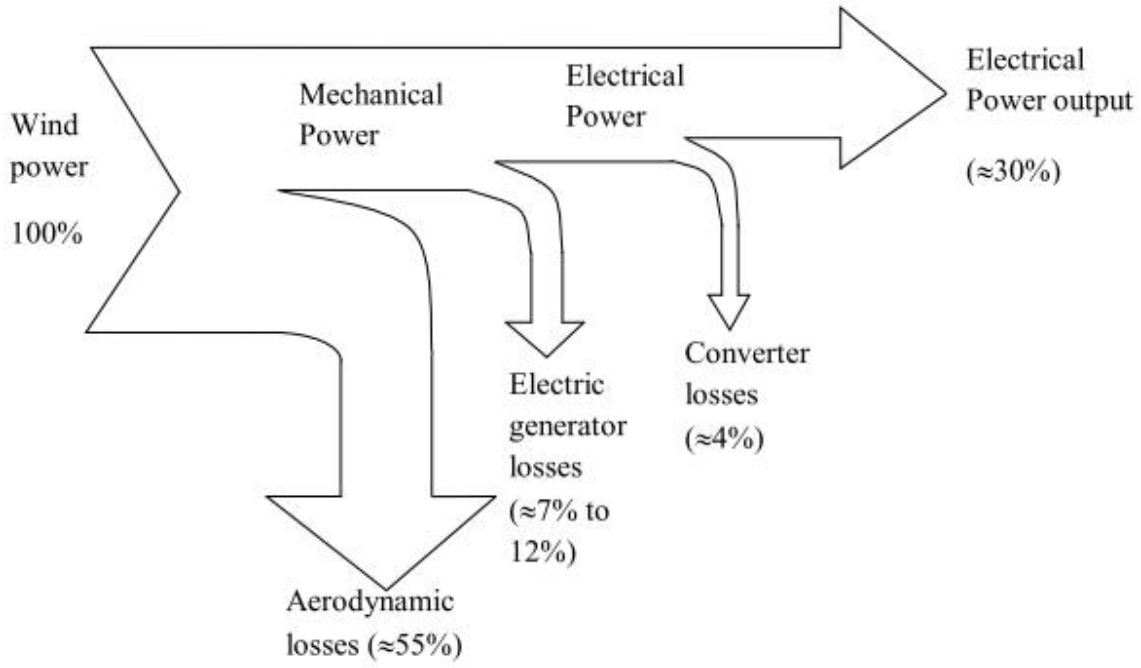

Figure 3.7 Power flow in a wind energy conversion system [66]

In theory, the power of the wind, P, is governed by the Eqn. 3.1.[9]

$$P \propto V_w{}^3 A\rho \qquad \text{Eqn. 3.1}$$

Where, V_w is the wind velocity (m/s), $A\ (\pi r^2)$ is the swept area (m^2) with radius r (m) and ρ (kg/m^3) is the density of air. From Eqn. 3.1 it can be seen that if the radius of swept area is doubled, power is increased by four times and if speed is doubled, power is increased eight times. The relation between wind speed and power for a turbine, most commonly, is presented as a power curve such as in Figure 3.8. This curve has three main parts

differentiated with respect to wind speed: speeds between zero to the cut-in wind speed (the lowest speed at which the turbine is able to generate any power which is usually around 3 or 4 m/s), speeds between the cut-in wind speed and rated wind speed (the speed at which the turbine produces its rated power, typically around 11-12 m/s) and speeds between rated speed and cut-out speed (beyond which turbine is not able to generate, often about 25 m/s). Generally, a site's wind characteristics and a turbine's power curve are used in combination to determine how much energy the turbine will generate at the given site over a period of time. Wind speeds increase with height above ground, so the higher a turbine is mounted, the greater the power that can be generated. Obstacles such as buildings and trees can cause sheltering and turbulence, depending on their distances to the turbine and relative heights.

When considering the performance of the wind turbine at any particular site, or compared to other sites, a capacity factor is used. The capacity factor is the ratio of the amount of electricity actually produced in a certain period to the amount of electricity that would have been produced over the same period had the turbine been generating continuously at its rated power.

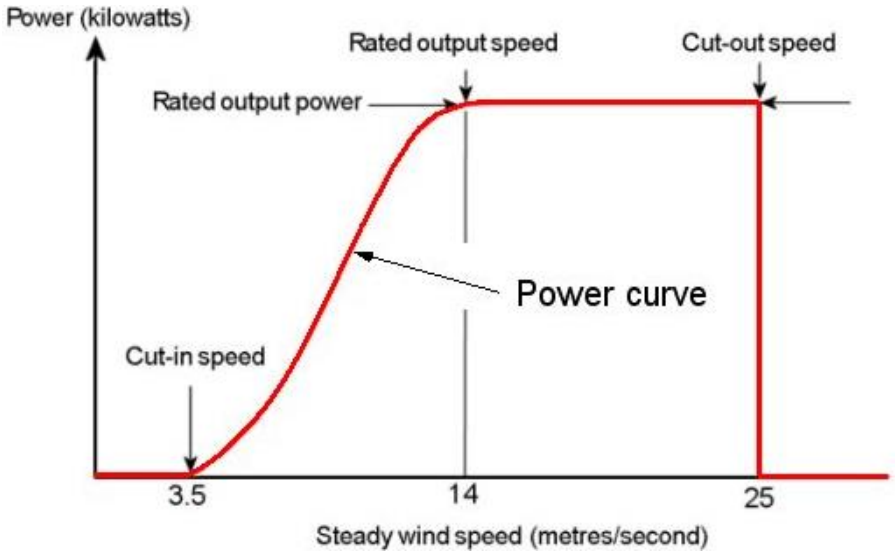

Figure 3.8 Power curve of a wind turbine [67]

There is lack of performance analysis done on domestic scale wind turbines. The results of a field trial by the Energy Saving Trust [68], indicate that there is potential to generate up to 3,500 GWh electricity per annum from domestic scale wind turbines in the UK but the installation has to be done properly and in appropriate locations, where the average wind speed should be above 5 m/s. As wind speed is the primary factor for a wind turbine to generate electricity, its variability and difficulty in prediction is the prime concern. Accurate wind speed data is not available especially for those in urban locations. There is a need for rigorous research into wind speed frequency distributions for small scale wind turbines [69]. The results from a wind trial in Warwick [70], also show that the wind speed and power curve data that are available to predict the performance of the given wind turbine is not accurate, giving an error ranging from +/- 25%. García-Bustamante *et al.* [71] have shown a comparison of manufacturers' power curves and effective power curves (directed from turbine power production data) showing that manufacturers' power curves generally

overestimated at high wind speeds and underestimated power output at low wind speeds. The economic viability of small wind turbine are mainly influenced by two factors, not clearly presented by equipment manufacturers; the power curve and the ratio between the rated power and the rotor swept area [72]. In many instances they are not viable due to high capital cost and long payback period. However, with much more accurate wind speed data and power curve data, together with support from government with grants and incentives the small scale wind turbine could be viable in the future.

3.3 Benefits of Distributed Generation

Installation of DG can improve reliability, reduce costs and reduce emissions. However, the benefits of DG highly depend on the characteristics of each installation and characteristics of the local power system. Table 3-1 briefly highlights the benefits of DG.

Table 3-1 Benefits of distributed generations [73]

Reliability	Economic	Environmental
1. Increased security for critical loads. 2. Transmission and distribution congestion relieved. 3. Impacts from physical and cyber-attacks are reduced. 4. Generation diversity increased.	1.Fuel cost is reduced due to overall efficiency and free fuel when renewable energy source used. 2.Investments for network upgrade are deferred. 3.Lower operating costs due to peak shaving. 4.Reduced costs associated with power losses. 5.Reduced land use for additional generation.	1. Transmission line losses reduced. 2. Pollutant emission is reduced due to high overall higher efficiency.

Improved system reliability results from the ability of DG units to maintain supply to local loads in the event of system outage by operating in 'islanding' mode. When a distribution feeder is disconnected from a faulted area an 'island' is created. Successful islanding operation requires sufficient power generation to meet the demand and necessary distributed system control capability. However, in the current situation operating DG in island mode is not allowed due to safety and technical issues.

Customer sited DG reduces revenue for the utility but can offer long term electricity cost stability and, in some cases, savings which can come in different forms such as feed-in-tariff.

DG connected to the grid via power electronic inverters such as in case of PV, fuel cells and most wind turbines are widely understood to be sources of voltage waveform distortion. However, if designed and implemented properly, the power electronics could cancel grid distortions and help voltage regulation [74]. DG capable of providing constant uninterrupted power can improve power quality by mitigating voltage problems and flicker.

Apart for the above advantages, DG will also help to fulfil part of the electricity demand which is expected to increase in future despite the improvements in household and non-domestic energy efficiency and partly compensate for the closure of existing power generating plants over the next decade as they are getting old or becoming more polluting.

In realization of the above advantages, the UK government has introduced different schemes such as Carbon Price Floor (CPF), Feed-in-Tariff (FIT), Renewable heat Incentive (RHI) and standards such as the Emissions Performance Standards (EPS) to drive decarbonisation

and help investment in low-carbon generation technologies and limit the emissions from new fossil-fired power stations.

3.4 Impact of Distributed Generators on Low Voltage Networks

Existing electrical power distribution systems have been designed to transmit power from the high voltage end to the low voltage end. The power transmission system accepts bulk power from central power generation stations and then transmits to the distribution centre from which power is carried to customer delivery points. Configuration of power lines and protective relays are designed based on this arrangement. So far, a small number of DGs are connected to the distribution network and these are regarded as simply a reduction in load. However, this situation changes as the penetration of DG increases and becomes significant. The distribution network will not only become a distributor but also a source of power supplied from remote customers. Therefore, the control of the distribution network will be required to change.

The problems that could arise when connecting a large number of any types of DG on the distribution network are: change in voltage level, increase in short circuit contribution (fault levels), reverse power flow, malfunctioning of the electrical protection system and potential voltage unbalance.

3.4.1 Voltage change

Voltage control is the main problem when connecting a large number of DGs to the low voltage network. In the UK, the statutory voltage limits are -6% to +10% of nominal at 400 V and -6% to +6% of nominal voltage for systems above 400 V up to 132 kV. Change in

voltage levels and potential violation of voltage limits can be a voltage rise, when the voltage exceeds the statutory upper limit and voltage drop, when it falls below statutory lower limit.

When there is no DG connected to the LV network, the voltage will drop as the distance from the distribution transformer increases. However, when a DG is connected, the voltage at the point of common coupling (PCC) can increase as the DG supplies power and effectively reduces the voltage drop. During the time of peak demand, the voltage at the PCC decreases but is kept within limits by the operation of the tap changer. During the time of minimum demand and maximum DG output, (for example in the case of micro-CHP early in the morning), the voltage at PCC will increase because of export of more power.

When DG is connected to LV network it will generally reduce the voltage drop and may cause the network voltage to exceed the limit. However if the DG failed, there would be a sudden voltage drop, which could bring voltage levels below the statutory limit.

3.4.2 Reverse power flow

If power generated by DGs connected to a distribution network exceeds the load power demand and network losses, the net power flow become negative. Power will then flow from the PCC into the network thus reversing the direction of power flow, which is not what the network was designed for. Reverse power flow will lead to malfunctions of the protection system in the network which is designed for unidirectional power flow. Also, the primary transformer's tap changer is not usually designed to accept significant flow of reverse power.

3.4.3 Increased fault level

In an electrical network, the possibility of electrical faults on a section of line or cable is always there which may be due to short circuit faults, lighting strikes, earth faults or electrical and mechanical equipment failure. To prevent the equipment from damage due to such faults, relays and circuit breakers are installed at different location of the network. When a generator is connected to the network, including DG, fault levels close to the PCC will increase due to the contribution of the generator during the fault. The peak short circuit current from a DG may increase more than 3-4 times the nominal current rating of the machine during the fault. Due to the addition in fault level, the overall fault level increases and could exceed the rating of the existing circuit breaker.

3.4.4 Voltage unbalance

Voltage unbalance is the percentage difference between the average of all three-phase voltages and the individual phase voltages. According to the Engineering Recommendation P29, the maximum recommended limit for voltage unbalance is 1.3%. Voltage unbalance only occurs when a very large number of DGs are connected to one phase and very few on adjacent phases. Barbier *et al.* [18] have shown that voltage unbalance occurs when there is very high amount of penetration in one phase compared to others which is unlikely to happen in the near future.

3.5 Energy Storage Systems

Energy storage system (ESS) plays an important role for energy management. Energy storage system can be thermal or electrical.

3.5.1 Thermal energy storage

Adding thermal storage to a micro-CHP system allows the micro-CHP to operate continuously and limit switching on/off of the device. Furthermore, the operational time of the micro-CHP unit will be extended which means more electricity generation, more energy saving and less CO_2 emission. Research has shown that micro-CHP with thermal storage can have higher overall system efficiency [75-77].

Inadequate sizing of thermal energy storage device is frequent [75]. The size of the thermal storage device is also an important consideration during the design stage of micro-CHP as it affects the economics. Large thermal storage can store more thermal energy and gives more flexibility. At the same time stray heat loss can increase as a result of which it becomes less cost effective and larger space requirement can be another problem. On the other hand, a smaller thermal storage device makes the storage process less flexible.

In domestic application with micro-CHP, a hot water tank is mostly used as thermal energy storage by increasing the temperature of water. The use of a hot water tank (HWT) with phase change material (PCM) as storage is gaining the potential. Nallusamy *et al.* [78] and Sharma *et al.* [79] have shown that HWT with PCM has potential to reduce or shift peak load demands.

3.5.2 Electrical energy storage

The effective usage of an electrical storage device can increase the usefulness of a micro-CHP system. Fluctuating electrical loads can be supplied from the electrical storage and consequently resulting in fewer disturbances on the low voltage distribution network. The

presence of an electrical storage device influences the import and export of electricity from the grid. Used effectively, storage can increase the versatility of a micro-generation system by satisfying the highly variable electrical load of an individual dwelling.

Electrical storage devices can be rechargeable batteries, flywheels and super-capacitors; rechargeable batteries being the most common. A rechargeable battery comprises three major components: the positive electrode (cathode), the negative electrode (anode) and the electrolyte, solid or liquid, which together form an electro-chemical cell. The electrodes are immersed in the electrolyte and the cell produces a voltage. Usually this voltage is less than 2 V, but several electrochemical cells connected in series provide the output voltage. Depending on the electrodes and the electrolyte, there are many different batteries such as Lead-acid, Lithium-ion (Li-ion), Nickel-metal hydride (NiMH) Sodium-sulphur (NaS) and Nickel cadmium (NiCd). Flywheels take advantage of storing electrical energy as kinetic energy. When it charges, the flywheel accelerates. When it discharges, the kinetic energy is withdrawn. There are two main types: low- and high-speed, also termed as high-power and high energy, respectively. The first type is cheaper but has a short discharge time (some seconds to a few minutes). The second type can supply energy for more time (up to an hour) but is about 100 times more expensive. The advantages of this technology are its apparent immunity to the number of cycles, the speed of charging and discharging, power rating and modularity. The drawbacks are the limited energy storage for the low-speed type and the cost of the high-speed type. In case of super-capacitor, energy is stored in the electric field produced between the two electrodes of the capacitor. Compared with normal capacitors, super capacitors make use of their particular structure to provide an outstanding capacitance. The main features are their exceptional efficiency, the performance at low temperatures, no

need for maintenance, immunity to deep discharges, speed of response, and extreme durability. Drawbacks are the high cost, high self-discharge, and low energy density.

Table 3-2 General table of technologies and their characteristics.[80]

	Lead-acid	**Ni-Cd**	**NiMH**	**Li-ion**	**NaS**	**Fly wheels**	**Super Capacitors**
Power rating (MW)	0.001-50	0.001-46	0.01 to (~)1	0.1-50	0.05-34	0.002-20	0.001-10
Discharge duration (h)	H	s-h	s-h	0.1-5	5-8	5-130	0.05-30
Gravimetric energy density (Wh/Kg)	30-50	50-75	30-110	75-250	150-240	5-130	0.05-30
Volumetric energy density (Wh/L)	50-80	60-150	140-435	200-600	150-240	20-80	100,000+
Power density (W/Kg)	75-300	150-230	250-2000	100-5000	150-230	400-1600	500-5000+
Efficiency (%)	70-92	60-70	60-66	85-90	75-90	80-99	97+
Durability (years)	5 - 15 (~10)	5-20	3-15	5-20	15	15-20	20+
Durability (cycles)	500-1200	1000-2500	200-1500	1000-10000	2000-5000	1,000,000	1,000,000+
Capital cost ($/KW)	300-600	500-1500	-	1200-4000	1000-3000	250-350	100-300
Capital cost ($/KWh)	200-400	800-1500	-	600-2500	300-500	1000-5000	300-2000
Technological maturity level (1-lower to 5-higher)	5	4	4	4	4	4	3

Similar to thermal storage, sizing of electrical storage is also important as the larger the storage the more expensive it is. Jenkins *et al.* [81] have shown that micro-generation with suitably sized storage can reduce export substantially and choosing the size of the storage should be based on the level and type of micro-generation. An electrical energy storage system has economical as well as technical advantages. Economical: electricity will not be sold cheaply and can replace the import of expensive electricity from grid; technical: the

effect on the grid due to export of electricity can be minimized. However the capital cost of the electrical storage is high.

Lead-acid batteries are considered common for storing of onsite generations, however their capacity degrades with continuous charge and discharge cycles and thus affects the lifetime of the battery [81].

Chapter 4 Thermal Modelling of Building and Heating Systems

4.1 Introduction

When developing strategies to minimise the energy consumption within the building, it is crucial to understand the dynamics of energy generation, transfer and loss. Recently, simulation of building thermal performance using different software has been an active area of investigation in order to identify the measures to minimise the heating demand of the building and improve carbon emissions. Over time, the simulation domain has grown richer and more integrated with tools integrating simulation of heat and mass transfer in the building fabric, airflow in and through the building, daylight and a vast array of system types and components. Yet, at present, there are still many difficulties to answer with available simulation tools.

Dynamic thermal modelling is an advanced way to simulate the thermal environment of a building and so requires a description of all energy paths. A thermal model of a building represents the actual heat loss and generation within the building. In order to analyse energy loss from a building, three modes of heat transfer must be considered. These modes are radiation, conduction, and ventilation. Heat loss due to heat flow from a hot region to a cold region through walls and windows are conduction losses. Whereas, direct movement of hot air out of the building through cracks and gaps as well as deliberate ventilation is the losses that come under ventilation. Heat loss due to conduction and radiation involves a temperature difference; the standard method of modelling such heat losses is to make heat

flows proportional to the temperature difference between the two regions. The main source of heat within the building is the heating system and the sunlight coming through windows. The effect of a building's occupants, cooking and heat dissipated by the electrical appliances can also be sources of heat. Climatic data, location of building, building structure and constructions and occupancy pattern are the factors that determine the heat loss from the building to the surroundings.

In the precise area of building thermal modelling, issues of model accuracy and computational efficiency becomes important. In recent years, significant progress has been made for investigating the thermal behaviour of buildings and its associated heating and ventilation systems. A number of modelling software tools, available commercially and free of charge, already exist to simulate the individual component and of whole buildings [82]. These tools were developed for comprehensive analyses of the dynamic energy balance in buildings and are appropriate for evaluation of standard building designs but not suitable for analysis of innovative components, such as building integrated heating and cooling systems [83]. A different modular modelling approach is used by TRNSYS. Strand *et al.* [85] discussed differences between modular modelling approach and integrated modelling approach and concluded that the major shortcomings of building energy simulation programs have been, so far, the inability to accurately model HVAC system that are not considered standard. The advantage of a modular approach is that new components can easily be included, if necessary. This approach is used in this research to represent the building envelope and modules represents walls, window, heating system, gains, ventilation and the air within the building.

4.2 Building Thermal Model Input Variables

The energy balance within the building can be influenced by many factors: weather, casual heat gains, the heating system and building design and construction as shown in Figure 4.1.

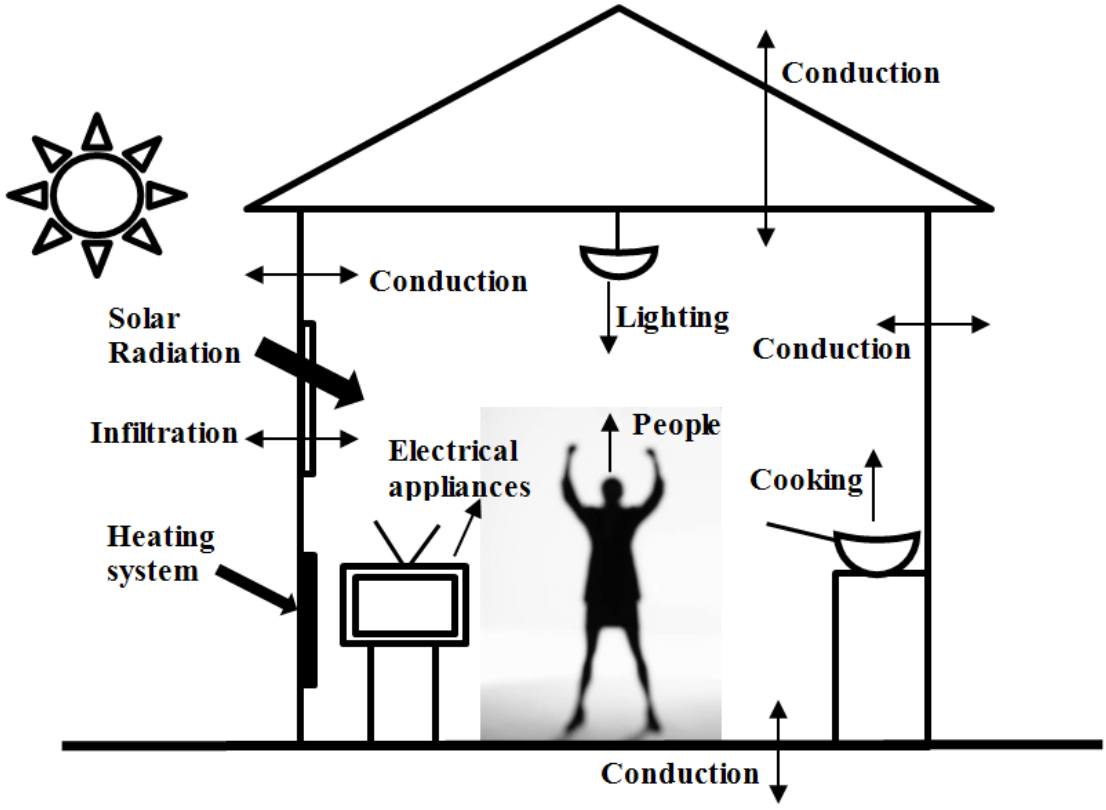

Figure 4.1 Building energy balance

Solar gain to the building space is mostly through the windows by direct radiation. It depends on site-specific factors and dynamic factors. Site specific factors consist of surface area, angle of tilt of window, composition of glass in windows, orientation of the building, geographical location of the site and any local shading factors. Dynamic factors include time of the year, prevailing cloud conditions and the existence of any adjustable shading mechanisms such as internal blinds. Maximum gain through vertical south-facing windows

in the northern hemisphere tends to occur in spring and autumn when the sun-angle is low. With careful window and shading design, the solar gain can assist in winter heating whilst giving minimum nuisance overheating in summer.

Little solar heat reaches the internal part of external walls and roof due to the high thermal capacity of heavy construction which tends to delay the transmission of the heat. So, the solar heat gains through the roof and external walls are considered negligible.

According to the ISO 13790 [86] standard, "Internal heat gains, heat gains from internal heat sources, including negative heat gains (dissipated heat from internal environment to cold sources or sinks) consist of any heat generated in the conditioned space by internal sources other than the energy intentionally utilised for space heating, space cooling or hot water preparation". The internal heat gains include: metabolic heat from occupants and dissipated heat from appliances; heat dissipated from or absorbed by hot water, cold water and sewage systems; heat dissipated from lighting devices; heat dissipated from or absorbed by heating, cooling and ventilation systems; heat from or to processes and goods. Casual heat gains or internal heat gains can be sensible or latent heat gain. The major sources of internal heat gains being the occupants (sensible and latent), electrical appliances (sensible), cooking (sensible and latent) and lighting (sensible). Numerical models of the building created for the simulation calculations of energy balance, often based on the assumption that internal heat gains are constant over time, or only part of them is changing. Values of the heat gains are calculated on a basis of coefficients referring to living area.

4.3 Building Model

Different approaches to model the heat flow in the building can be found in the literature such as lumped parameter method, finite element or finite difference method and impulse response method. Lumped parameter methods, through its simplicity, have established themselves as computationally efficient approach that can give sufficient accuracy for short time horizon investigations. In this work, a lumped-parameter building modelling method is used. This has the advantages of relative simplicity (and, hence, reduced computational time) whilst also allowing a full treatment of the dynamic characteristics of the building energy flows to be captured.

Modelling based on first-order lumped capacitance elements is useful for certain types of simplified problem solving but breaks down in certain instances, in particular when modelling heat transfer through high thermal capacity elements. A high-order lumped parameter method used for the building envelope has the advantage of providing sufficient accuracy and rigour to capture a wide range of transient effects. The method proposed by Gouda *et al.* [87] through the use of constrained optimization is adopted which considers a second order element for each significant thermal capacity pathway. The second order lumped parameter method retains the simplicity, has excellent computational efficiency and overcame the problems associated with the heat transfer through high thermal capacity elements.

Any construction element consists of several layers of different materials, each material having its own thickness, specific heat capacity, thermal conductivity and density. These construction elements can be represented as ‘lumped’ thermal resistances and capacitances

and can be represented as equivalent electric R-C circuits as shown in Figure 4.2. This circuit can represent a wall, floor or roof of n layers using two capacitors, C_i, C_o and three resistors R_i, R_m and R_o. These five parameters of the second-order element may be adjusted such that the response of the element is nearly identical to that of a fully distributed element with equivalent overall thermal resistance, *R*, and thermal capacitance, *C*. Gouda *et al.* [87] suggest a minimum of 20 layers for a typical multiple layer construction element would yield a most accurate outcome at least from a modelling point of view. The parameter adjustment was then treated using optimisation that can be stated as follows.

If the overall element resistance and capacitance can be expressed as:

$$\begin{aligned} R_i &= x_i R \\ R_m &= x_m R \\ R_o &= x_o R \\ C_i &= y_i C \\ C_o &= y_o C \end{aligned} \qquad \text{Eqn. 4.1}$$

then:

$$\begin{aligned} &\text{Minimise: } f(\varepsilon) \\ &\text{Subject to: } x_i + x_m + x_o = 1 \\ &x_i; x_m; x_o \geq 0 \\ &y_i + y_o = 1 \\ &y_i; y_o \geq 0 \\ &L_{bound} \leq \varepsilon \leq U_{bound} \end{aligned} \qquad \text{Eqn. 4.2}$$

in which the single object function, *f(ε)*, is the square root of the sum-square error between the distributed and second order elements and L_{bound} and U_{bound} are the lower and upper tolerance bounds respectively on ε. In the work reported by Gouda et al. [87] the Kuhn–

Tucker system of Lagrange multipliers was used as a basis for cancelling gradients between the objective function and active constraints at solution points. Though each construction element type needs to be uniquely parameter-fitted to use this method, results for a wide range of construction types show only moderate variation in results.

The equations for this second-order approach to element modelling are as follows

$$\frac{dT_s}{dt} = \frac{1}{y_i C}\left[q_{rad} + \frac{(T_i - T_s)}{x_i R} - \frac{(T_s - T'_s)}{x_m R}\right]$$

$$\frac{dT'_s}{dt} = \frac{1}{y_o C}\left[\frac{(T_s - T'_s)}{x_i R} - \frac{(T'_s - T_o)}{x_o R}\right] \qquad \text{Eqn. 4.3}$$

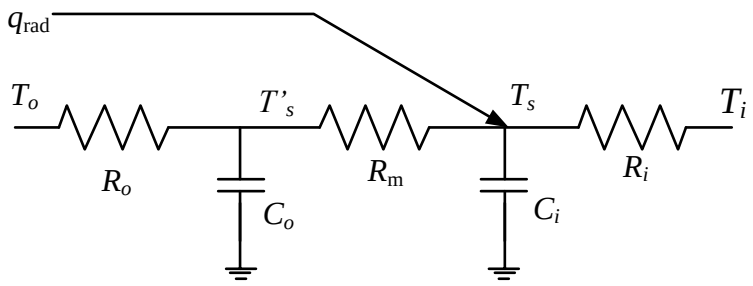

Figure 4.2 Second-order lumped-parameter construction element

Energy balance about each element can be written as second order matrix differential equations, as given by Eqn. 4.4 for the external wall element [88].

$$\begin{bmatrix} \dot{T}_s \\ \dot{T'}_s \end{bmatrix} = \begin{bmatrix} -\frac{1}{RC(x_i y_i + x_m y_i)} & \frac{1}{RCx_m y_i} \\ \frac{1}{RCx_m y_o} & -\frac{1}{RC(x_m y_o + x_o y_o)} \end{bmatrix} \times \begin{bmatrix} T_s \\ T'_s \end{bmatrix} + \cdots$$

$$\ldots \begin{bmatrix} \frac{1}{RCx_i y_i} & \frac{1}{Cy_i} & 0 \\ 0 & 0 & \frac{1}{RCx_o y_o} \end{bmatrix} \times \begin{bmatrix} T_i \\ q_{rad} \\ T_o \end{bmatrix} \qquad \text{Eqn. 4.4}$$

Where the resistance (R), capacitance (C) and 'rations' ($x_{i,m,o}$; $y_{i,o}$) are obtained using the method described by Gouda *et al.* [87].

Eqn. 4.1 can be readily and efficiently represented in Simulink using a state-space block. Further details of the application of the method can be found in [89].

Along with the building elements, building space is modelled by two first order equation representing air moisture and room air temperature and a simple air change ventilation model is incorporated.

Figure 4.3 illustrates the relationship between the various energy transfer paths in the building space using a lumped parameter methodology.

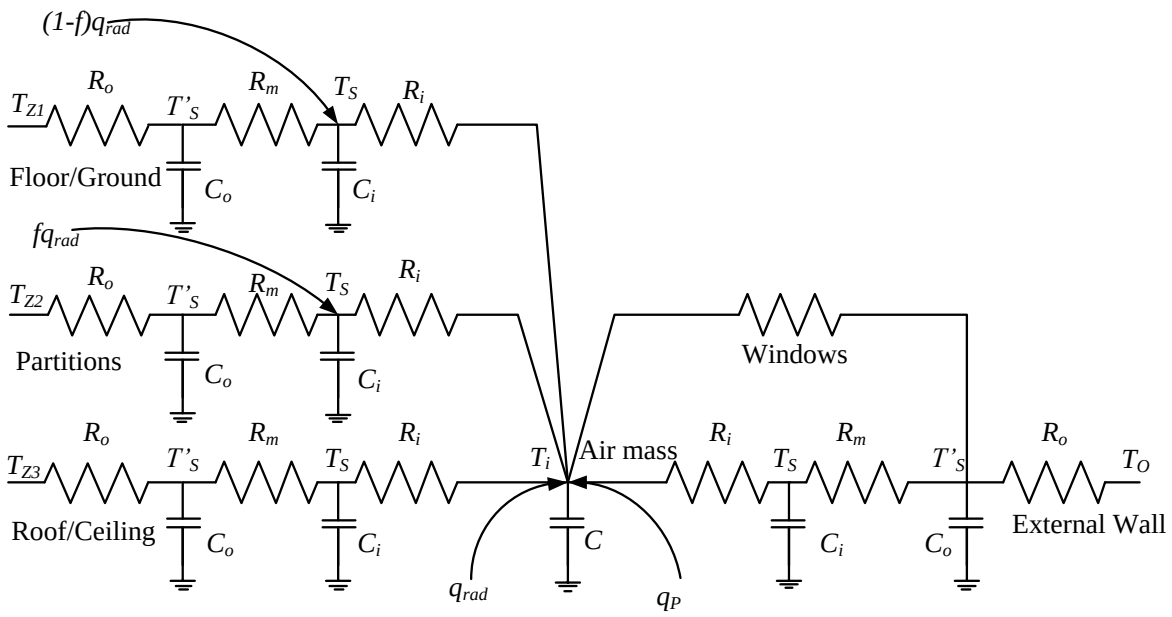

Figure 4.3 Simplified building energy transfer paths

Where, *T*, *C*, *R* and *q* represents temperature, thermal capacity, thermal resistance and heat inputs respectively. Subscripts *z*, *i*, *o*, *rad* and *p* represents zone, internal, outer, solar and heating system respectively.

In order to maintain the internal temperature (T_i), the heat input only from the heating system (q_p) is controllable through changing the flow rate of hot water or changing the temperature of hot water. In this study, the heat gain from solar radiation coming through the window is assumed to be constant with time, although in reality this may be controllable using the blinds or curtain.

4.4 Solar Radiation Model

In the proposed modelling, weather data is based on measured data from weather stations. The solar radiation measurements from such stations tends to be global horizontal irradiation

(i.e. the combination of direct and diffuse radiations measured on the horizontal plane). Therefore to estimate the incident solar irradiation on a surface at any orientation, estimations of the diffuse and direct fractions of incident radiation on the horizontal plane are required. Then from these values, an estimate of incident radiation on a tilted surface may be made.

For this purpose, two algorithms were combined. Firstly, the diffuse and direct fractions were estimated from the measured global solar radiation by using the algorithm presented by Skartveit and Olseth [90]. The obtained estimated results were then used to determine the radiation incident on a building surface by using the algorithm of Liu and Jordan [91] as presented in [92]. The solar irradiation model does not consider any blinds, curtains or internal shading devices. All radiant sources (both short wave and long wave) are assumed to be distributed uniformly to all opaque room surfaces with the exception of the direct component of solar radiation which is assumed to be absorbed by the floor surface only.

4.5 Heating System Model

The current practice for heating buildings is through hot water emitters which are controlled by a valve. There are three possible ways to control the heat emitted from the emitter in order to heat the room: variable flow-rate constant temperature, constant flow-rate variable temperature and variable flow-rate variable temperature. In most of the domestic applications, hot water supplied from a central boiler is delivered at constant temperature and the valve controls the water flow rate through each emitter. Valves of this type are often referred to as ‘thermostatic radiator valves’ though they mostly provide a continuous adjustment of flow. For the emitter, Underwood and Yik [88], suggest that a satisfactory

trade-off between accuracy and computational cost for most heat emitters can be achieved with a third-order model (Figure 4.4).

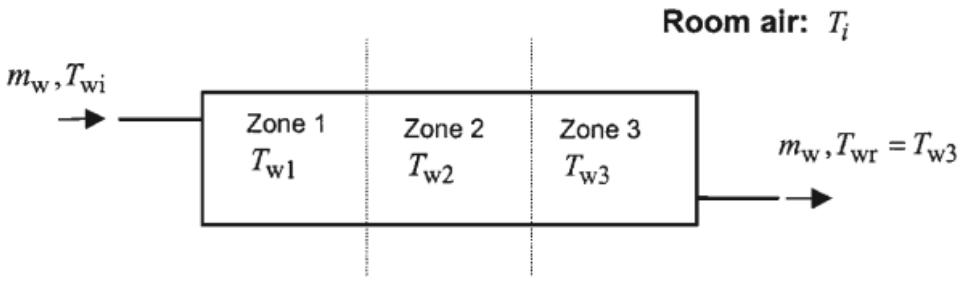

Figure 4.4 Third order room emitter

A general third-order model for an emitter can be written as:

$$C_W \frac{dT_{w1}}{dt} = 3m_w c_p(T_{Wi} - T_{W1}) - K_e(T_{W1} - T_i)^n \qquad \text{Eqn. 4.5}$$

$$C_W \frac{dT_{w2}}{dt} = 3m_w c_p(T_{W1} - T_{W2}) - K_e(T_{W2} - T_i)^n \qquad \text{Eqn. 4.6}$$

$$C_W \frac{dT_{wr}}{dt} = 3m_w c_p(T_{W2} - T_{Wr}) - K_e(T_{Wr} - T_i)^n \qquad \text{Eqn. 4.7}$$

Where, C_w is the overall thermal capacity (includes the radiator material and water), K_e is the overall heat transfer coefficient of the emitter and n is the heat transfer index (typically 1.3 for convector-radiators and 1.5 for pure convector).

In a heating system, a valve can have two purposes: to isolate different parts of the system and to enable the regulation of water flow. For heating control applications, valves are used to regulate the heat transfer through changing flow rate.

For liquids, modelling of control valves are generally based on expressing the relationship between the position of the valve stem and the flow rate passed by the valve; the valve characteristics [93]. Thus, a valve can be expressed by an inherent characteristics G_{inh} (effect of connected system not present), leading to an installed characteristic G_{ins} (effect of connected system included). The inherent characteristics can be expressed as a linear or equal percentage as follows [94]:

$$G_{ins} = [1 + N(\frac{1}{G_{inh}^2} - 1)]^{-1/2} \quad \text{Eqn. 4.8}$$

$$\text{Linear: } G_{inh} = G_o + u(1 - G_o) \quad \text{Eqn. 4.9}$$

$$\text{Equal Percentage: } G_{inh} = G_o^{(1-u)} \quad \text{Eqn. 4.10}$$

Where, G_o is the let-by (can be obtained from manufacturer), the valve authority '*N*' can be assumed between 0.3 and 0.5 inclusive, and u is the stem position.

The "let-by" refers to the closure flow rate arising from the need to maintain a small clearance between plug and port. Valve authority is the ratio of the pressure drop across fully open valve to the pressure drop across the whole circuit. In this work, an equal percentage valve characteristic is assumed.

4.6 Model Implementation

In the UK, one of the most common types of house is a semi-detached house, which accounts for 26 % of total housing stock [95]. This forms the basis for a case study of a two floor semi-detached house located in Newcastle upon Tyne facing predominantly south with three bedrooms and a gross floor area of 94 m^2, as shown in Figure 4.5.

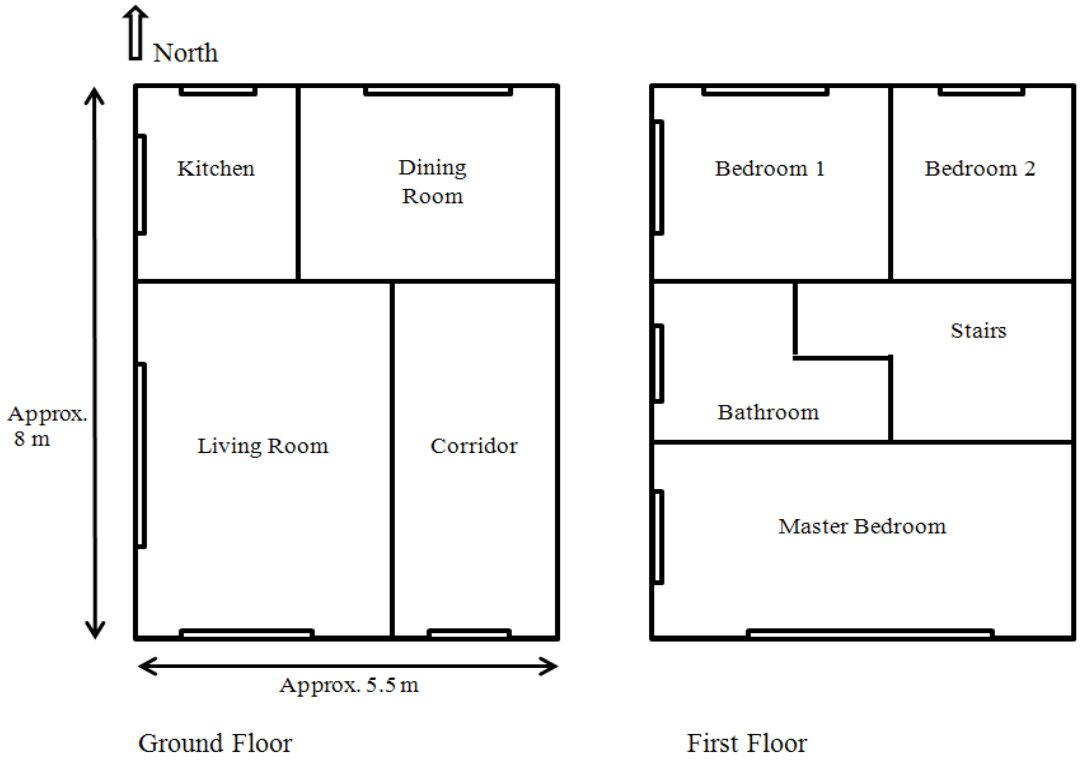

Figure 4.5 Plan view of semi-detached house

The combined building model, solar model and heating system model were applied to the case study. It is assumed that the double glazed house is occupied by medium size family of four members: two adults (working full time) and two children (of school age) with active occupancy (when occupied and awake) pattern for weekdays and weekends, as given in Table 4-1.

Table 4-1 Active occupancy pattern

Days	**Active Occupancy Period**	
weekdays	07:00 – 09:00	17:00-23:00
weekends	08:00 – 23:00	

On the basis of designed temperature i.e. heating requirement, the whole house is divided into three separate zones. All three zones are heated and controlled. First zone, Zone 1 refers to the living room and is set to an internal design temperature of 21 °C. Second zone, Zone 2, refers to the three bedrooms and is designed at 16 °C. Third zone, Zone 3 (referred as balance zone) is the rest of the house which is designed at 18 °C. This is a common assumption for domestic energy modelling in the UK [96]. The house constructions were assumed to be in accordance with typical recent construction standards as set out in the UK's National Calculation method database [97] and the UK Building Regulations, Part L 2006. The internal casual heat gain were based on those used by Anderson *et al.* [96]. The house was assumed to be ventilated at an average rate of 0.5 air change per hour (including external air infiltration) with respect to the whole house volumes. A typical International Weather for Energy Calculations (IWEC) weather data file for the north east of England (Finningley) [98] was used. International Weather for Energy Calculations (IWEC) contains "typical" weather files, suitable for use with building energy simulation programs outside Canada and the USA. The IWEC files contain hourly weather observations such as dry bulb temperature, dew point temperature, wind speed, and wind direction and present at least 12 years of record up to 25years. These files are derived from Integrated Surface Hourly (ISH) weather data originally archived at the National Climatic Data Centre. The ISH database

does not contain measured solar radiation, so the hourly total horizontal solar radiation is calculated using an empirical model based on the sun-earth geometry, reported cloud cover, temperature difference from three hours previously, relative humidity, and wind speed [98].

The control of the central heating system is a time-led operation that follows the heat demand in a house, which is defined by the occupancy pattern. Thermostatic radiator valves are used to modulate the output of individual radiators to match the desired temperature of the room. It uses the principle of thermal expansion with a mechanism to steadily close the valve as the room approaches the desired temperature. This mechanism is modelled by using the air temperature block and valve block.

Figure 4.6 shows the air temperature of the three different zones with internal gains but no heating for a week. It can be seen that the temperature of the bedroom, which has larger window and facing north, increases faster than others zone when the solar radiation comes into effect and decreases as the solar radiation reduces. In this model it is assumed that the ground temperature is 14 °C and constant so the temperature of the living room and balance zone (most part is on the ground floor) is higher than the temperature of the bedroom which is on the first floor.

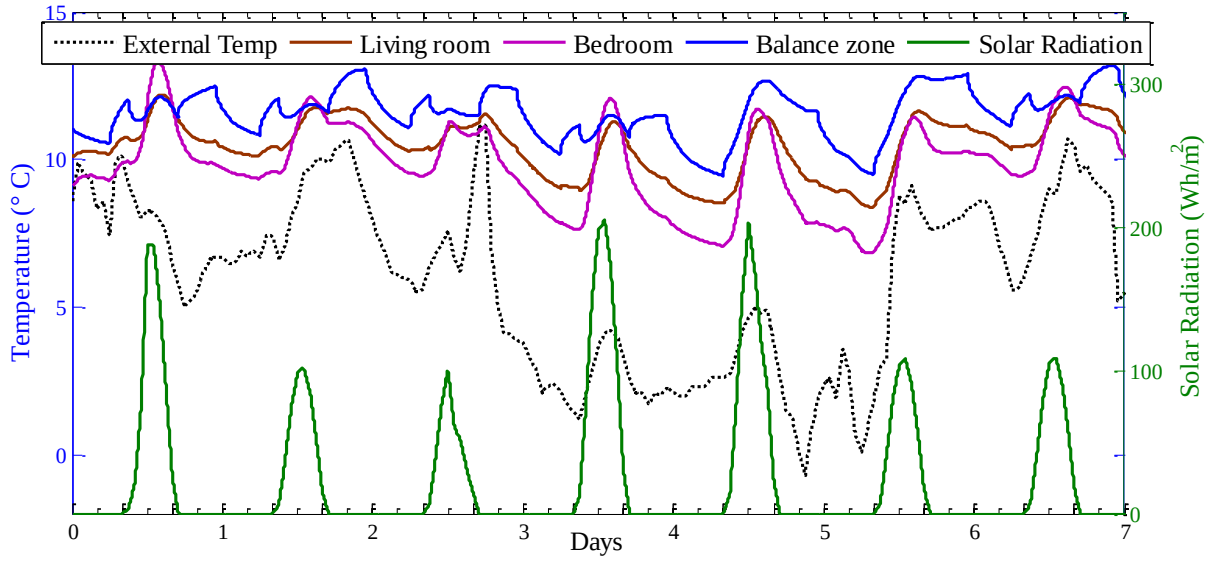

Figure 4.6 Zone air temperatures with no heating

Similarly, Figure 4.7 shows the temperature of the three zones for a week (in which day 5 and 6 are weekends) when the heating comes into effect along with the corresponding external air dry bulb temperature and global (horizontal) solar radiation. The heating system is controlled on the basis of occupancy pattern and the desired set temperatures. The heating system uses variable flow constant temperature strategy, in which room temperature sensor (usually placed in lobby) and the control valve seeks to vary the hot water flow rate into the emitter in response to room temperature to obtain the desired temperature. In the application given here, the house is occupied intermittently during the weekdays. Thus two characteristic peaks in zone temperature can be seen for each day for morning and evening periods during which the house is occupied often with a free float mid-day. Slight rise in temperature during the mid-day is due to the increase in solar radiation. More detail of Figure 4.7 is shown in Figure 4.8 for weekdays and a weekend.

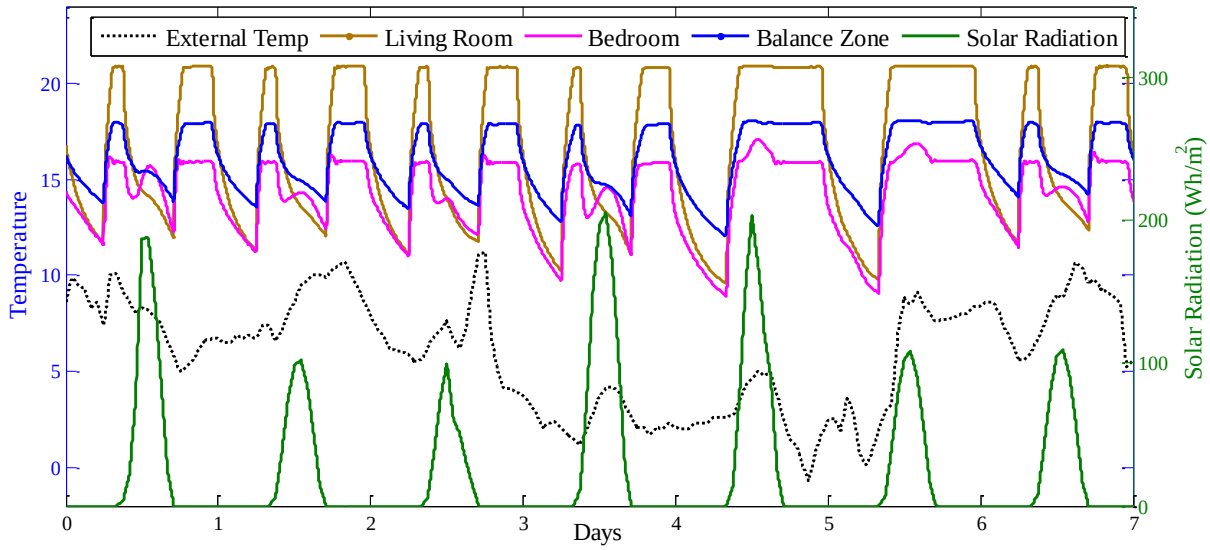

Figure 4.7 Zone air temperatures for a week

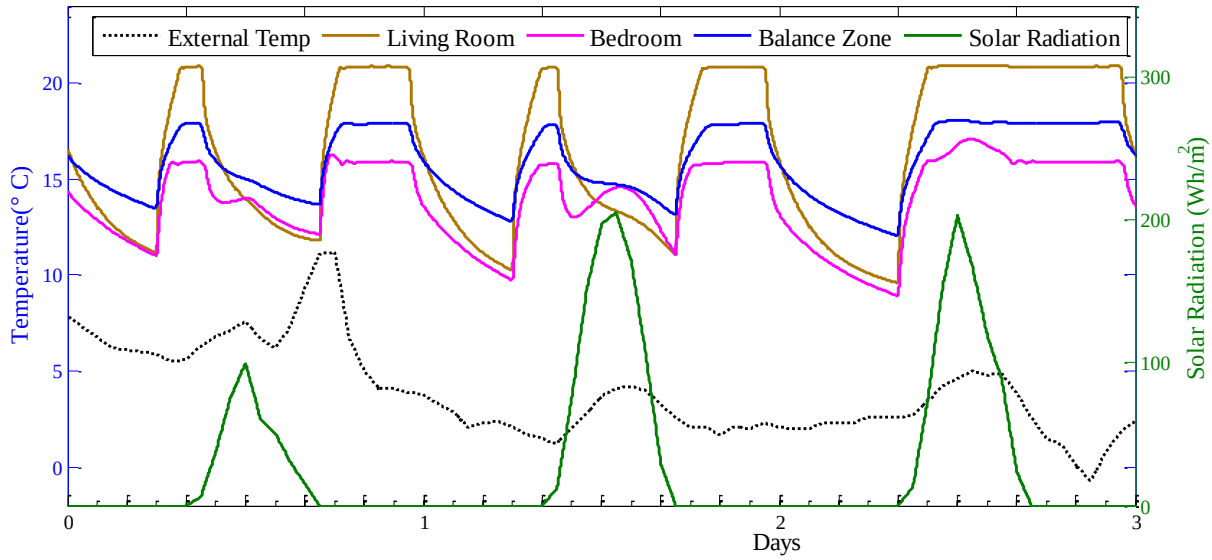

Figure 4.8 Zone temperatures for weekdays (1&2) and weekend (3)

Figure 4.9 shows the amount the heat emitted by the emitter to maintain the desired set temperature in three zones along with external temperature and global solar radiation. More detail is shown in Figure 4.10 for weekdays and a weekend. As the desired set temperature for living room is the highest (21 °C), the heat emission in the living room is greater than the

other Zones. Point to note here is that on day 5 and 6, which are weekends and heating is 'on' all day from morning to night, when solar radiation comes into effect, the room gets heated so the heat emitted by the emitter reduces during mid-day. The heat demand for one winter week of the living room, bedroom and balance zones are 60.2 kWh, 42.54 kWh and 39.5 kWh respectively.

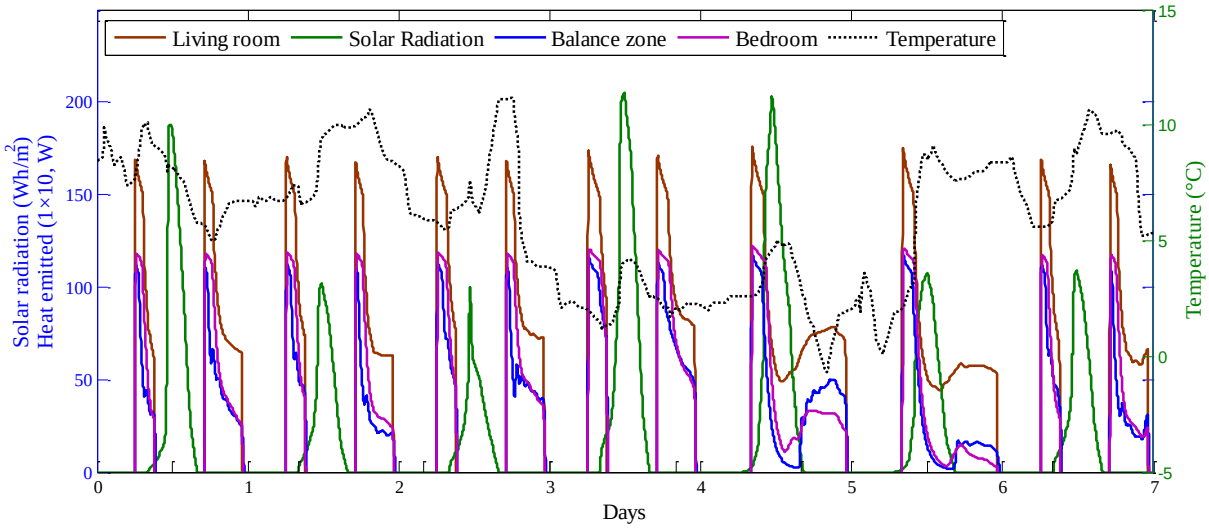

Figure 4.9 Heat emitted in three zones

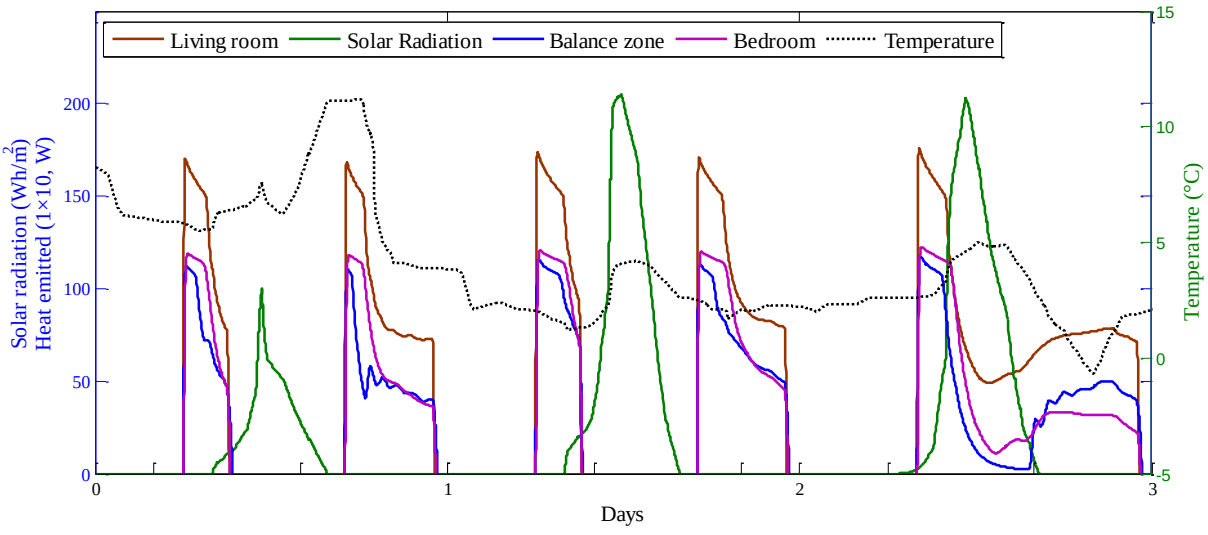

Figure 4.10 Heat emitted for weekdays (1 & 2) and weekend (3)

4.7 Model Verification

A verification test is essential for the improvement in the quality of a model and to boost the confidence in the predicted results. There has been much effort done at the International Energy Agency (IEA) [99], the American Society of Heating Refrigeration and Air-Conditioning Engineers (ASHRAE) [100] and others to create methodologies, tests and standards to verify the reliability and accuracy of building models. Bowman and Lomas [101] have proposed three validation methods: Analytical verification, Empirical validation and Comparative testing.

In analytical verification, exact known solutions are compared with the model predicted values. This type of verification has limited application and is useful for investigating errors in algorithms.

Empirical validation compares a program's prediction with monitored data. The monitored data can be based on experiment tests or measured in a real environment. In principle, this method gives real world results restricted by the reliability or comprehensiveness of the measurements. This approach is limited due to the complex and expensive design and operation of experiments.

In comparative testing, a program is compared to other programs. This includes both sensitivity testing and inter-model comparisons. Results from two or more programs are compared (with identical inputs) in inter-model comparison. This method of testing enables an inexpensive comparison at different levels of complexity. However, in practice the difficulties in matching the program inputs can lead to a significant uncertainty in performing inter-model comparisons.

In this work, the inter-program comparative testing is used to validate the thermal house model developed and as a diagnostic tool to identify the errors associated with the implementation of the model. The results obtained from the model developed in Matlab are compared with the results obtained from the Design Builder software. Design Builder forms an interactive front-end and uses EnergyPlus for the energy calculations. In turn, EnergyPlus has been tested against the IEA Building Energy Simulation Test (IEA BESTest) building load and HVAC tests.

A two storey, three bedrooms, semi-detached house was built in Design Builder with identical construction elements for the building envelop. Activities and internal gains in Design Builder are scheduled as occupancy pattern. Design Builder has the ability to merge different rooms in a house to be considered as a single zone giving out single temperature for a zone. Figure 4.11 shows the comparison of air temperature of the balance zone obtained from the developed Matlab/Simulink model and from Design Builder without a heating system, for a week period. The pattern of air temperature in the balance zone obtained from Simulink gives a reasonable comparison with that of Design Builder with the difference in temperature of 1°C at few points. Similarly, Figure 4.12 shows the comparison of air temperature of the balance zone when the heating system is turned ‘on’.

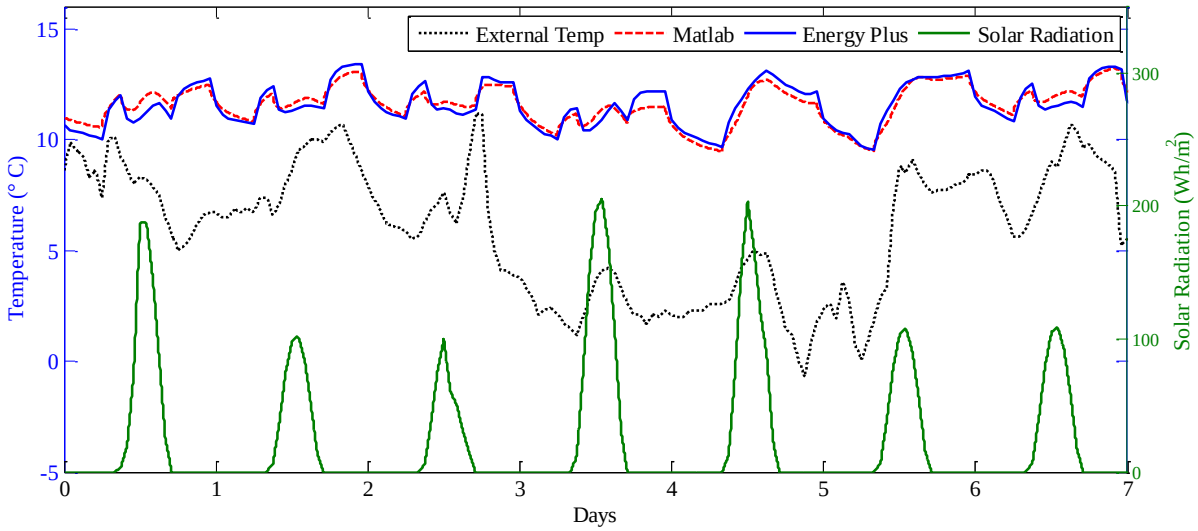

Figure 4.11 Comparison of balance zone air temperature without heating

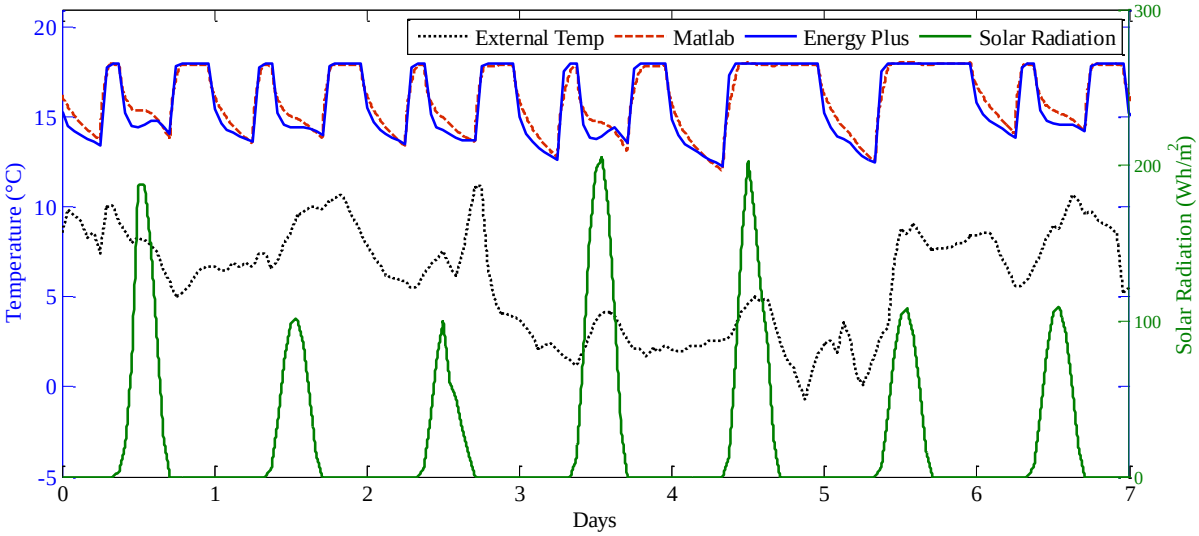

Figure 4.12 Comparison of balance zone air temperature with heating

Figure 4.13 and Figure 4.14 shows the patterns of air temperature in the living room without heating and with heating respectively. As can be seen, the Simulink model consistently under predicts the temperature of the living room which is due to the heat coming from

ground. The influence of heat coming from the ground to the balance zone is not significant as the volume of the balance zone is much larger than that of living room.

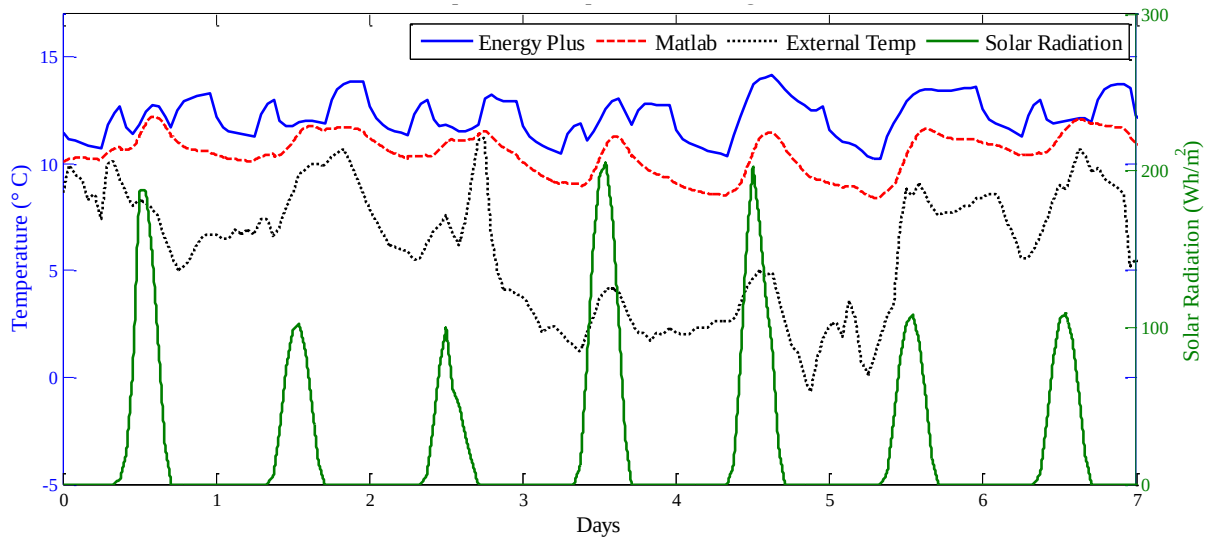

Figure 4.13 Comparison of living room air temperature without heating

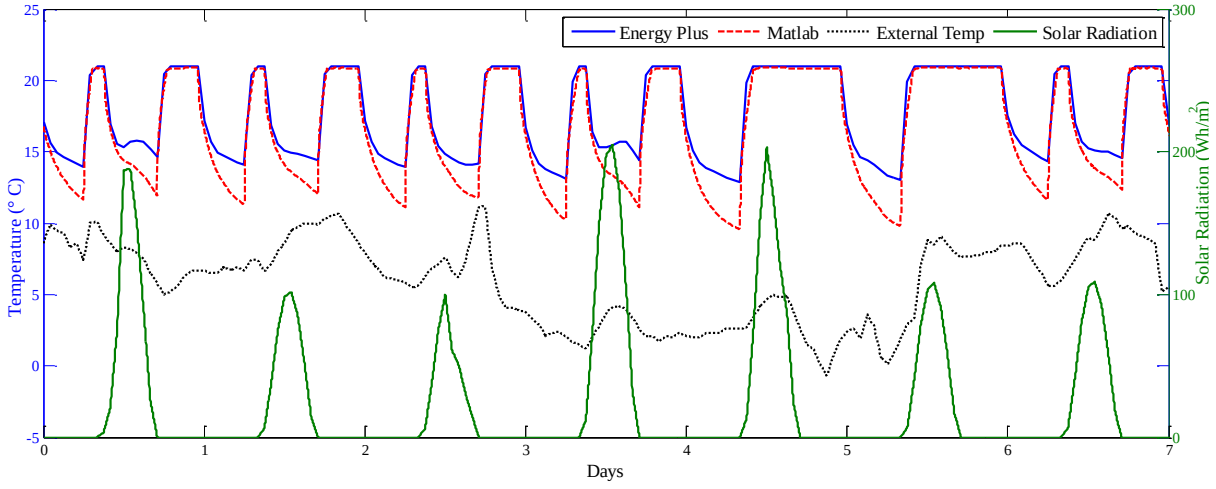

Figure 4.14 Comparison of living room air temperature with heating

Chapter 5 Modelling of Distributed Generation and a Typical Low-Voltage Network

5.1 Introduction

This chapter presents details of the mathematical modelling of different distributed generators that could be installed in a house and a typical low-voltage (LV) distribution network in the UK. Distributed generators include the Stirling Engine based micro-CHP, micro photovoltaic and wind turbine systems.

A mathematical model is the way to describe the system and its performance using mathematical concepts. Mathematical modelling has many advantages such as precision, concise language with well-defined rules. However, it is not always possible to model the real world due to its complication and any small change in structure of equation may results in different outputs.

5.2 Stirling Engine Micro-CHP Modelling

For dynamic simulations of micro-CHPs, it is necessary to treat the problem rigorously because these systems tend to exhibit quit long run-up time. Whilst having the advantage of generic applicability, a rigorous theoretical approach will lead to a complex model requiring high computational power for its solution and would also most likely to require at least some parameterisation from empirical data. Such is the case with the model developed by Lombardi *et al.* [48] for Stirling engine based micro-CHP. In situations where experimental transient response data are available it is suggested that an empirical model fitted to such

data is a preferred choice on the grounds of computational cost (i.e. relative model simplicity) and accuracy. This is the approach adopted in this work.

5.2.1 Experimental setup

A transient response test was carried out on Whispergen, a natural gas-fired domestic micro-CHP module, discharging into hot water panel radiators or domestic hot water and local electricity network in laboratory conditions as shown in Figure 5.1. The laboratory heating system test rig was configured using conventional panel radiators with a combined capacity similar to what might be found in a typical family house in the UK. The test micro-CHP module has a nominal rated capacity of 6 kW (thermal output) and 1 kW (single phase power output). The test rig installation included:

- A 120 litre domestic hot water (DHW) storage cylinder for the production of hot water via a 3.5 kW internal indirect water/water coil heat exchanger. The cylinder also incorporated a DHW cylinder thermostat for 'on/off' DHW temperature control.
- An open vented, gravity fed, hydronic circuit.
- Implementation of a UK standard 'W' plan control system incorporating:
    - A 3-way mid-position control valve for direction of engine coolant into respective components of the space heating or hot water cylinder circuits.
    - A room thermostat.
    - A programmable controller to provide independent 'on' and 'off' for space and DHW heating schedules.
- Two heat meters; one in the DHW cylinder heating coil circuit and one in the space heating circuit (4 radiators).

- PC for data logging from the Whispergen engine management system.

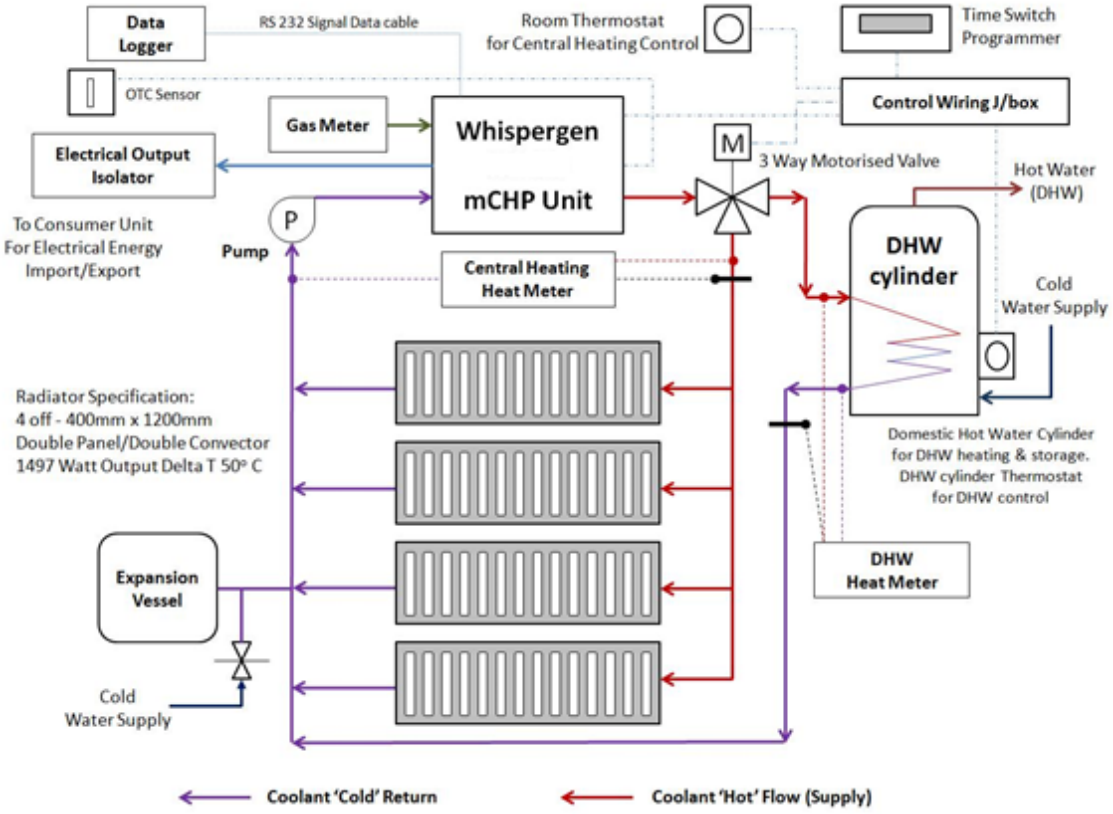

Figure 5.1 Micro-CHP system test rig [102]

5.2.2 Modelling

After running the test rig for several hours electrical and heat generated by the micro-CHP was collected. Inspection of the data suggested that a transfer function of the following form could be fitted as in Eqn. 5.1.

$$G(s) = \frac{Ke^{-t_d s}}{(\tau s + 1)} + \varepsilon(s) \qquad \text{Eqn. 5.1}$$

Where *G(s)* is a transfer function expressing the response in power output or heat output of the micro-CHP module, *K* is the gain, t_d is a pure time delay, τ is a time constant and $\varepsilon(s)$ is a uniformly distributed error term.

Fitted parameters to Eqn. 5.1 for the test module are given in Table 5-1.

Table 5-1 Model parameters for the test case micro-CHP module

State	K (kW)	τ (s)	t_d (s)
Switch on – heat	6	91.4	60
Switch on – power	1	131.4	120
Switch off – heat	4	161.4	0
Switch off – power	0	-	-

The error term reflects a random pattern of variance about a nominal mean and mainly arises from variation in the heating water flow rate. Such variations are evident in most flow measurements of this kind due to small variations in pump operating condition and the presence of small bubbles of air etc. and cannot generally be individually explained in detail. This was modelled in the time domain as a Gaussian random number sequence with a mean of zero and variance equal to the standard deviation of the heat output value or power output value with respect to their respective mean values during the steady load period of the response. The Simulink models of micro-CHP with heat and power components are shown in Figure 5.2.

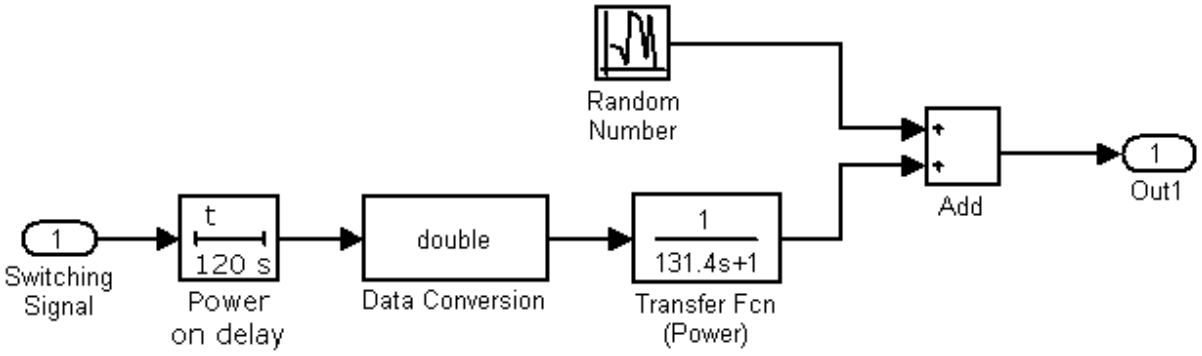

(a) Power component

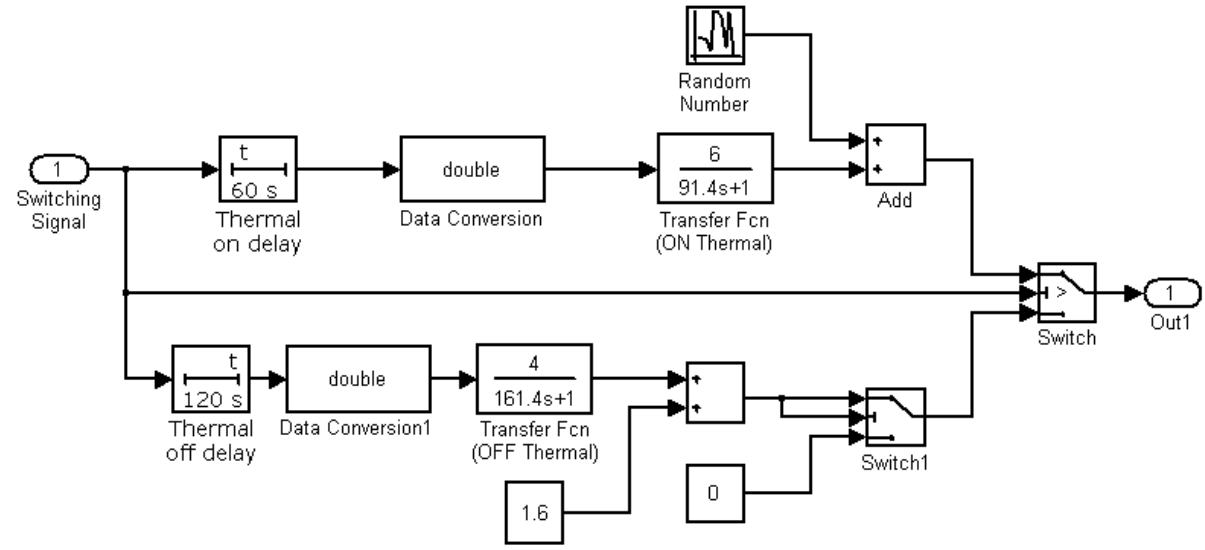

(b) Heat component

Figure 5.2 Simulink model of micro-CHP (a) Power component (b) Heat component

5.2.3 Results

Results of the test including the fitted model response data are given in Figure 5.3 and Figure 5.4. The data to which the model was fitted reflects a cold-start situation in which the laboratory air (and the heating emitter water contents) was at an initial steady temperature of approximately 18°C.

Figure 5.3 compares the actual electrical and thermal output from the test rig with the modelled output for electrical and thermal respectively. Similarly, Figure 5.4 shows a comparison of the temperature of the coolant coming out of the micro-CHP unit. These graphs show good agreement between the actual measurements and the modelled results. The root mean square error between the actual data and modelled data for thermal output, electrical output and coolant temperature are 0.143, 0.023 and 0.24 respectively.

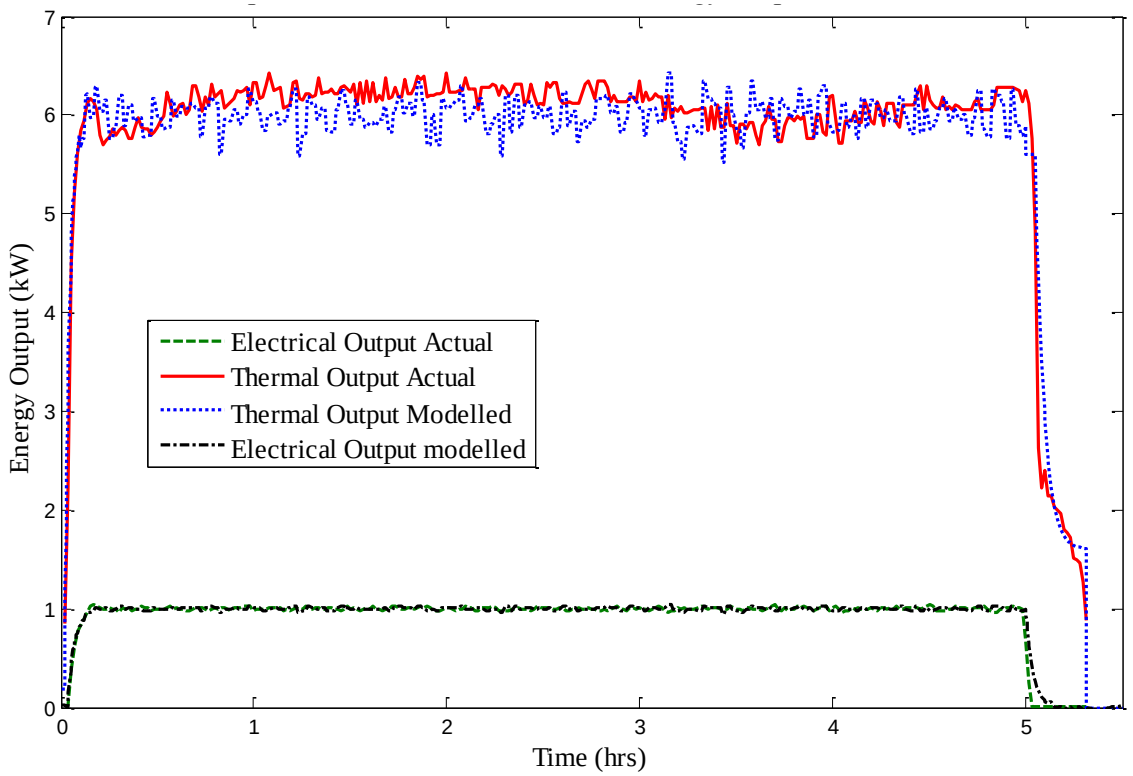

Figure 5.3 Fitted model to micro-CHP data

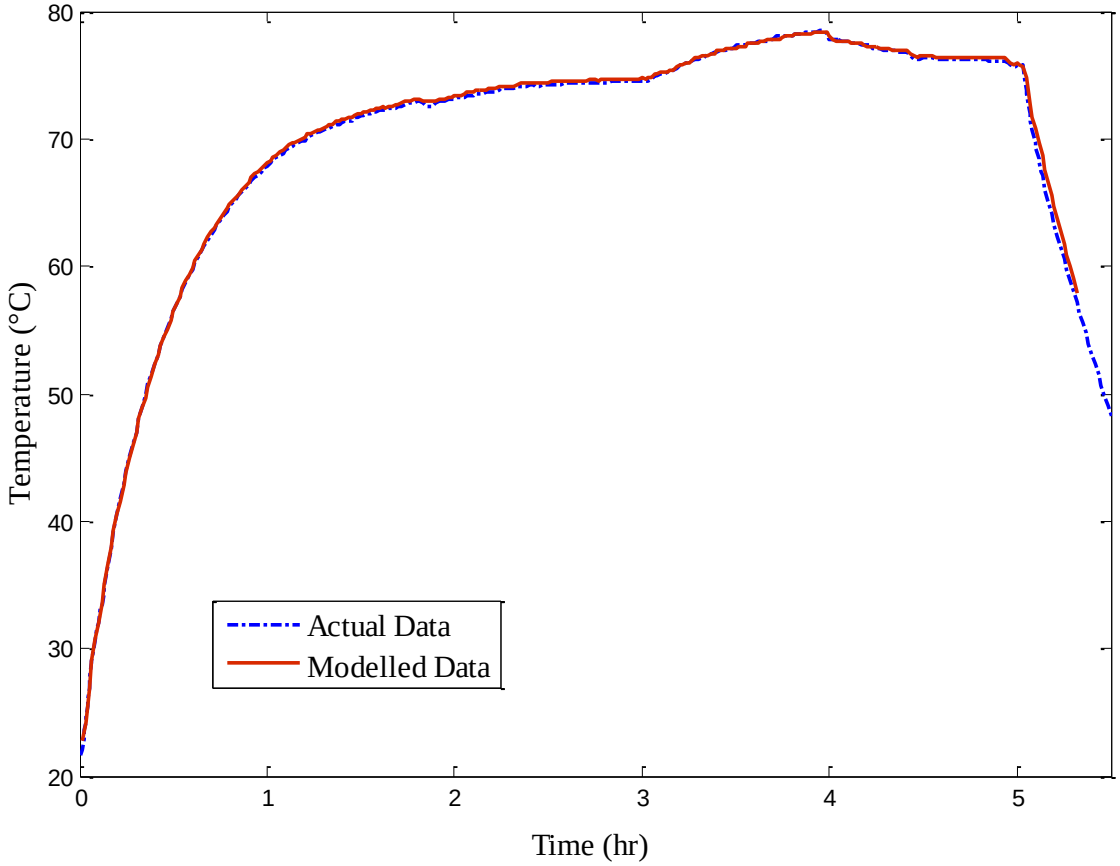

Figure 5.4 Comparison of coolant outlet temperature

5.3 Photovoltaic (PV) Modelling

In this section, modelling of PV cell using equivalent circuit (Shockley diode equation) and methodology to evaluate both the IV characteristics and MPPT of the PV system with various environmental conditions such as temperature and solar radiation are presented. To ensure the accuracy of the model, the simulation results obtained are compared with available commercial data sheets.

5.3.1 Modelling

Photovoltaic modelling primarily involves the estimation of the non-linear I-V curves (refer to Figure 3.6). Many other different models can be found in the literature which includes characteristics of the model when subjected to environmental variations such as changes in irradiance and temperature. The simplest model is the single diode model, which consists of a current source representing the ability of the cell to produce the current when exposed to light and a diode representing the p-n junction. In addition to the single diode, the model includes a series resistance, R_s, [103] representing the resistance between the silicon, electrical conductor and the surface of the cell and a shunt resistance, R_p, representing energy losses due to the imperfection of the cell [104] .

The single diode model is based on the assumption that the recombination loss in the depletion region is absent. However, in actual solar cells, the recombination represents a substantial loss which cannot be represented in the single diode model. Therefore, the concept of a two diode model evolved [105]. Figure 5.5 represents the two diode model with series and shunt resistances.

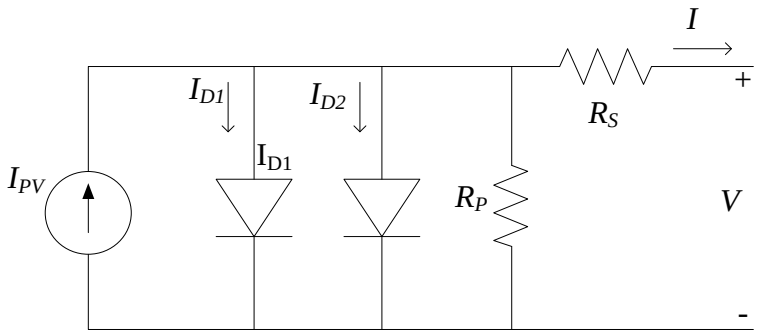

Figure 5.5 Two diode model of PV cell

The output current, *I*, for two-diode model can be represented by Eqn. 5.2 and Eqn. 5.3 [106].

$$I = I_{PV} - I_{O1}\left[\exp\left(\frac{V + IR_s}{a_1 V_{T1}}\right) - 1\right] - I_{O2}\left[\exp\left(\frac{V + IR_s}{a_2 V_{T2}}\right) - 1\right] - \left(\frac{V + IR_s}{R_p}\right) \quad \text{Eqn. 5.2}$$

$$V_T = \left(\frac{N_s kT}{q}\right) \quad \text{Eqn. 5.3}$$

Where, I_{PV} is the current generated by the incidence of light on the solar cell, I_{o1} and I_{o2} are the reverse saturation currents of diode 1 and diode 2 respectively, V_{T1} and V_{T1} are the thermal voltages of the respective diodes, N_s is number of cells connected in series, q is the electron charge (1.60217646×10^{-19} C), k is the Boltzmann constant (1.3806503×10^{-23} J/K), T is the temperature of the p–n junction and a is the diode ideality factor. The term I_{o2} in Eqn. 5.2 compensates for the recombination loss in the depletion region.

The 3rd term on the right hand side of Eqn. 5.2 (with I_{o2}) is due to the presence of the second diode and the 4th term is due to the presence of the shunt resistance, R_p.

Using the two-diode model to represent the solar cell, greater accuracy can be achieved. However, many parameters such as I_{PV}, I_o, I_{o2}, R_p, R_s, a_1 and a_2 have to be computed.

In this work, the model proposed by Ishaque *et al.* [106] has been used for the two-diode PV model. The equation for PV current, $I_{PV,}$ can be written as [107] Eqn. 5.4.

$$I_{PV} = \left(I_{PV\_STC} + K_I \Delta T\right)\frac{G}{G_{STC}} \quad \text{Eqn. 5.4}$$

Where I_{PV_STC} is the light generated current at STC, $\Delta T = T - T_{STC}$ (in Kelvin, T_{STC} =25 °C), G is the surface irradiance of the cell and G_{STC} (1000 W/m^2) is the irradiance at STC. The constant K_I is the short circuit current coefficient (provided by the manufacturer).

Reserve saturation current for both diodes are assumed to be equal in magnitude and is represented as in Eqn. 5.5.

$$I_{O1} = I_{O2} = I_O = \frac{I_{SC\_STC} + K_I \Delta T}{exp[(V_{OC\_STC} + K_V \Delta T)/\{(a_1 + a_2)/p\} V_T] - 1} \quad \text{Eqn. 5.5}$$

Where, K_V is the open circuit voltage coefficient and V_{OC_STC} is the open circuit voltage at STC.

The value for a_1 was set at 1 and a_2 was found to be ≥ 1.2 [106]. Since, $(a_1 + a_2)/p = 1$ and $a_1 = 1$, then p can be chosen to be ≥ 2.2. Thus Eqn. 5.2 can be re written as

$$I = I_{PV} - I_O \left[\exp\left(\frac{V + IR_s}{V_T}\right) + \exp\left(\frac{V + IR_s}{(p-1)V_T}\right) + 2\right] - \left(\frac{V + IR_s}{R_p}\right) \quad \text{Eqn. 5.6}$$

Parameters R_s and R_p, are determined simultaneously through iteration. The procedure proposed by Villalva *et al.* [108] is used to calculate the values of these parameter. The approach is to match the calculated maximum power point (P_{mp_C}) with the experimental maximum power point (P_{mp_E}) by iteratively increasing the value of R_s while simultaneously calculating the R_p value. From Eqn. 5.6, at the MPP condition, the expression for R_p can be rearranged and rewritten as

$$R_p = \frac{V_{mp} + I_{mp} R_s}{\left\{I_{PV} - I_o \left[\exp\left(\frac{(V_{mp} + I_{mp} R_s)}{V_T}\right) + \exp\left(\frac{(V_{mp} + I_{mp} R_s)}{(p-1)V_T}\right) + 2\right] - \frac{P_{max\_E}}{V_{mp}}\right\}} \quad \text{Eqn. 5.7}$$

Where, P_{mp_E} is the maximum power point from data sheet (experimental), I_{mp} is the output current during maximum power and V_{mp} the voltage during the maximum power.

The initial conditions for both resistances are:

$$R_{s0} = 0;\ R_{p0} = \frac{V_{mp}}{I_{sc} - I_{mp}} - \frac{V_{oc} - V_{mp}}{I_{mp}} \qquad \text{Eqn. 5.8}$$

The initial value of R_p is the slope of the line segment between the maximum power points and short circuit point. The output current of the PV cell is determined using the Newton-Raphson method. Each iteration updates R_s and R_p towards the best model solution. A flowchart describing the algorithm is given in Figure 5.6.

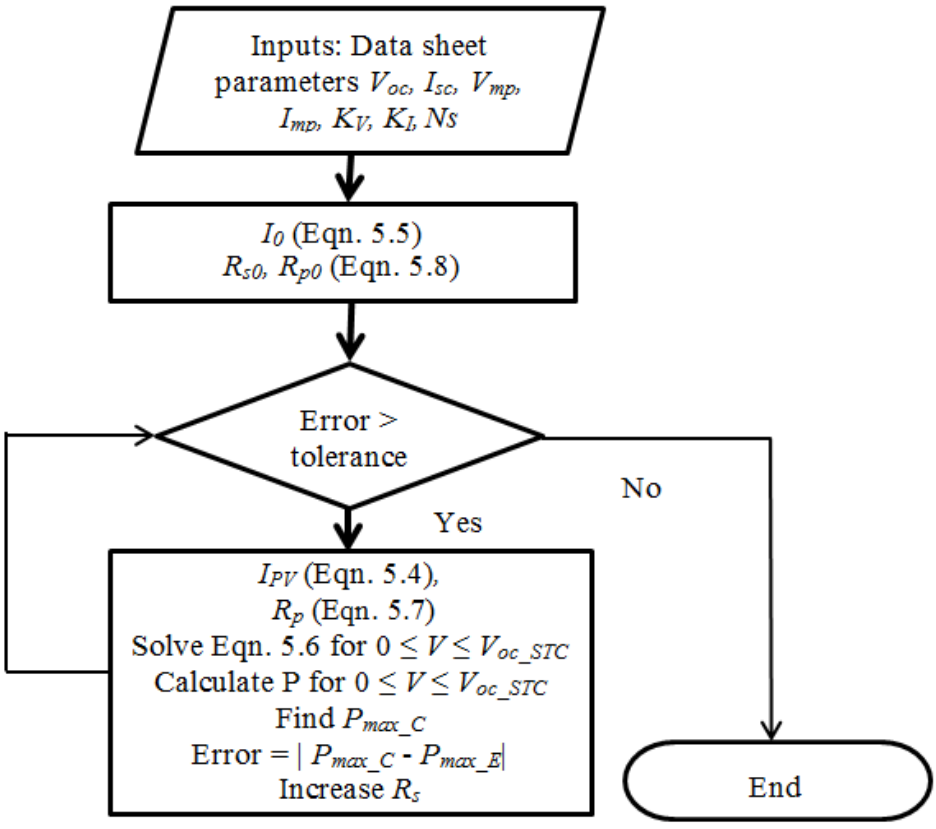

Figure 5.6 Algorithm used to adjust the I-V model

5.3.2 Results and validation

The I-V and P-V characteristics of the PV model are shown in Figure 5.7 along with its three main points: short circuit current, open circuit voltage and maximum power point. The PV model was then verified against a commercially available PV panel. Solarcentury's 185 W solar module [109] was selected for this. It uses 72 highly efficient monocrystalline PV cells delivering a module efficiency of 14.7%. The specification of the Solarcentury's 185 W solar module is given in Appendix B: Specification of 185 W Solar Module.

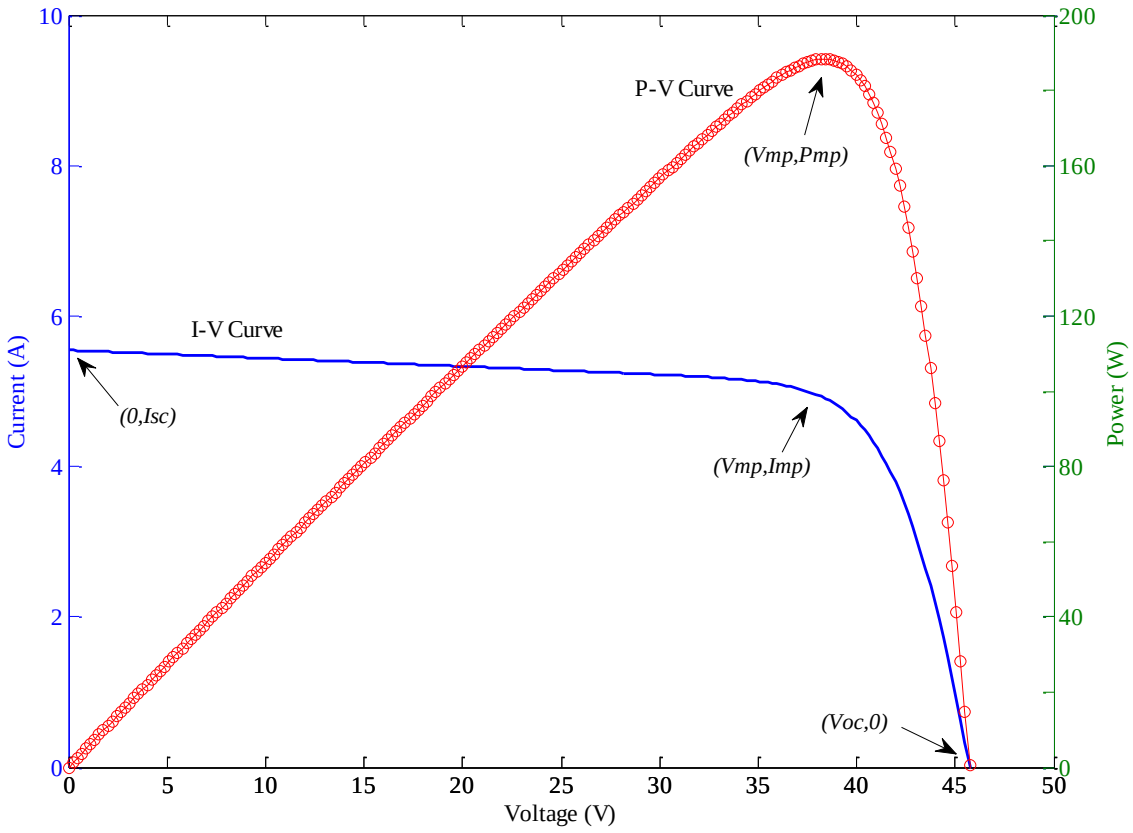

Figure 5.7 I-V and P-V characteristic curves

Figure 5.8 shows a comparison of the I-V characteristic generated by the PV model at different irradiation with the curves presented in the data sheet for the corresponding

irradiation. The graphs show a good agreement between them. The root mean square error between the modelled data and actual data are 0.695, 0.413 and 1.131 for 600 W/m^2, 800 W/m^2 and 1000 W/m^2 respectively. In real PV system test conditions, different losses occurs such as PV loss due to irradiance level and temperature, module quality loss, module array mismatch loss and ohmic wiring loss. These losses are not taken into account when modelling so there is a slight difference in the slopes of the graphs.

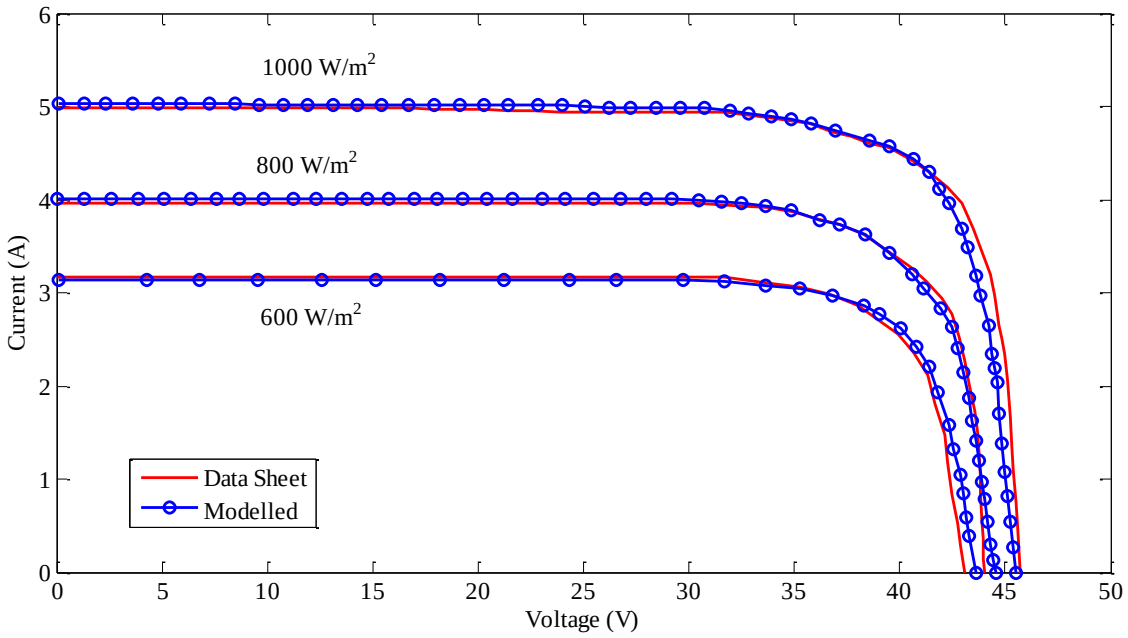

Figure 5.8 Comparison of I-V curves of PV model with data sheet value at different Irradiation

5.3.3 PV Maximum power point tracking (MPPT)

A PV system has a few drawbacks such as high cost, low efficiency of the PV system, fluctuation in power output with changing climatic conditions etc. With changes in climatic conditions the maximum power point also changes. To track this and get more benefit out of

the PV system a MPPT is used. A review of different MPPT techniques on the basis of their advantages, disadvantages, control variables involved, complexity of algorithm, hardware implementation and application has been presented by Subudhi and Pradhan [110].

It is generally agreed in the literature that the maximum power extracted from the PV depends strongly on three factors: cell temperature (ambient temperature), irradiation and load profile (load impedance). An increase in temperature will mainly decrease the output voltage and vice-versa. Similarly, an increase in irradiation will mainly increase the output current which can also be seen in Figure 5.8. So with change in environmental conditions output power of the PV system changes and this can be far from the maximum power output. A simple maximum power point tracking method based on the 'Lambert W function' proposed by Jiang *et al.* [111] is used in this work. Lambert W function, also called the omega function or product logarithm, is a set of functions, namely the branches of the inverse relation of the function $z = f(W) = We^W$ where e^W is the exponential function and W is any complex number.

In PV array, the relation between voltage and current is highly nonlinear and their combination determines the power output from the PV. A 'Lambert W function' is used to determine the optimum operating voltage at given temperature and irradiation level, Eqn. 5.9, directly which is then used by the PV model to generate maximum power as shown in Figure 5.9.

$$V_{mp} = \frac{\omega\left(e\left(1+\frac{[I_{SC}+K\Delta T]}{\frac{I_{SC}}{\frac{qV_{OC}}{e^{N_S KaT}-1}}\times\left(\frac{T}{T_{STC}}\right)^{\frac{3}{a}}\times e^{\frac{qE_G}{ka}\left(\frac{1}{T_{STC}}-\frac{1}{T}\right)}}\times\frac{G}{G_{STC}}\right)\right)-1}{\frac{q}{N_S kaT}} \quad \text{Eqn. 5.9}$$

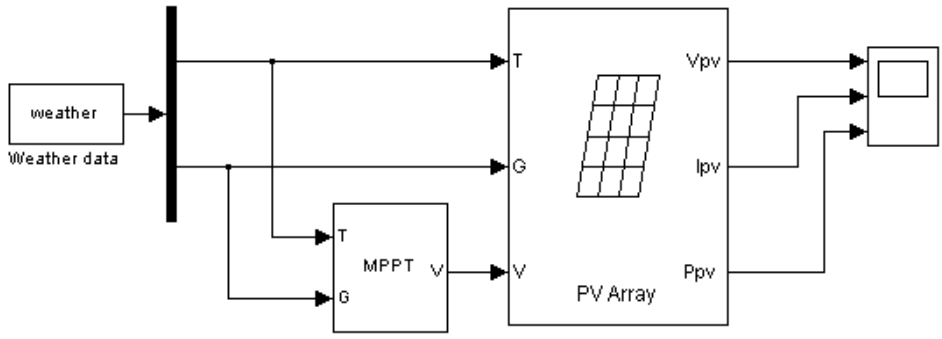

Figure 5.9 PV model with MPPT in Matlab/Simulink

Figure 5.10 shows the power generated by the PV model when combined with the MPPT. Real weather data which is used in section 4.6 is given as input and a total of 14 panels were connected.

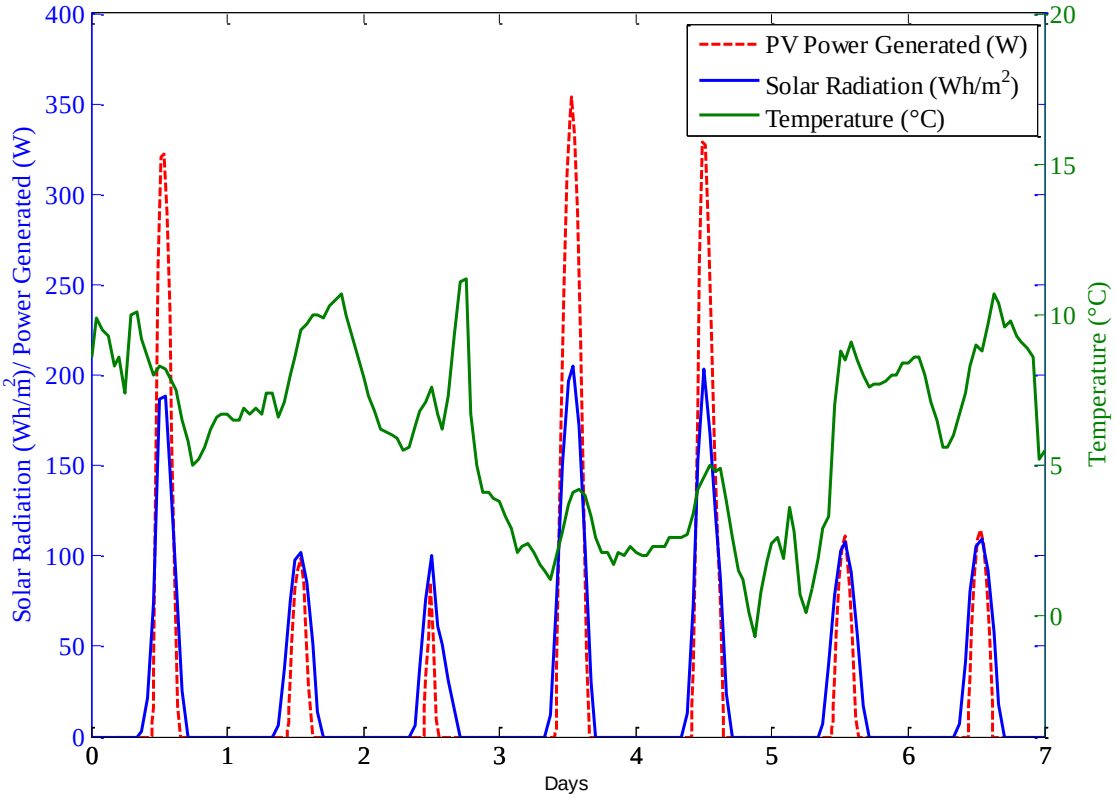

Figure 5.10 PV power generation during a winter week

5.4 Small Scale Wind Turbine Modelling

Small scale wind turbines consist of a wind rotor, a generator (normally a permanent magnet generator, PMG) and a power demand controller. To understand the operation of the wind turbine system and to maximise the energy capture, the combined performance of these components needs to be analysed. In commercial small scale wind turbines, the wind rotor is directly coupled with the electrical generator so the length of drive shaft is very small and its effects on power transmission can be neglected. The schematic diagram of a small scale wind turbine power system is shown in Figure 5.11.

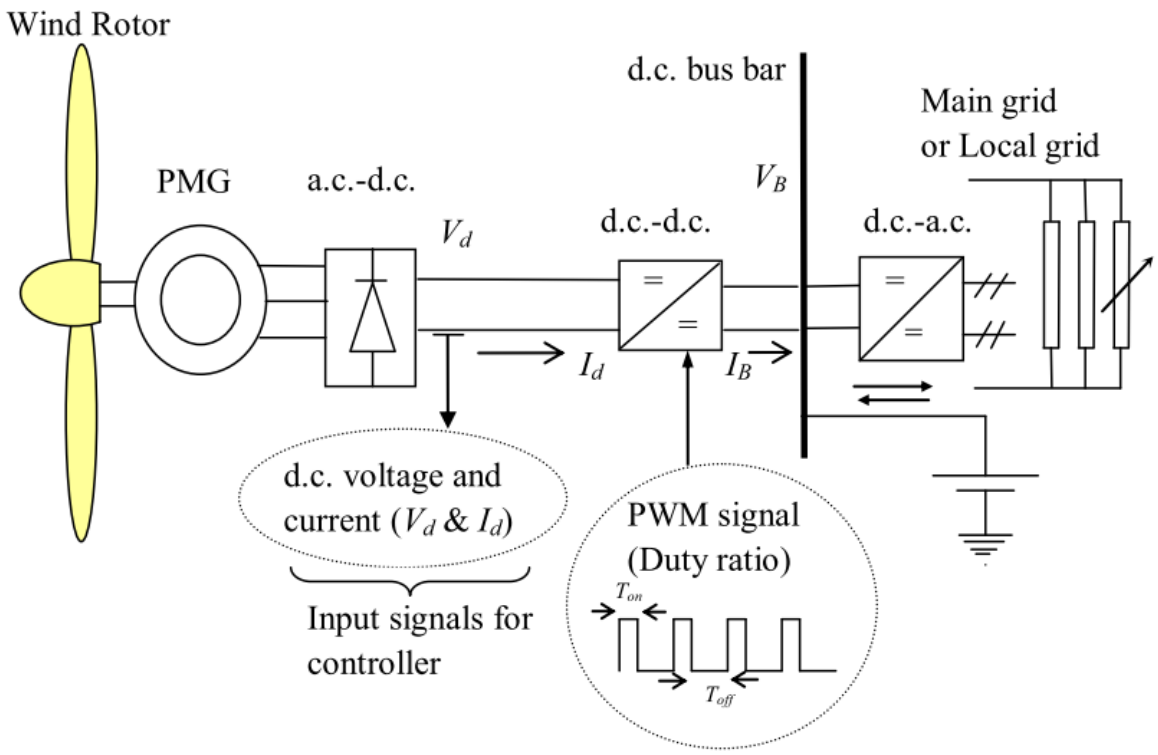

Figure 5.11 Schematic diagram of small scale wind turbine power system [66]

Variable speed wind turbines, generally, have higher efficiency than fixed speed wind turbines and hence are becoming more popular, particularly for small wind turbines. Usually, power electronics are used to regulate the torque and speed of the turbines in order to maximise the output power in the variable speed wind turbine. Variable pitch aerodynamically controlled wind turbines are more complicated to build and expensive. Therefore, a variable speed fixed pitch design for the wind rotor is a more popular scheme for small scale wind turbine systems.

To evaluate the actual performance of a wind rotor, a detailed and representative wind flow-model is required. It should be noted that, although the incoming flow is usually assumed to be steady, uniform and axial in a basic design process, the flow field generated by a wind

rotor is very complex [64]. Therefore, accurate modelling the flow-field around the wind rotor is a difficult process.

Control strategies in small scale wind turbines are different than those used in large scale wind energy conversion systems. Power electronic converters are mostly used for MPPT control in wind energy conversion systems depending upon the type of generator which can be a permanent magnet synchronous generator, induction generator, doubly fed induction generator or synchronous generator. In real systems, exact tracking of the maximum power points with variation of wind speeds can lead to high mechanical stress and aerodynamic fluctuations in the system. Therefore, exact MPP tracking may not be possible and for some systems, control limitation is employed to smooth the power output and avoid structural failures. A review and analysis of different MPPT techniques for WECS has been presented by Kazmi *et al.* [112].

In this work, a most common lookup table based MPPT technique is used to maximise the system efficiency. In this technique a pre-programmed 2D lookup table with stored values of rotational speed or d.c. voltage and the corresponding maximum power or maximum torque at various wind speeds is adopted. Figure 5.12 shows a block diagram of the maximum power tracker using PI controller employed in this work.

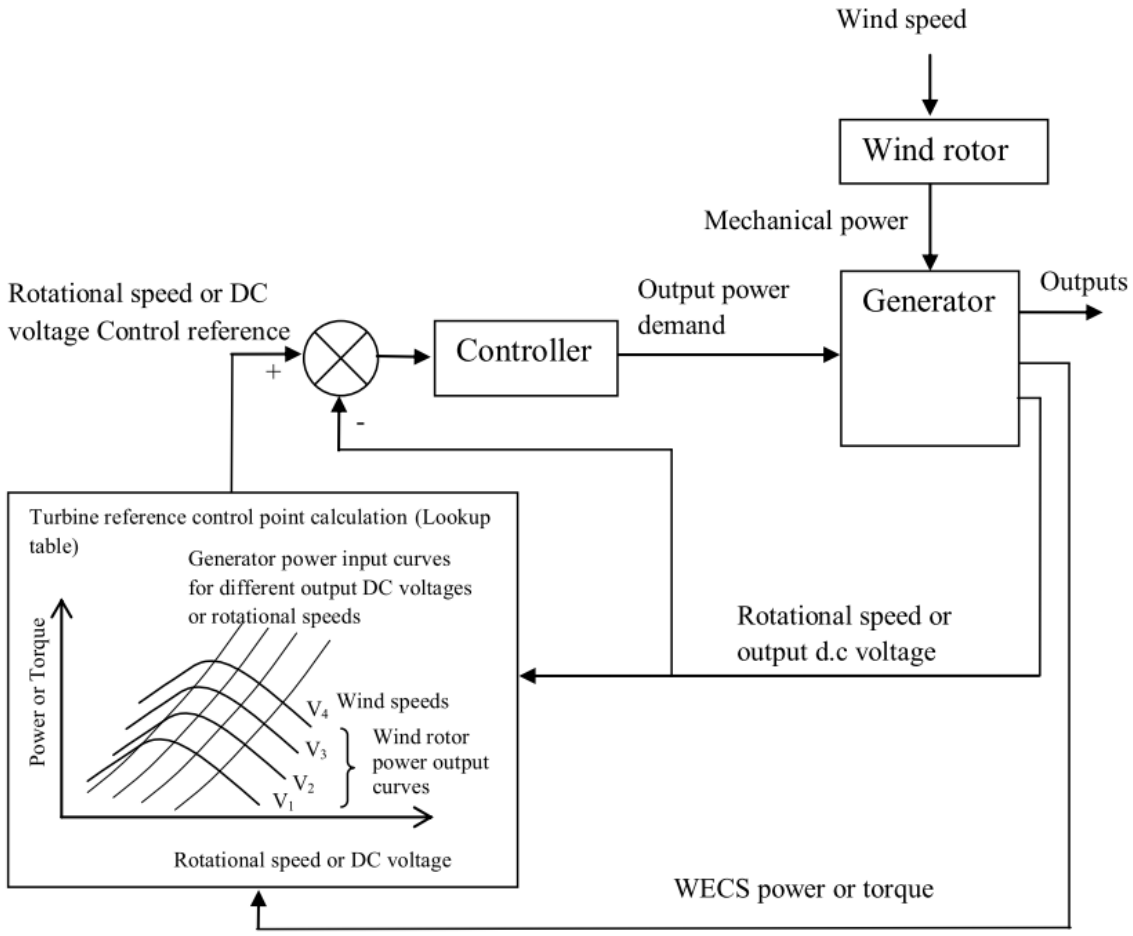

Figure 5.12 Control system for WECS using lookup table method [66]

5.4.1 Wind rotor model

The energy extracted from the wind is transmitted through the wind rotor shaft as a torque, and the air is acted upon with a reactive torque that makes the wake, which rotates opposite to the wind rotor motion. This implies that the downstream air has axial and rotational motions, which represents a kinetic energy. Indeed, this energy component represents a part of energy in air which could not be absorbed by the rotor [64]. Thus the energy extracted from the wind may be represented as [64]

$$P = \frac{1}{2}\rho\pi {R_r}^2 {V_w}^3 C_P \quad \text{Eqn. 5.10}$$

Where, P is the power captured by the wind rotor, R_r is the radius of the wind rotor, ρ is the density of air, V_w is the speed of the incident wind and C_P is the power coefficient.

The power coefficient of a wind turbine is a measurement of how efficiently the wind turbine converts the energy in the wind into electricity, which for a given wind rotor depends on the pitch angle of the wind rotor blades and the tip speed ratio (λ). The tip speed ratio is defined in Eqn. 5.11 [64].

$$\lambda = \frac{\omega . R_r}{V_w} \quad \text{Eqn. 5.11}$$

Where, ω is the rotational speed of the wind rotor.

German physicist, Albert Betz, who calculated that no wind turbine could convert more than 59.3% of the kinetic energy of the wind into mechanical energy turning a rotor. This is known as the Betz Limit, and is the theoretical maximum coefficient of power for any wind turbine.

The aerodynamic torque (T_a) of a wind rotor can be obtained as

$$T_a = \frac{P}{\omega} \quad \text{Eqn. 5.12}$$

Thus substituting Eqn. 5.10 and Eqn. 5.11 in Eqn. 5.12, we get

$$T_a = \frac{1}{2}\rho\pi {R_r}^3 {V_w}^2 \frac{C_P}{\lambda} \quad \text{Eqn. 5.13}$$

$$T_a = \frac{1}{2}\rho\pi {R_r}^3 {V_w}^2 C_t \qquad \text{Eqn. 5.14}$$

Where, C_t is the torque coefficient of wind rotor.

The characteristics of a wind rotor are usually given by the variation of power coefficient with respect to the tip speed ratio as shown in Figure 5.13. The power coefficient has a maximum value for an optimal tip speed ratio value (λ_{opt}) which peaks at around the optimum tip speed ratio resulting in maximum power extraction at any wind speed. Therefore for a variable speed wind turbine, when wind speed varies, the wind rotor speed should be adjusted proportionally to maintain the optimum tip speed ratio to extract maximum power from the wind.

From Figure 5.13, it can be noted that the maximum value for the power coefficient and torque coefficient occur at different values of tip speed ratio. The maximum torque coefficient occurs at lower rotational speed compared to that for the maximum power.

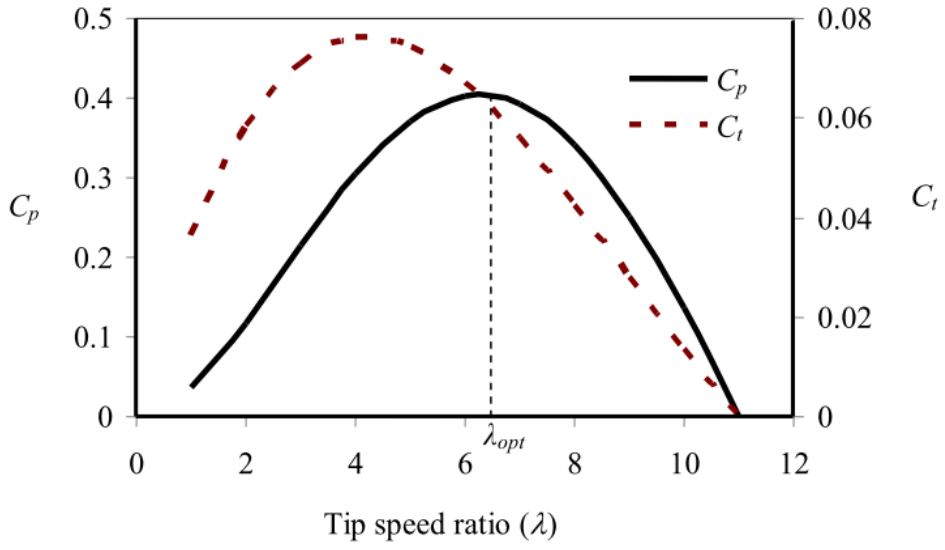

Figure 5.13 The wind rotor characteristics [66]

The lookup table for the wind rotor characteristics used in this work is presented in Appendix A. To calculate the tip speed ratio for each step, the rotational speed is multiplied by the rotor radius and divided by the wind speed as in Eqn. 5.11. The aerodynamic torque delivered by the wind rotor is estimated by using Eqn. 5.10. The Simulink computer model of the wind rotor is shown in Figure 5.14.

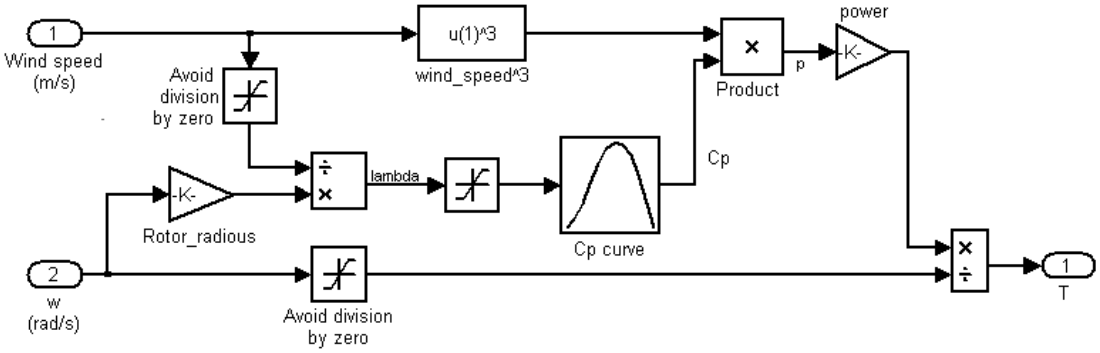

Figure 5.14 Simulink model of wind rotor

5.4.2 Equivalent d.c. model of three-phase PMGs

Three phase permanent magnet generators (PMGs) are generally used for small scale wind turbines. In small scale wind energy systems, a three phase-bridge rectifier is used to convert a.c. to d.c. and may be used to charge the battery directly or inverted back to a.c. for connecting to the grid. The d.c. load circuit of a PMG and the equivalent d.c. circuit of a PMG, as seen from the three-phase rectifier d.c. terminals, is shown in Figure 5.15 and Figure 5.16 respectively. Note that L_a, L_b, L_c are the phase inductances, R_a, R_b, R_c are the phase resistances and for electric and magnetic symmetry: ($L_{ph} = L_a = L_b = L_c$ and $R_{ph} = R_a = R_b = R_c$) [113].

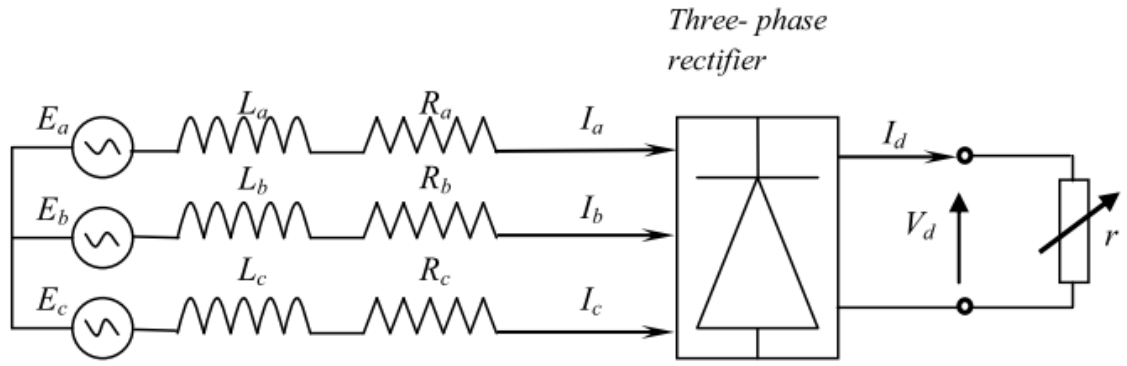

Figure 5.15 The d.c. load circuit of a PMG [113].

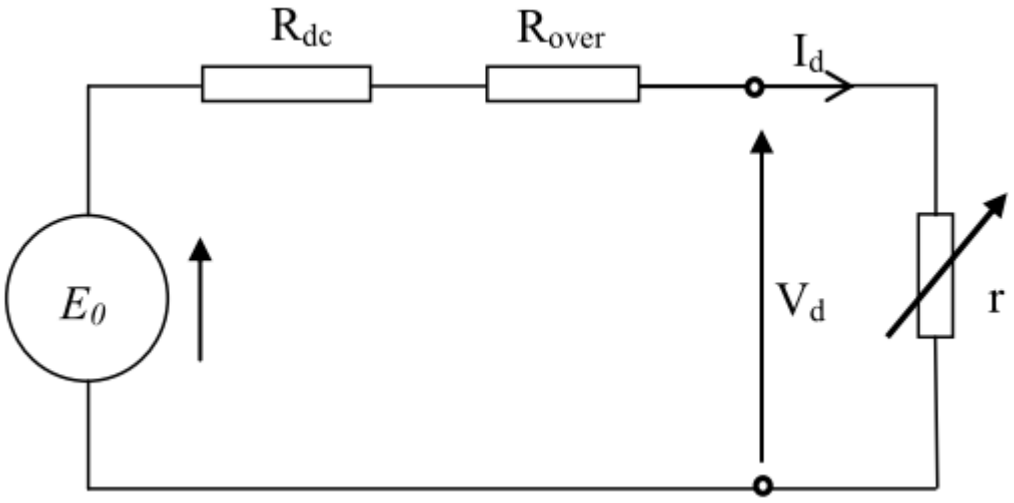

Figure 5.16 The equivalent d.c. circuit of PMG [113]

For three-phase rectifier, the effective armature resistance is approximately twice the phase resistance [113] i.e.

$$R_{dc} \approx 2R_{ph} \qquad \text{Eqn. 5.15}$$

The overlap resistance is given by [113]

$$R_{over} = \frac{3}{\pi}\omega_s L_{ph} \quad \text{Eqn. 5.16}$$

Where, $\omega_s = p\omega$, L_{ph} is phase inductance, ω_s is rotational speed of electric field, p is No. of pole pairs.

The WECS output terminal d.c. voltage is:

$$V_d = E_0 - I_d(R_{dc} + R_{over}) \quad \text{Eqn. 5.17}$$

Where, V_d is d.c. output voltage, I_d is d.c. current and E_0 is generated EMF.

Let,

$$R = R_{dc} + R_{over} \quad \text{Eqn. 5.18}$$

Therefore,

$$E_0 = V_d + I_d R \quad \text{Eqn. 5.19}$$

$$\text{As, } E_0 = k'\omega, \quad \text{Eqn. 5.20}$$

$$k'\omega = V_d + I_d R \quad \text{Eqn. 5.21}$$

Where k' is a fixed parameter, that depends on magnetic flux linkage and number of pole pairs ($k' = p\,\varphi_m$; φ_m is the magnetic flux linkage, p is number of pole pairs).

For lossless operation, the electromagnetic torque is given as ($P_{WR} = E_0 I_d$; without electrical and mechanical losses);

$$T_e = \frac{P_{WR}}{\omega} = \frac{E_0 I_d}{\omega} = \frac{k'\omega I_d}{\omega} = k' I_d \qquad \text{Eqn. 5.22}$$

The generator torque is a function of the generator current (I_d), magnetic flux linkage and number of pole pairs [114]. Therefore, the electromagnetic torque of a generator (T_e) can be varied by controlling the current. Electrical losses can be expressed as $I_d^2 R$. Therefore, higher losses occur at high torque operation due to high flow of current.

The Simulink model of the PMG equivalent d.c. model is shown in Figure 5.17. The input to the equivalent d.c. PMG model is aerodynamic torque and output is the d.c. voltage applied across the load through the rectifier bridge. The output d.c. voltage is externally controlled by a buck-boost converter and is controlled by PI controller.

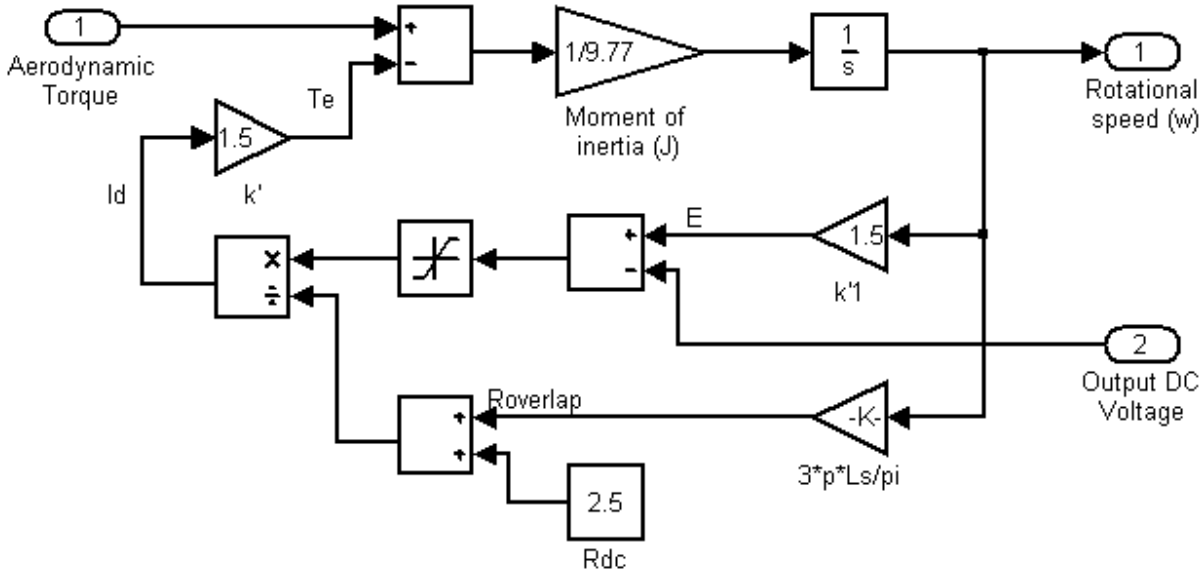

Figure 5.17 Simulink model of PMG equivalent d.c. model

For the buck-boost DC-DC converter (shown in Figure 5.11);

Voltage ratio[17],

$$V_B = -V_G \left(\frac{D}{1-D}\right) \quad \text{Eqn. 5.23}$$

And the corresponding current

$$I_B = -I_G \left(\frac{1-D}{D}\right) \quad \text{Eqn. 5.24}$$

$$\text{Where, } D = \left(\frac{T_{on}}{T_{off}+T_{on}}\right) \quad \text{Eqn. 5.25}$$

Where, V_B is the voltage at DC bus, V_G is the generator side voltage, I_B is the current flow towards the d.c. bus, IG is the current flow from the generator. T_{on} and T_{off} represents the on and off times of the duty cycle respectively.

Since the duty ratio '*D*' varies from 0 to 1, the output current and voltage can also vary from lower to higher values. The duty ratio is controlled by using PI controller.

5.4.3 Results

Using the same weather data used in section 4.6, the power generated by the wind turbine model is shown in Figure 5.18 for two weeks. The specification of the wind rotor and permanent magnet generator are given in Appendix C: Specification of the Wind Turbine. The wind turbine's rated power is 400 W and its cut in speed is 12 m/s.

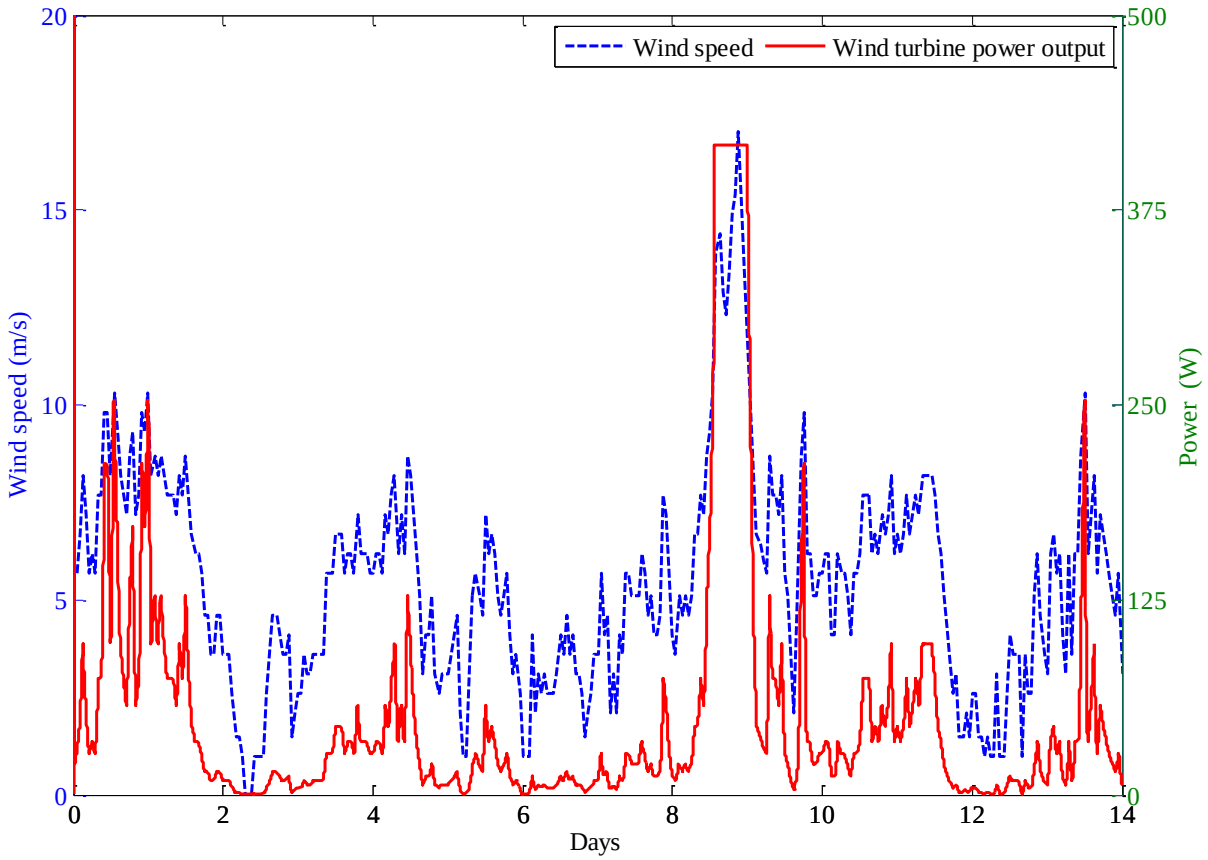

Figure 5.18 Power generated by small scale wind turbine power system

5.5 Low-Voltage Network Modelling

5.5.1 Introduction

The purpose of modelling of low-voltage (LV) distribution network is to analyse the voltage profiles at different parts of the LV network with different scenarios such as at different penetration levels of small scale distributed generation. The voltage profiles generated are used as one of the inputs for the controller of the micro-CHP which will be discussed in section 7.3.

The model represents a typical UK LV distribution network and includes voltage level between 33 kV and 400 V [18]. The distribution network includes a 33 kV (500MVA) source as a grid supply point, which is connected to a 33/11 kV substation. Two on-load tap changer (OLTC) 15 MVA 33/11 kV transformers are present in the substation. Six 11 kV outgoing feeders are supplied from this substation and each 11 kV feeder supplies eight low voltage distribution substations. Each low voltage distribution substation contains a 500kVA 11kV/400V distribution transformer. This distribution transformer is equipped with an off-load tap changer. A schematic single line diagram of the LV network model is shown in Figure 5.19. Details of components of the network along with the feeder parameters are given in Appendix B.

In the distribution network model, only one of the six 11 kV feeders (brown colour) together with its connected loads was modelled in detail and the other five 11 kV feeder were modelled as a lumped load connected to the main 11kV busbar. Similarly, only one out of the eight 11 kV/400 V substations (red transformer) including the connected feeders and loads was modelled in detail whilst other seven 11kV/400V substations were represented as a lumped load. There are four radial 400V feeders coming out of this substation out of which three were modelled as lumped loads (Green load) and one in detail (red loads) with connected loads.

Actual distribution network data was used for the detailed 400 V feeder modelling which includes loads for 56 individual consumers [18]. An assumption was made that loads on the other three 400 V feeders were equivalent to the load of 328 individual domestic consumers. Hence the total number of consumers supplied by each 11 kV/400 V substation was 384 (=

56 + 328). This resulted in a modelled total load connected to an 11 kV feeder to be equivalent to the load of 3072 (= 8 × 384) domestic customers and modelled total load supplied from the 33/11 kV substation to be equivalent to 18432 (= 6 × 3072) domestic consumers.

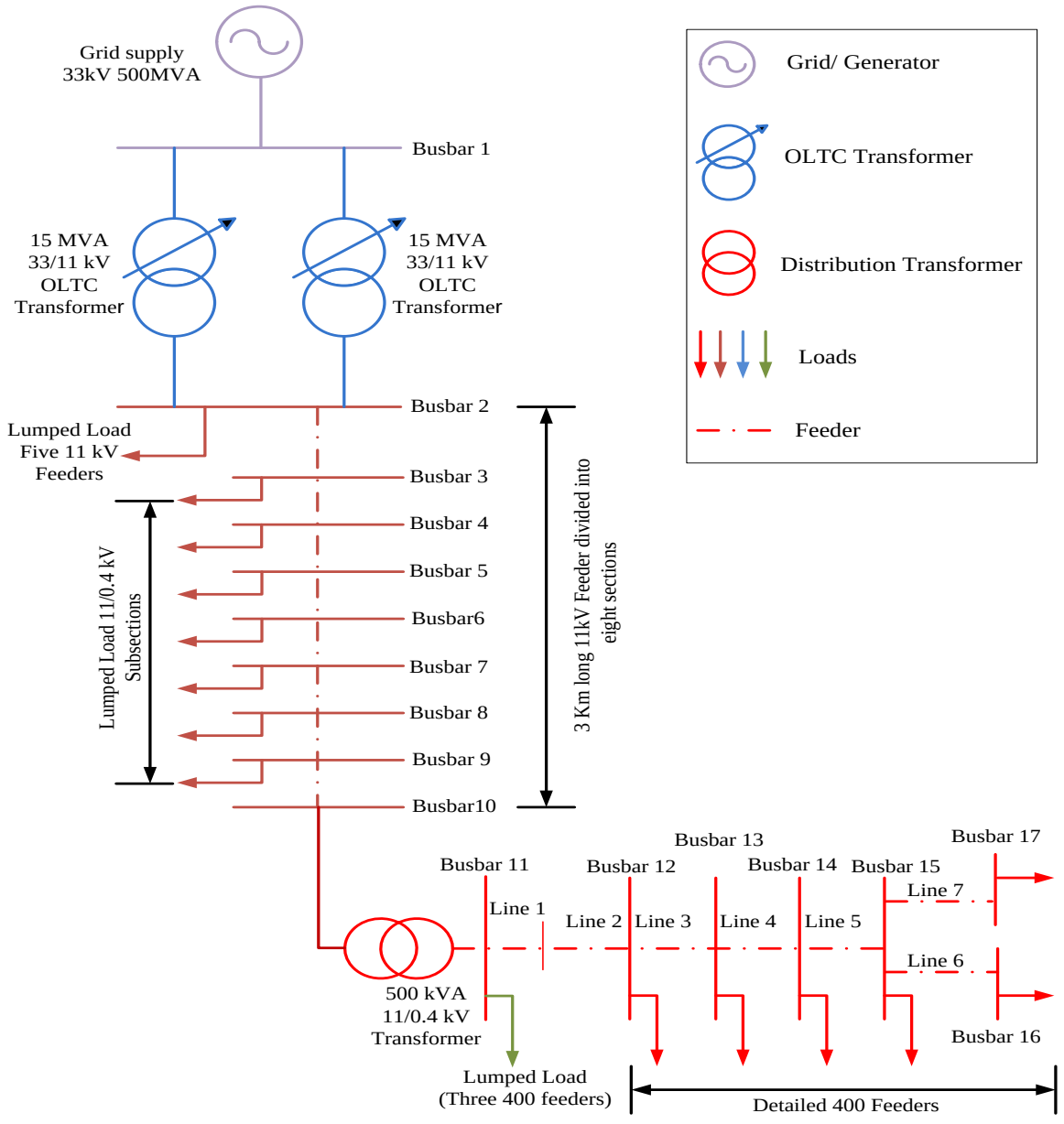

Figure 5.19 Single line diagram of typical low voltage network in UK

5.5.2 Modelling

The above mentioned low voltage distribution network is developed in Simulink which is shown in Figure 5.20. Block 'Lumped 400 V feeder in 11 kV' in Figure 5.20 is a subsystem of all lumped loads consisting of 11/0.4 kV substation connected to an 11 kV feeder (brown feeder and loads in Figure 5.19) and detailed as shown in Figure 5.21. Similarly, block 'Low voltage feeder (400 V)' at the right most end of Figure 5.20 is a subsystem in which details of the 400 V feeder is modelled (red and green colour feeder and loads in Figure 5.19) and the detailed model is shown in Figure 5.22.

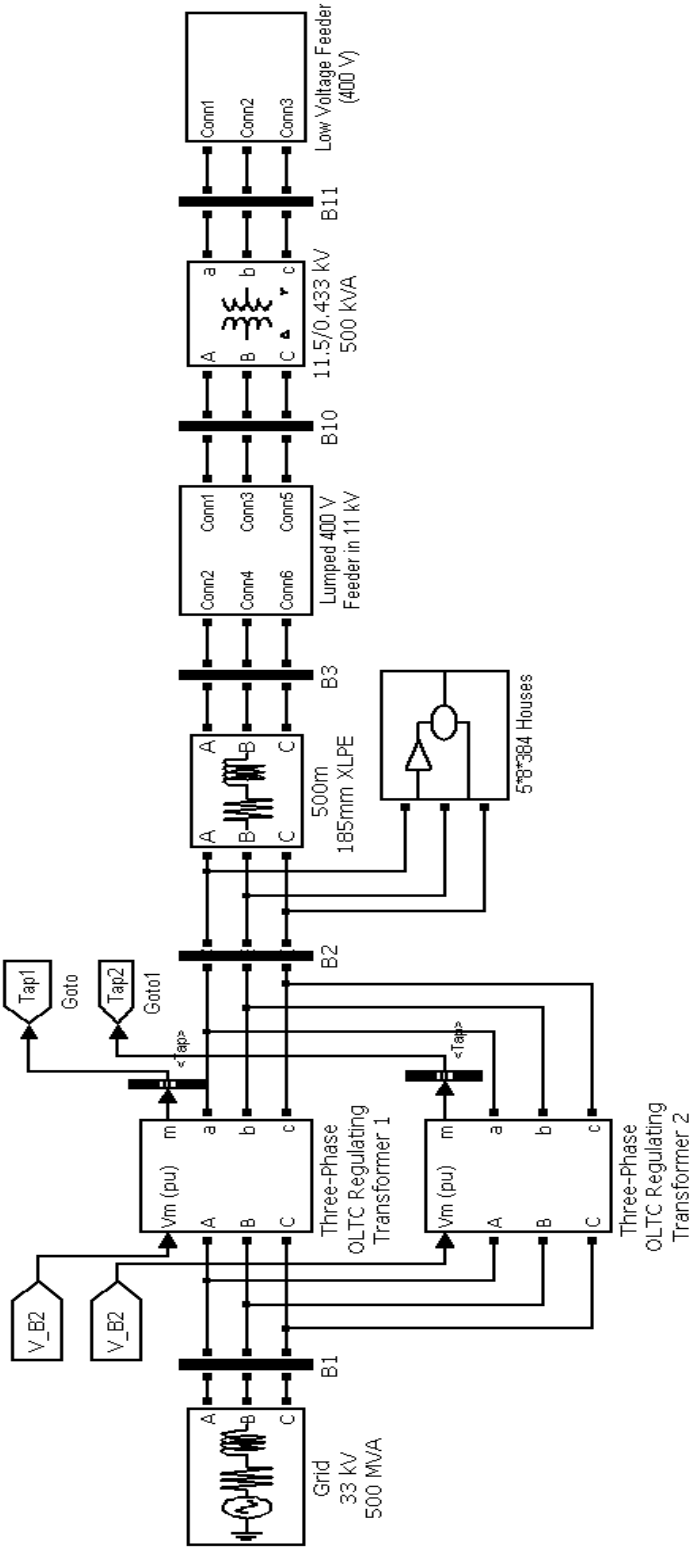

Figure 5.20 MATLAB/Simulink model of the typical low voltage network in the UK

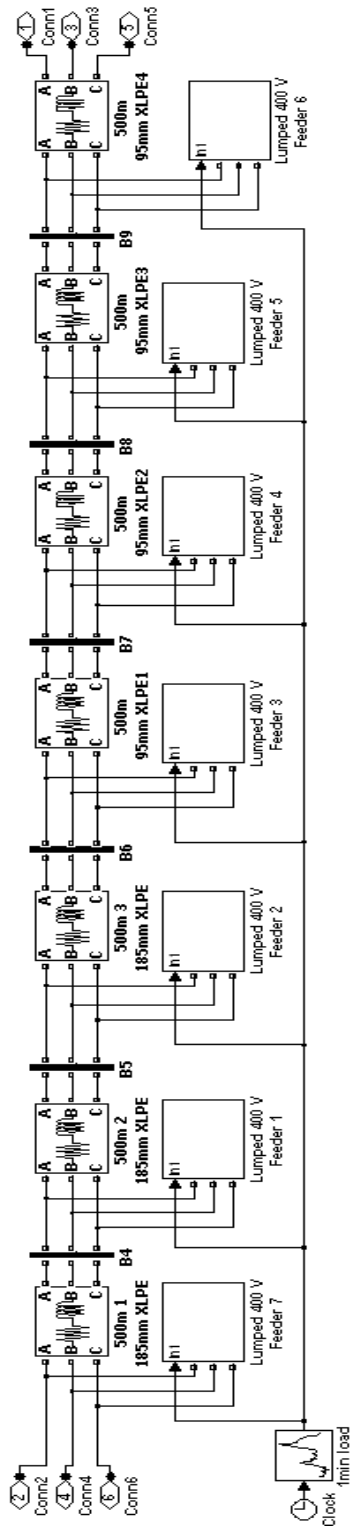

Figure 5.21 Detail of lumped 400V feeder in 11kV

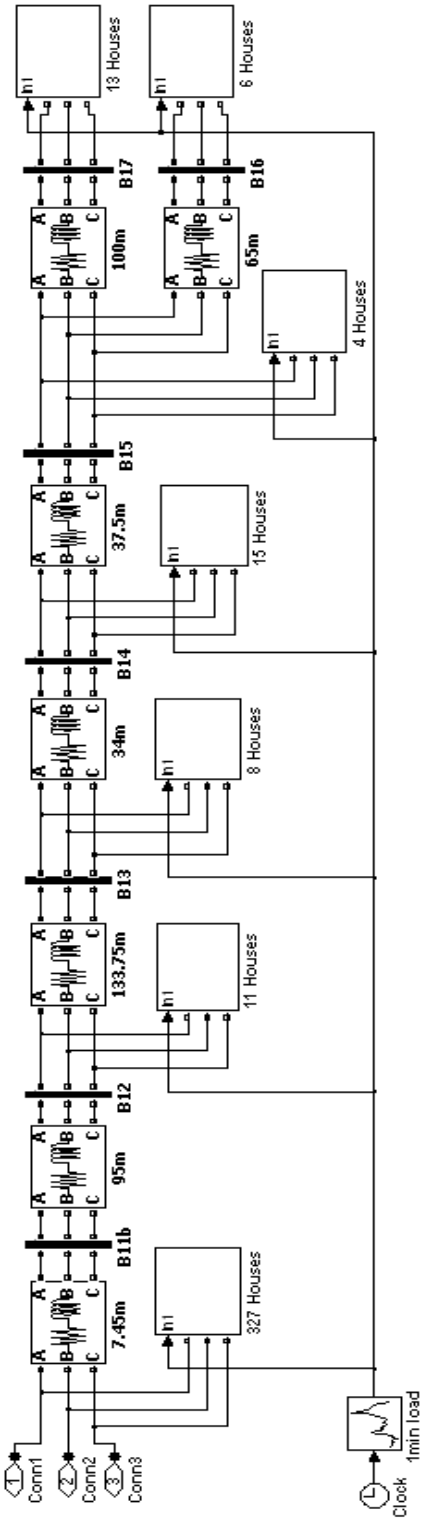

Figure 5.22 Detail of low voltage feeder (400V)

5.5.3 Results

The voltage profiles in a distribution network depend on the consumer loading conditions and these vary with respect to the time of day and the season. So, a typical demand load profile for winter was used to analyse the network performance.

Figure 5.23 shows the averaged power demand load profile (7043 domestic consumers) for the February month of 2011inclusive of weekdays and weekends. Figure 5.23 is data that has been converted to kW from half-hourly averaged electrical energy consumption in kWh. These domestic customers do not own any low-carbon technologies [115].

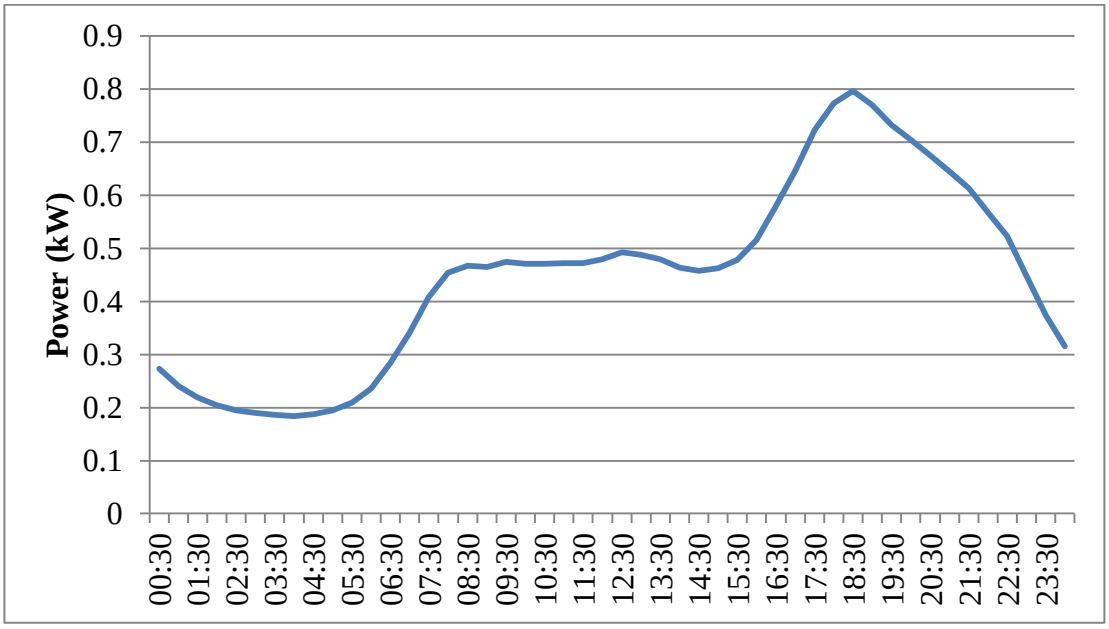

Figure 5.23 Averaged daily load profile for month of February [115]

Figure 5.24 shows the voltage profile obtained from the modelled network between busbar 2 (nearest to the OLTC transformer) and busbar 17 (farthest point on the LV side). The voltage drop increases further away from the OLTC transformer along the distribution

network. Busbar 17 is farthest away and hence is the weakest point in the LV network. The voltage at any busbar in the network depends on to the loads connected to the network. As the loading increases, the voltage at the busbars decreases and vice-versa. The OLTC transformer in the network is designed in such a way that if voltage at busbar 2 goes beyond ±0.0125 p.u. from 1 p.u. (i.e. 1.0125 and 0.9875), the transformer reacts by changing the tap position and tries to bring the voltage towards 1 p.u. This can be seen clearly at 7:00 when the voltage at busbar 2 goes below 0.9875 p.u. and the tap changer respond to push to voltage close to 1 p.u.

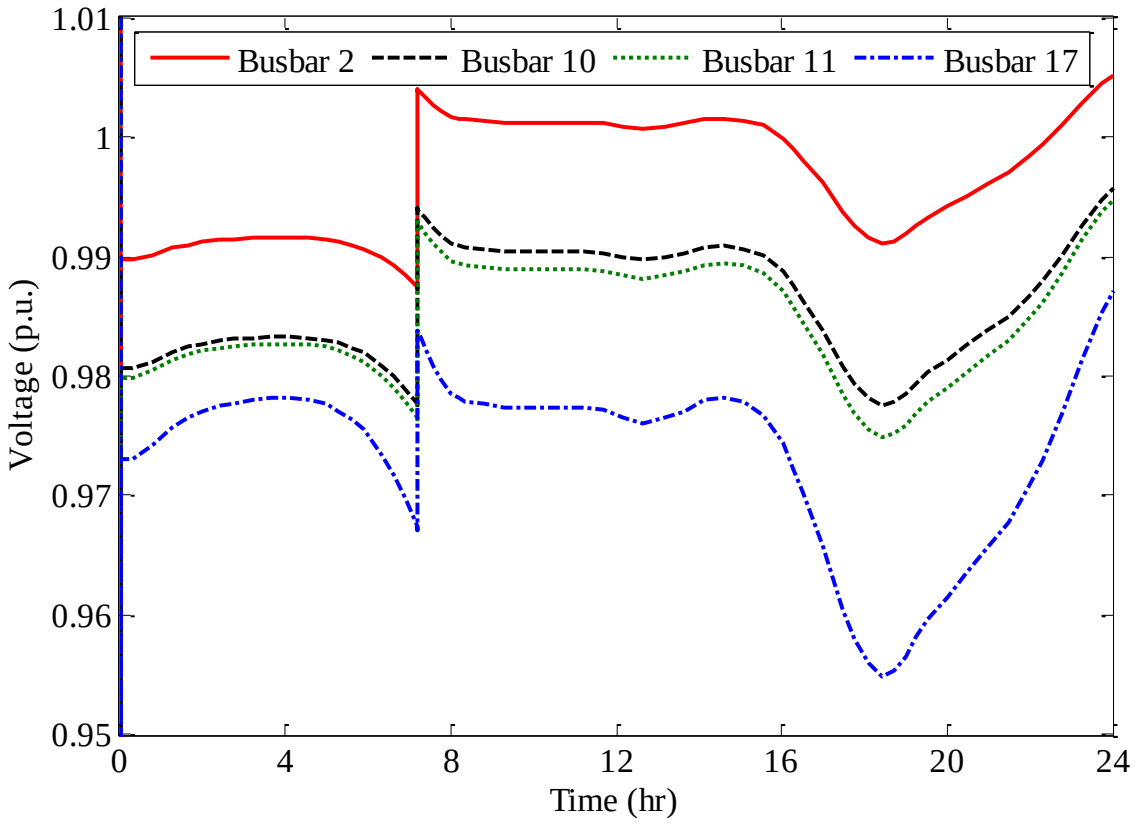

Figure 5.24 Voltage profile at different busbar of the distribution network

Chapter 6 Integration of distributed generators and thermal model of the building

6.1 Introduction

The cost of PV and wind turbine generated electricity is expected to decline as production continues to climb and benefits the economics of them. So, there is high possibility of having more than one distributed generation in a dwelling. Renewable energy sources are on one hand free of greenhouse emissions and they are unlimited but on the other hand they are site-dependent. Furthermore, renewable energy sources such as wind and solar have an intermittent nature, the output powers are dependent on weather conditions. Therefore their power production varies with month, days, hours and seconds. Research has shown that combining PV with micro-CHP overcomes the inherent challenges of intermittency and enables the share of solar PV to be expanded without completely depending on a storage system [116]. Apart from emissions, advantages of having these technologies together are diversity in fuel source and reliability. Hybrid system options offer market entry strategies for technologies that cannot currently compete with the lowest-cost traditional options.

The Simulink models developed in Chapter 4 and 5 are integrated together as shown in Figure 6.1. The ‘space heating’ block masks the three-zones of the house model, heating system and its thermostatic control as discussed in Chapter 4. The time series input data are read from files as follows:

- Domestic hot water demand

- Weather data (external air temperature, wind speed, global horizontal solar radiation).
- Occupancy activity schedule
- Electrical power demand

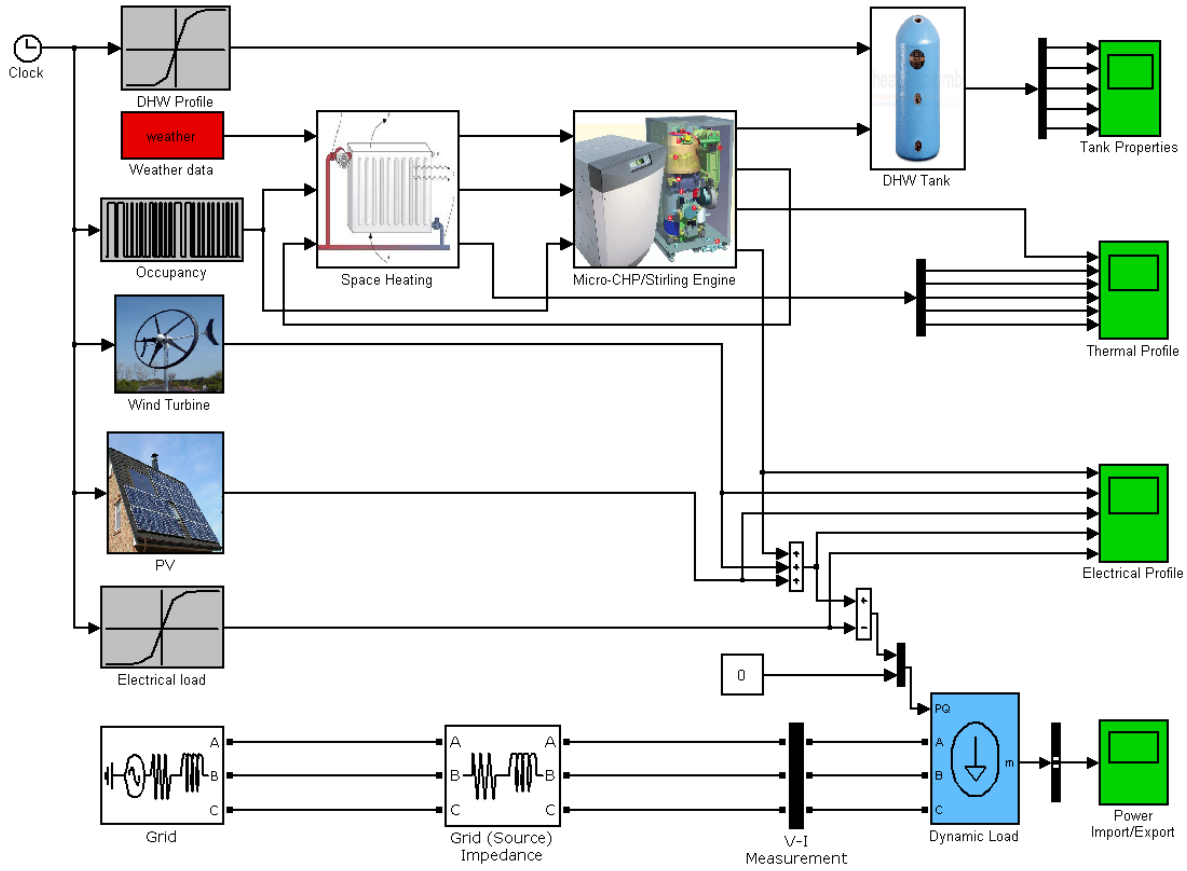

Figure 6.1 Integrated simulation model

6.2 Application

The integrated model was applied to two typical UK family house types: a semi-detached house (as shown in Figure 4.5) and a larger detached house (as shown in Figure 6.2) as they will have different energy demand profiles. In both cases, as a simplifying assumption, each

house was divided into 3 heating zones depending on the required internal temperature: the living room (21^{o}C), the bedroom (16^{o}C) and the balance zone (18^{o}C). The house constructions were assumed to be in accordance with typical construction standards as set out by the UK's National Calculation Methodology (NCM) simplified building energy modelling database [97] and the UK Building Regulations, Part L, 2006 for the semi-detached house and 1996 for the detached house. The occupancy pattern assumed was similar to section 4.6, consisting of two working parents with two children of school age, see Table 4-1,. Internal casual gains were calculated based on Table 6-1 using data from [96], as follows:

Table 6-1 Calculation of Internal Gains

Cooking
For Gas = (70.9 + 14.3×N) where, N is number of occupant = 4
Lighting
For Living room = MIN(20, 0.1×total floor area of house) + 6 (due to presence of children)
For Bedroom = MIN(5, 0.025×total floor area of house) + 1.5 (due to presence of children)
For Balance Zone = MIN(15,0.075×total floor area of house) + 4.5 (due to presence of children)
Metabolic Activity
For Living room = seated quiet (108 W)
For Bedroom = sleeping (72)
For Balance zone = work involving walking (160 W)

The values in Table 6-1 are based on 24 hour averages and incorporate utilisation factors: metabolic - 1, gas cooker - 0.5, lighting and appliances - 0.8 [96]. The same weather data as was used in section 4.6 for the north of England (Finningley) was used. The house was assumed to be ventilated at an average rate of 0.5 air change per hour, (including external

air infiltration) in winter and allowed to rise to 3 air change per hour in summer when heating is not operating and windows are opened [117] in an attempt to limit high summer time indoor temperature.

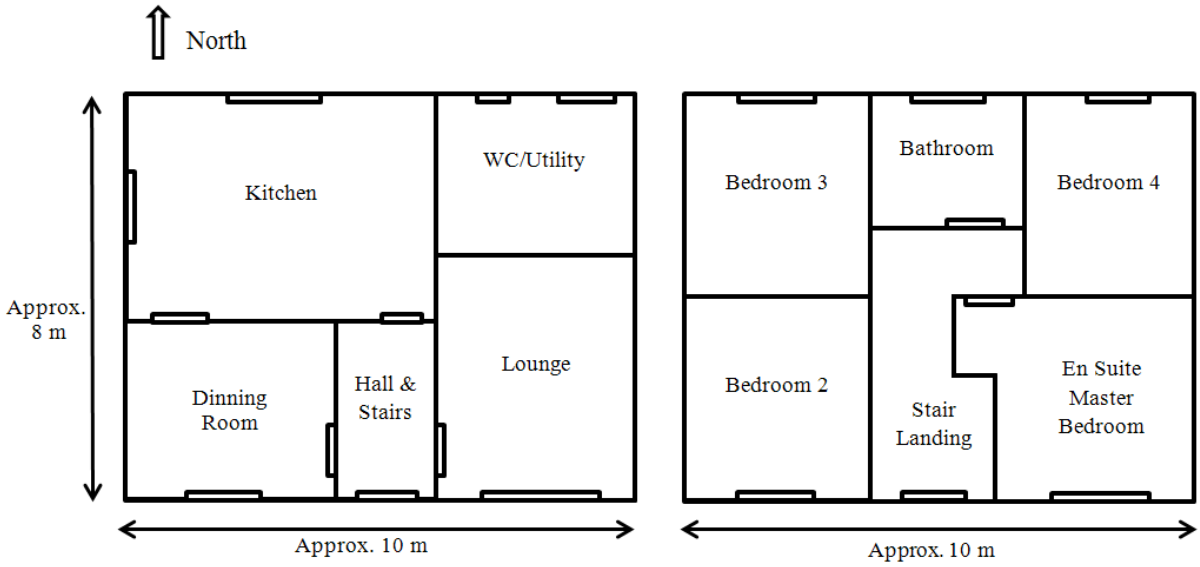

Figure 6.2 Plan view of detached house type

In both case studies, the micro-CHP module, presented in section 5.2, was configured for heat-led control. Thus when there is a heat demand in the house during occupancy (occupant(s) not sleeping), the module is activated providing 6kW of thermal energy and simultaneously providing 1kW of electrical energy servicing either the power demand of the house or exporting power to the grid (or both).

A domestic-scale wind turbine, presented in section 5.4, with a rated capacity of 400 W (at a cut-off wind speed of 12 m/s) was applied to the both house types. A detailed specification of the wind turbine is given in Appendix C: Specification of the Wind Turbine. Similarly, a PV array as discussed in section 5.3 was also applied to both houses. This comprised four roof-mounted mono-crystalline modules each with a rated power

output of 185W, (a detailed specification is given in Appendix B: Specification of 185 W Solar Module) applied to the semi-detached house and 14 modules to the much larger detached house.

Domestic electrical demand data measured at 1-minute resolution in 22 dwellings in the east midland region of England over two years (2008 and 2009) were obtained from UK Data Service [21]. Three different types of dwelling were included in these data: detached, semi-detached and terraced with numbers of occupants varying from 1 to 6. In this work, two houses with similar characteristics to those depicted in Figure 4.5 and Figure 6.2 (and the same numbers of occupants) were chosen. The one minute resolution data in both cases reflect the appliances in the monitored houses as summarised in Table 6-2. The resulting weekday and weekend electrical demand load profiles for the semi-detached type house and the detached type house are shown in Figure 6.3 and Figure 6.4.

Table 6-2 Electrical appliances in use in houses

Appliance Type	**Detached House**	**Semi-detached House**
Electric shower	Yes	No
Occasional use of electric heater	Yes	No
Economy-7 tariff	Yes	No
Use of time controls	Yes	No
Energy saving light usage (%)	25	25
Halogen lamp usage	12	4
Outdoor floodlight	No	Yes
Refrigerator	2 × Fridge/freezer	1
Freezer	No	1
Television	1 (tube)	1 (tube), 2 (plasma), 1 (LCD)

Computer	6	3
Electric oven	1	1
Microwave	1	1
Kettle	1	1
Toaster/sandwich toaster	1	2
Dish washer	1	1
Washing machine	1	1
Tumble drier	1	1

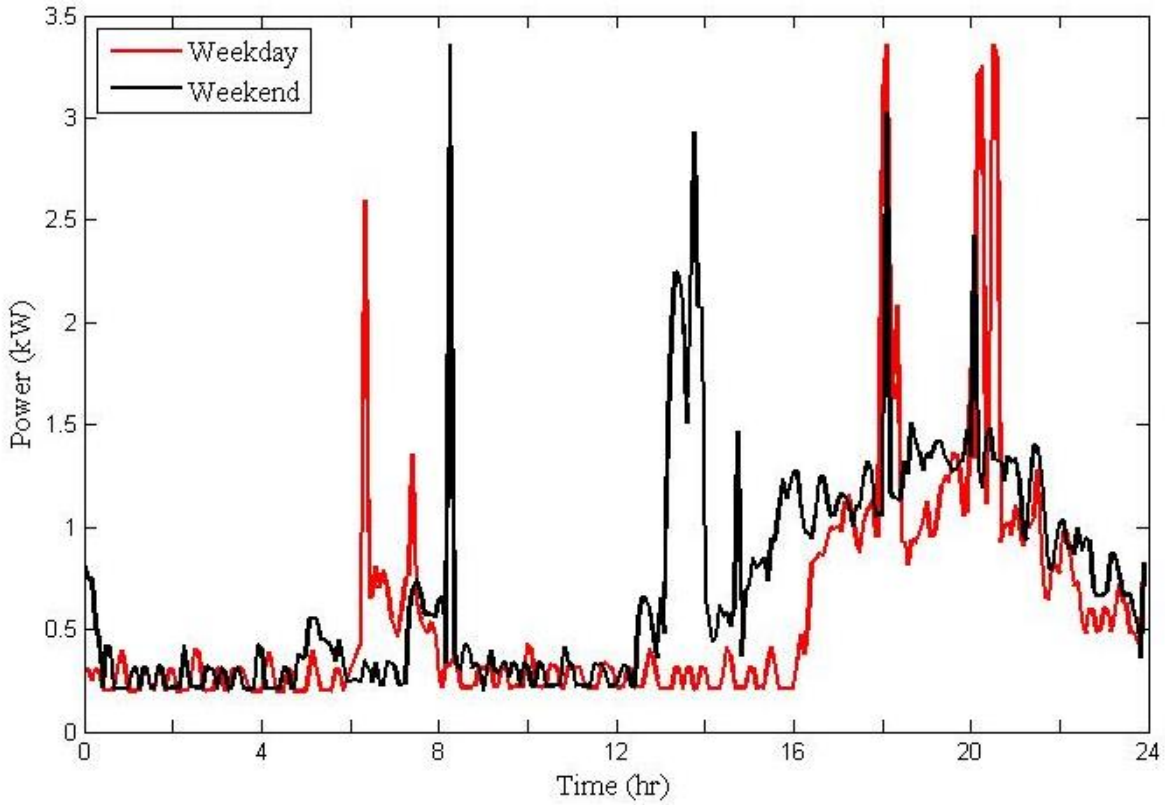

Figure 6.3 Daily power demand pattern for semi-detached type house

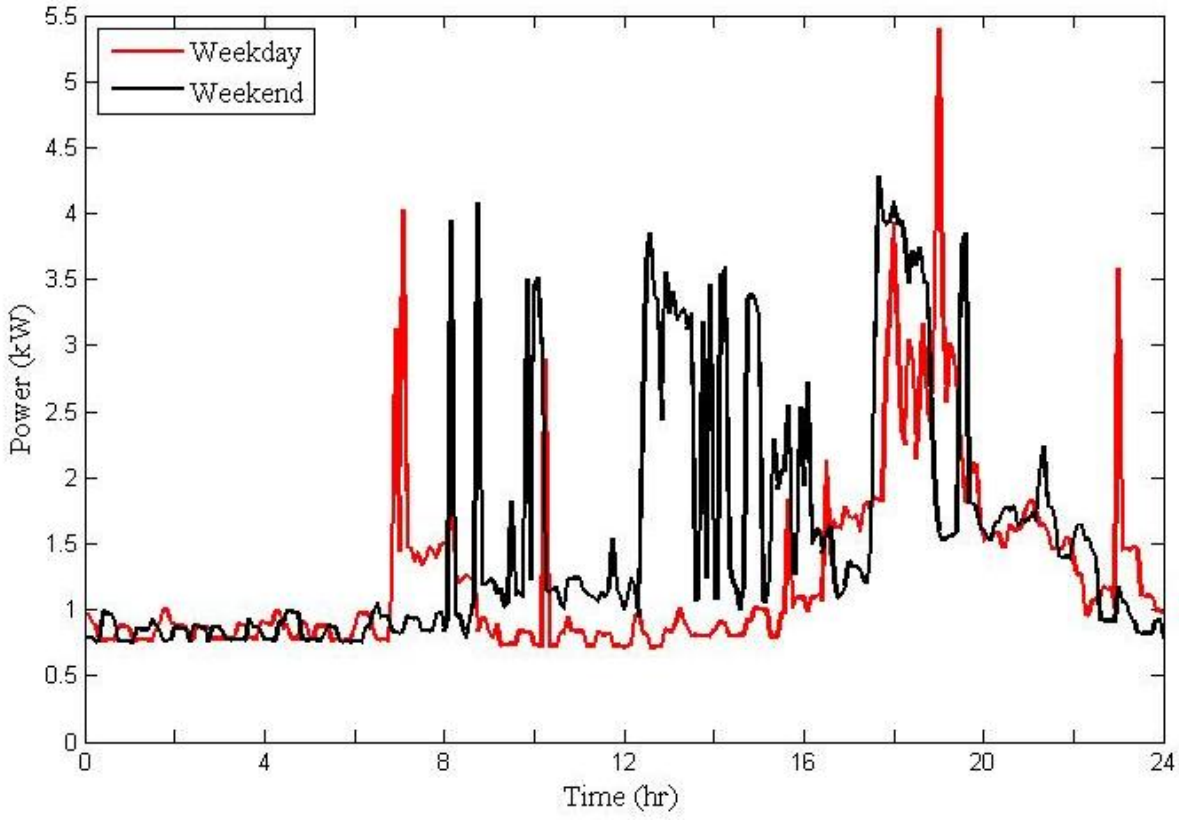

Figure 6.4 Daily power demand pattern for detached type house

The number of occupants is a key factor that influences the domestic hot water demand regardless of geographical location or type of boiler used in the house [16]. Therefore, the same domestic hot water demand profile can be used for both types of houses. The monitored hot water demand profile for a dwelling at an interval of 5 minutes for weekday and weekend is shown in Figure 6.5.

This is one of the main advantages of this model where the hot water demand pattern at a resolution of one minute has been used, whereas in other models the interval used is 15 minute [49] or higher. One minute resolution hot water demand profile can capture use of hot water for short intervals such as washing face or hand in kitchen sink or bathroom

basin. Thus resulting in decrease of hot water temperature and giving more accurate and frequent water temperature for the interaction with the micro-CHP to fulfil the hot water demand.

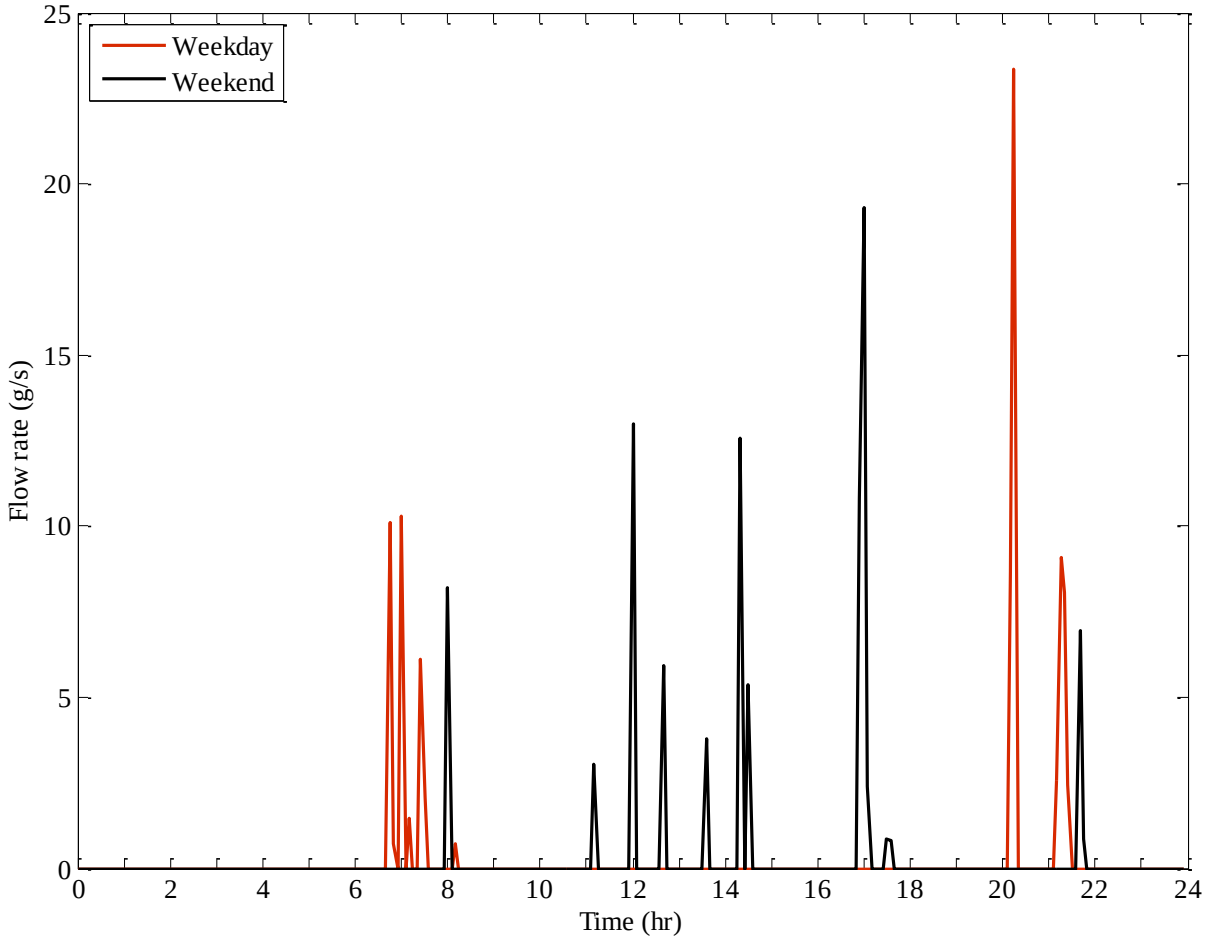

Figure 6.5 Domestic hot water demand profile

The integrated model consist of the equivalent LV distribution network (grid and grid source impedance blocks in Figure 6.1) to determine the amount of power exported and imported from the grid. The electrical load of a single dwelling and the power generation from the distributed generator of that dwelling are considered to be very low and will have very small effect on the grid voltage.

6.3 Results and Discussion

Full annual simulations were carried out with the integrated model for both houses using the input data described in section 6.2. Samples of results were extracted for a typical winter week (Figure 6.6, Figure 6.7 Figure 6.8) and for a typical summer week (Figure 6.9 and Figure 6.10) for the semi-detached house. Similar samples of results were also extracted for a typical winter week (Figure 6.11, Figure 6.12 and Figure 6.13) and for a typical summer week (Figure 6.14 and Figure 6.15) for detached house. Summaries of annual energy flows are given in Table 6-3 and Table 6-4 for both types of houses.

Zone temperatures for one typical winter week (starting with a weekend) are shown in Figure 6.6 for the semi-detached house (also plotted are the corresponding external temperature and solar radiation). In this case, the house is occupied intermittently during the day. Thus two characteristic peaks in zone internal temperatures can be seen for each day for the morning and the evening periods during which the house is occupied often with a free-float mid-day peak corresponding to an increase in solar radiation. Note that the heating is controlled from a thermostat mounted in the ground floor entrance lobby together with local thermostatic radiator valves. This is common practice in the UK domestic heating control. Therefore, heating control in this application is based on the temperature of balance zone. As a consequence, room temperature control involves wide variations among zones.

The electrical energy flows for a typical winter week are plotted in Figure 6.7 for the semi-detached house. This shows power generated by the three sources (micro-CHP, wind turbine and PV system) as well as power imported (shown as negative) and power exported

(shown as positive). Between two and three bursts of daily power from the micro-CHP can be seen in order to meet space heating and domestic hot water demands. It is encouraging that more frequent switching of the micro-CHP is avoided as this might lead to module wear and early breakdown. Renewable energy activity in this typical week is low with the exception of a windy day (day 2) giving rise to the wind turbine to operate at its rated capacity for a significant part of the day. Most of the power generated is used to fulfil the house demand even during the unoccupied periods during which standby loads absorb the available renewable power, through there are small contributions to export from the micro-CHP system when active.

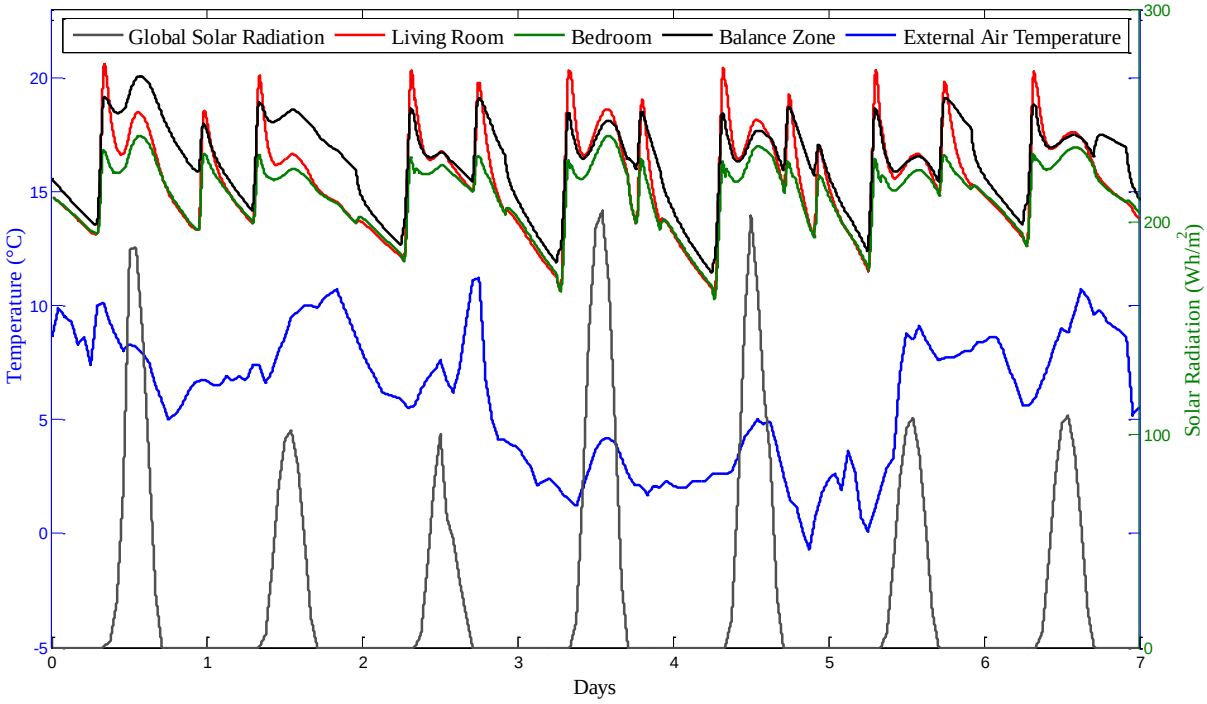

Figure 6.6 Typical winter week zone temperatures (semi-detached house type)

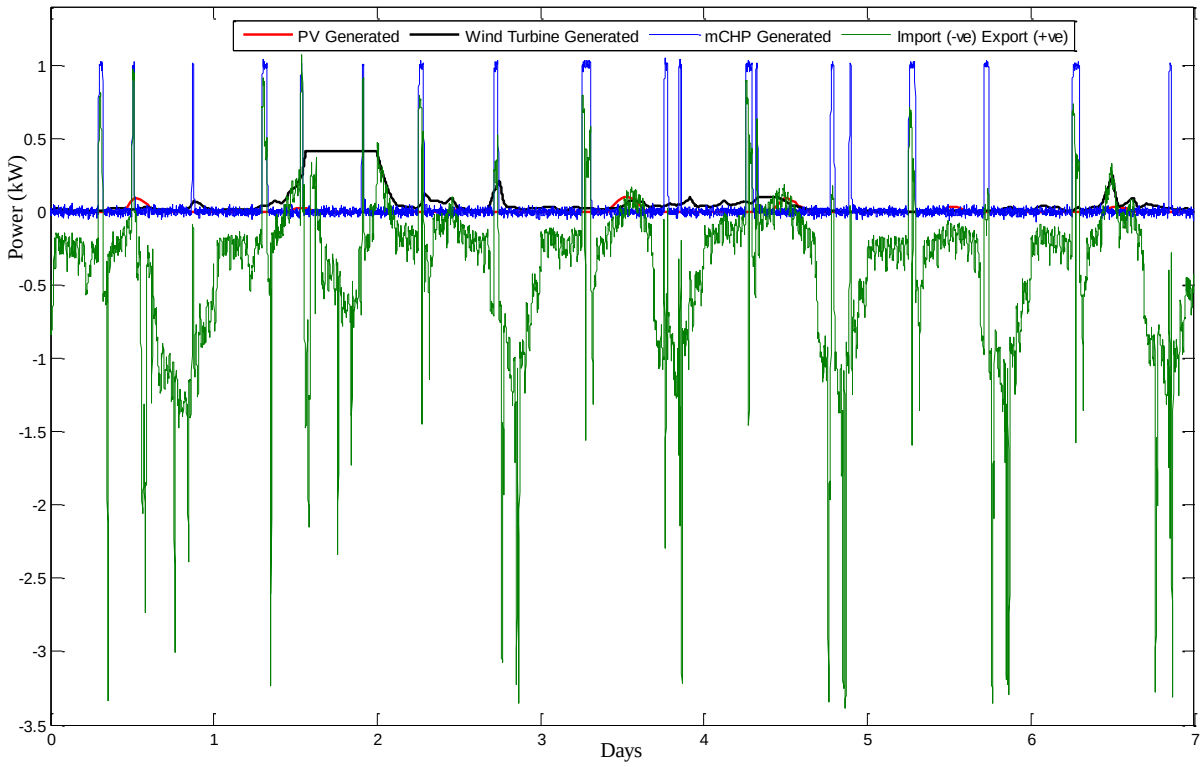

Figure 6.7 Typical winter week electrical power flows (semi-detached house type)

The thermal energy flow in a typical winter week is plotted in Figure 6.8 and typical summer week in Figure 6.9 for the semi-detached house. In winter, the micro-CHP is switched typically once in the morning and once or twice to meet the evening demand. Usually, just one or two relatively short charging cycles per day are needed for the hot water tank. When just one is needed, this tends to take place during the evening when the micro-CHP is also serving space heating loads. In summer, the micro-CHP is activated only to meet the domestic hot water demand and is activated once or twice a day usually when there is high coincident demand. From Figure 6.9 it is also clear that the temperature of water in the tank decreases at a higher rate when there is hot water demand and temperature decreases at a slower rate when there is no hot water demand, due to the heat loss from the

tank to the surrounding. In all cases, the high degree of damping (due to the space heating and the hot water tank) is such that frequent switching of the micro-CHP is avoided which is good for the module maintenance, operation and operating efficiency.

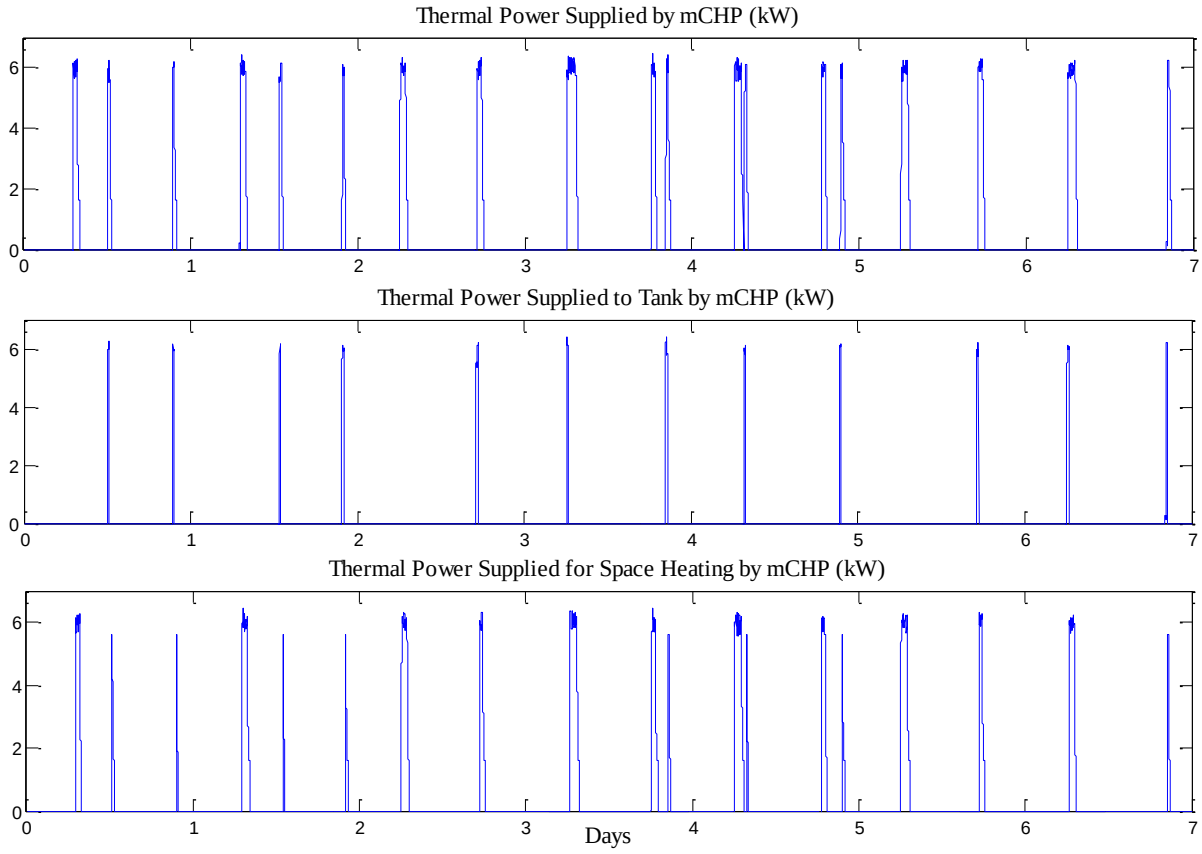

Figure 6.8 Typical winter week thermal power flows (semi-detached house type)

The electrical energy flow during a typical warm summer week is plotted in Figure 6.10 for the semi-detached house. On most days, micro-CHP is activated only once per day in summer and this is due to entirely domestic hot water demand. In summer, a stronger pattern of electrical export is seen and this is mainly due to daytime power generated by the PV modules (in this week, contribution from the wind turbine is very small). However, during this week power imported is high due to the restricted use of the micro-CHP since

the heating demand is now restricted to domestic hot water demand only and the power generated by PV system is outside the main occupied hours. The use of battery technology could be helpful at this point.

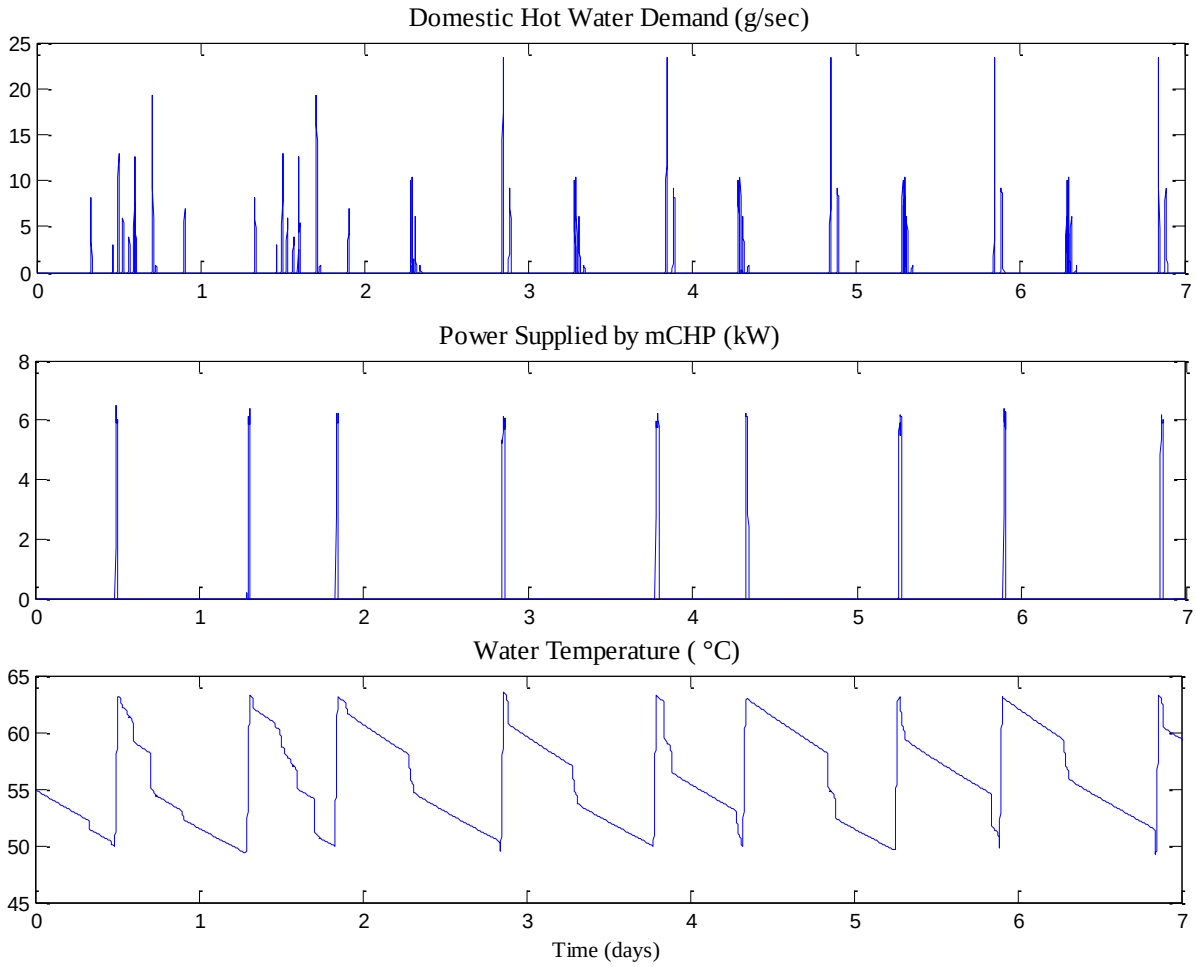

Figure 6.9 Typical summer week thermal power flows (semi-detached house type)

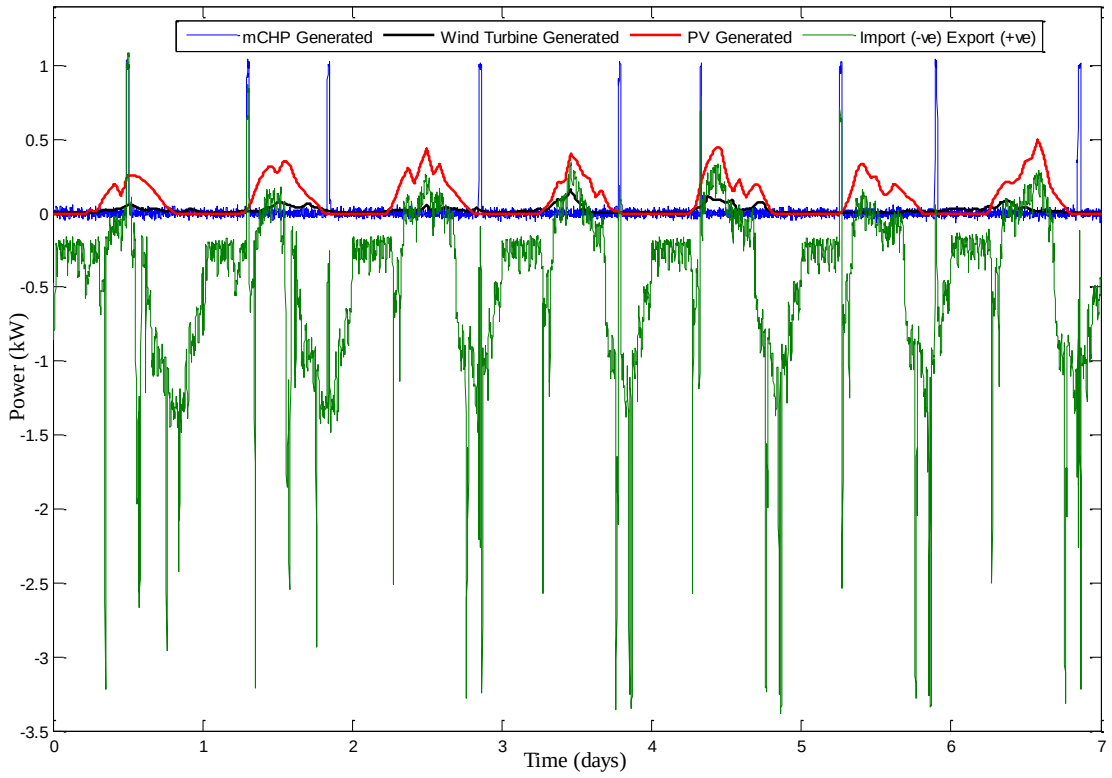

Figure 6.10 Typical summer week electrical power flows (semi-detached house type)

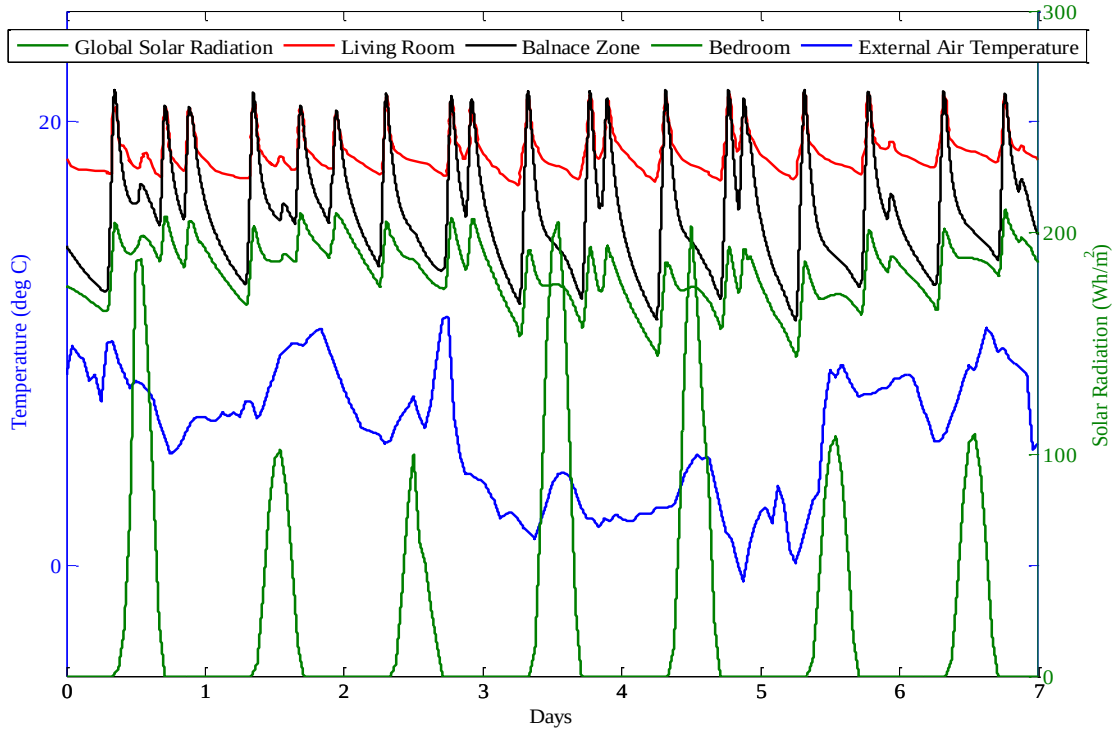

Figure 6.11 Typical winter week zone temperatures (detached house type)

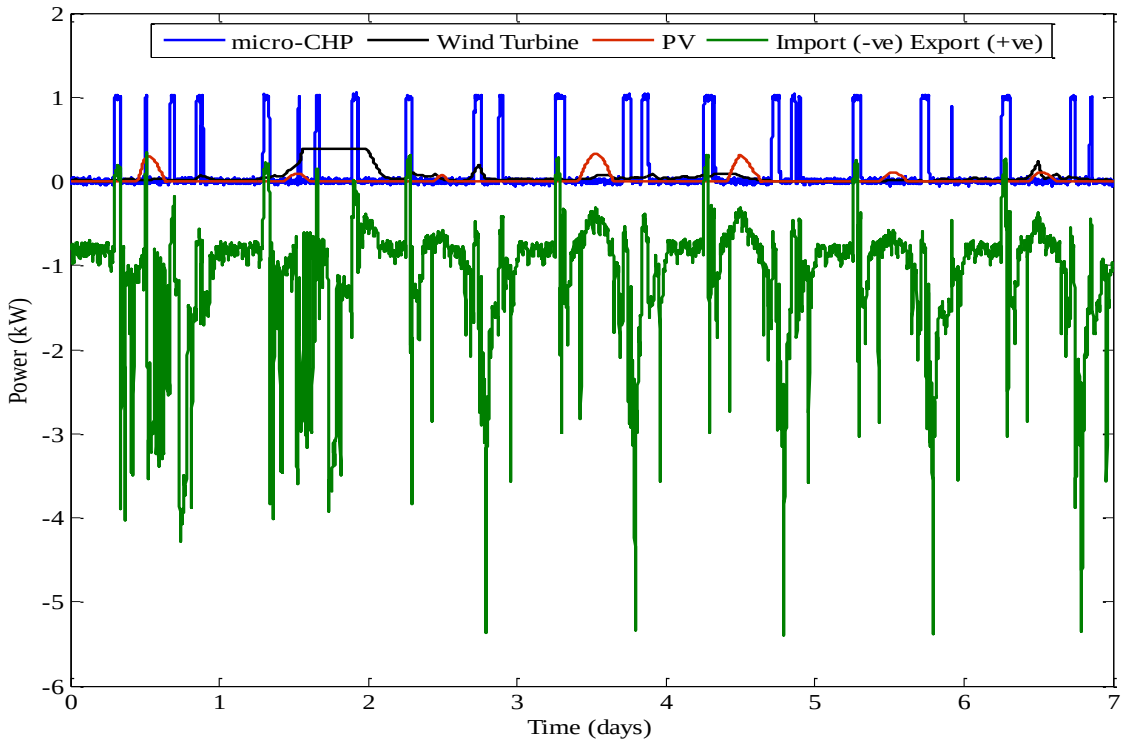

Figure 6.12 Typical winter week electrical power flows (detached house type)

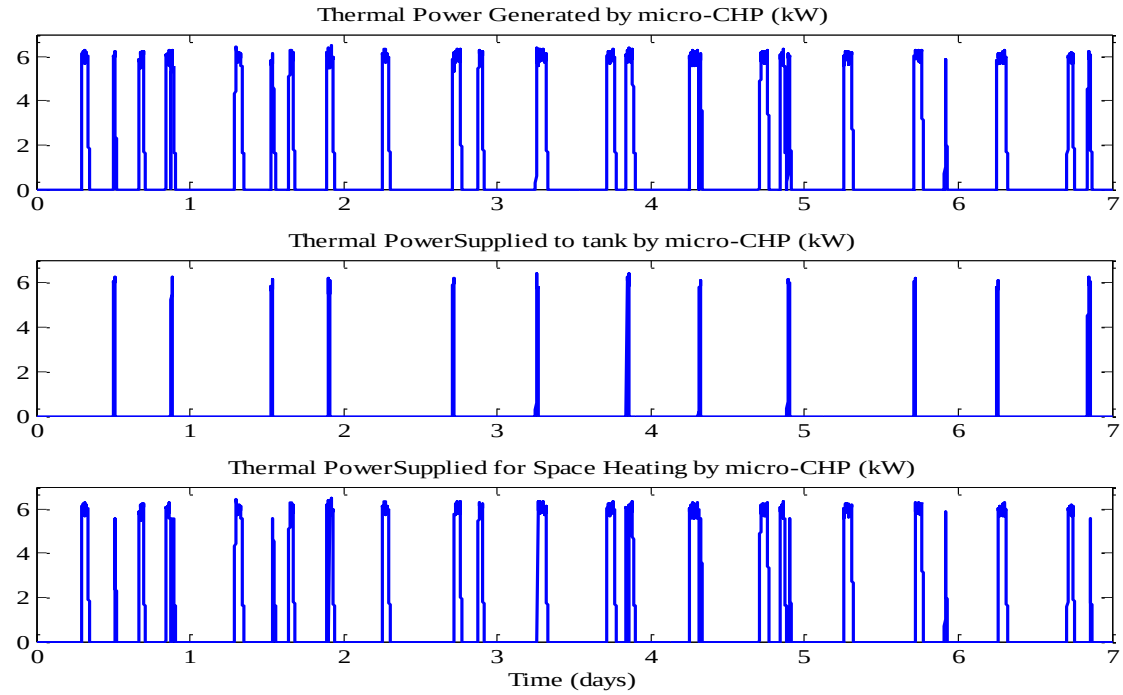

Figure 6.13 Typical winter week thermal power flows (detached house type)

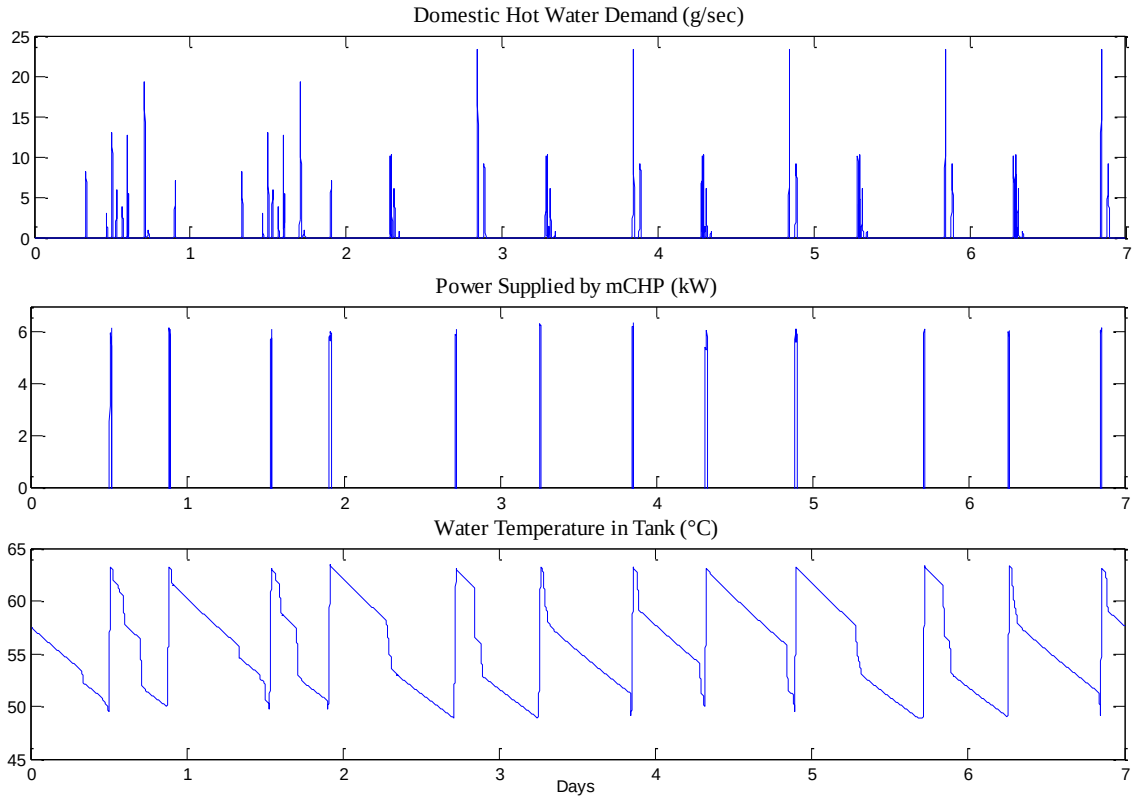

Figure 6.14 Typical summer week thermal power flows (detached house type)

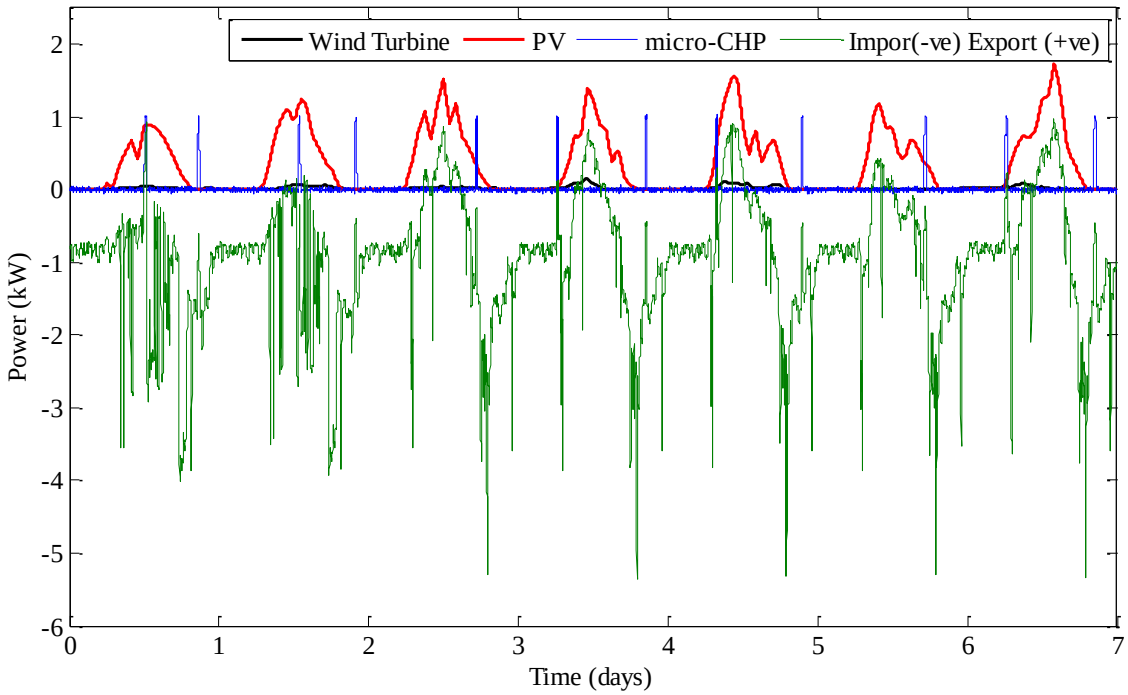

Figure 6.15 Typical summer week electrical power flows (detached house type)

The simulated annual total electrical and thermal energy loads are given in Table 6-3 and Table 6-4 for both house types. It is clear that heat-led strategy for the micro-CHP system restricts its ability to contribute electrical power. Indeed the power generated by the wind turbine and PV system both exceed that produced by the micro-CHP system (by a substantial degree in the case of the detached house type due to a much larger PV capacity). However, this is desirable in that the zero-carbon technologies dominate power in this application whereas the low carbon technology contributes a smaller share of the power but all of the heating. Combining technologies in this way, almost 20% of all power generated is exported by the semi-detached house but this falls to approximately 11% for the detached house due to its much higher power demand compared to semi-detached house which can be seen from Figure 6.3 and Figure 6.4. However, against the overall electrical demand for both houses, the micro-CHP system and renewable technologies met a similar proportion of around 20% of the demand of both house types (i.e. around 80% of the annual electricity demand needed to be imported). It is clear that the electrical contribution from the micro-CHP is heavily dependent on heating and hot water demand. To illustrate this point, consider the winter months November through February when very little renewable electricity is available (Figure 6.7), if all of the base demand for electricity (averaging approximately 250 W for the semi-detached house Figure 6.3, and 800 W for the detached house, Figure 6.4) was met by the micro-CHP system without regard to heating, then at least 720 kWh of electricity would be offered by the micro-CHP system to the semi-detached house (whereas the micro-CHP generated just 425.9 kWh in the entire operating year-Table 6-3) and 2304 kWh offered to the detached house (as against 719 kWh generated in the entire year-Table 6-3).

As to the heating (Table 6-4), the micro-CHP system met all of the domestic hot water demand and all of the space heating demand amounting to 2820 kWh for the semi-detached house and 5114 kWh for the detached house. The fuel consumption of the micro-CHP system was 4137 kWh for the semi-detached house and 7949 kWh for the detached house giving thermal efficiency of 68.2% and 64.5% and an electrical efficiency of 10.3% and 9.05% respectively. The overall fuel utilisations (electrical and thermal-to-fuel energy) are 78.5% and 73.4% respectively. The reason for the lower efficiency and fuel utilisation in the case of the larger detached house is due to greater number of cold system starts. The initial warm-up phase during a cold system start results in a short period of rated fuel usage during which the power and heat outputs are below their rated values.

The mean annual thermal efficiency of micro-CHP is 66.35% which is in consistent to [3] but lower by around 5% then [2] and as expected 10-15% lower than the condensing boiler. This is mainly due to some of the heat generated by micro-CHP is being used for the generation of electricity and more heat loss through the case of the micro-CHP systems compared to the condensing boiler [2]. Similarly, the mean electrical efficiency of micro-CHP is 9.67% which is again in consistent with [3] but higher by just over 3% than [2].

Table 6-3 Annual energy account (power)

ENERGY STREAM	**Semi-detached (kWh)**	**Detached (kWh)**
Generated by micro-CHP	425.9	719
Generated by wind turbine	256.87	256.87
Generated by PV modules	539.2	1752.7
Exported	233.6 (19.1%)	305.5 (11.2%)
Overall demand	5298	11542
Imported	4287 (80.9%)	9119 (79%)

Table 6-4 Annual energy account (heat)

ENERGY STREAM	**Semi-detached (kWh)**	**Detached (kWh)**
Demand due to space heating	1728	3995
Demand due to hot water	1092	1119
Annual fuel demand (natural gas)	4137	7949

Chapter 7 Proposed micro-CHP Controller

7.1 Introduction

As mentioned earlier in Chapter 2, most of the previous research in domestic micro-CHP has focused on the feasibility or performance of micro-CHP in a given scenario or on comparisons between different micro-CHP technologies with respect to carbon saving. In this chapter, a control tool for operation of micro-CHP system is designed using fuzzy logic control rules. This operation strategy allows a micro-CHP system to operate continuously with the aim to utilise the energy generated in an effective way to fulfil the energy demands. Another aim of the controller is to help the low voltage power network to get into a stable condition by determining whether to export the power generated or not. This strategy depends on the thermal demand in the building which is determined by monitoring the temperature of a key room and the temperature of hot water in the tank, as well as the state of the local LV grid. The added value about this control strategy is the response of micro-CHP with regards to the state of the grid. Here, the grid voltage is taken as a reference to determine the state of the grid whereas other parameters such as frequency, that define the stability of grid, can be used.

In addition to that, the influence of UK energy policies such as the Feed-in-tariff, carbon tax and alternative electricity trading scenarios may be considered during normal operating conditions (i.e. when the voltage of the grid is within the limit and there is thermal demand) is investigated using the fuzzy control strategy. These policies have different incentive mechanisms to encouraging the installation of micro-CHP technologies.

7.2 Fuzzy Logic Control

For the efficient operation of micro-CHP systems in domestic environment, different criteria have to be considered: the non-linear behaviour of micro-CHP, operation of micro-CHP during randomly varying electrical and thermal demand throughout the seasons and the impact that it could have on the grid. Due to these complexities inherent in the operation of micro-CHP, an intelligent technique is required for efficient operation. The fuzzy logic technique which aims to imitate the aspect of human cognition can deal with such complexities.

Fuzzy systems are based on fuzzy set theory and the associated techniques is pioneered by Lotfi Zadeh [118, 119]. Fuzzy logic control has gained considerable popularity in recent years. Fuzzy logic control is a knowledge-based approach consisting of linguistic If-Then rules that can be constructed using the knowledge and experience of experts in the relevant field. It can also exploit universal approximators that can realise nonlinear mappings. Unlike classical control strategies, which is point-to-point control, fuzzy logic control is a range-to-point or range-to-range control [120]. It cannot assure the global optimal performance of a system but it is capable of effectively providing a near optimal performance. Unlike Boolean logic, which describes that a given input is either a member of a given set (logic 1) or not (logic 0), fuzzy logic solves problems that change anywhere in the range from 0 to 1 [121]. Therefore, instead of sharp switching it offers smooth relocation of the output signal when one rule dominates the other. As a result, fuzzy logic is quite suitable to the system composed of nonlinear behaviours where an overall

mathematical model is difficult to obtain since the rules can be designed based on heuristics, intuition and human expertise [122].

The implementation of fuzzy logic control involves the following steps: fuzzification; a fuzzy inference process and defuzzification. Fuzzification converts data (crisp data) into fuzzy data or membership functions and these membership functions are combined with control rules to derive fuzzy output using a fuzzy inference process. During defuzzification, different methods are used to calculate each associated output.

Fuzzy logic is easy to implement, robust, flexible to change (in terms of inputs, outputs and rules) and it does not require any offline work. It is a transparent and qualitative technique, thus giving a simplified explanation of an operating technique. Fuzzy logic makes the application of a human language allowable for problem description and their solutions [123], however it requires good quality experiential knowledge and data about the controlled system's operating characteristics. It can be applied in many applications, especially when the system's model is unknown/uncertain or when the input parameters are unstable and highly variable [123]. This feature suits the purpose here as domestic energy demands have such characteristics. Changes in weather conditions or occupant behaviour could change the thermal energy demand (as modelled in Chapter 4) thus requiring immediate response from the micro-CHP. Fuzzy logic is applied in the modelling of vague systems which are imprecise and complex.

In terms of previous work, fuzzy logic based control techniques have been widely investigated for fuel cells as a source of energy in hybrid electric vehicles [124, 125] and as distributed generators [22, 51, 126] but has not been investigated for Stirling engine-based

micro-CHP. In [22] and [126] fuzzy logic controller has been used for controlling the power conditioning unit (DC–DC converter and DC–AC inverter circuits) where as in [51] fuzzy logic controller is used with an aim to minimise the operating cost and CO_2 emission of micro-CHP system. Consequently, fuzzy logic control would be developed and investigated for the Stirling engine based micro-CHP in this chapter.

The main idea about the fuzzy logic is to efficiently manage the energy generated by the micro-CHP system to fulfil the energy demands and help the local grid to maintain its stability. This principle can guarantee minimising the total amount of primary energy used and carbon emission. Minimising the total amount of primary energy used will result in minimisation of the total operating cost. The fuzzy logic controller is formulated in a generic form to allow its use for any micro-CHP system and any thermal energy demand patterns with the flexibility of giving the desired (or maximum) set temperature for the controlled room and hot water.

A fuzzy logic controller is designed in this work as the decision maker for the switching of the micro-CHP unit using three input variables: key (controlled space) room temperature, hot water temperature (i.e. water temperature inside the thermal storage device tank) and the voltage of the local LV network. Figure 7.1 shows a simple block diagram of the proposed fuzzy controller for the micro-CHP. In some literature [51], electricity demand of the house is also considered as one of the most influential input variables for the operation of the micro-CHP unit. The micro-CHP considered in this research is a Stirling engine-based micro-CHP which is heat-led so the electrical load is not considered as an input for the controller.

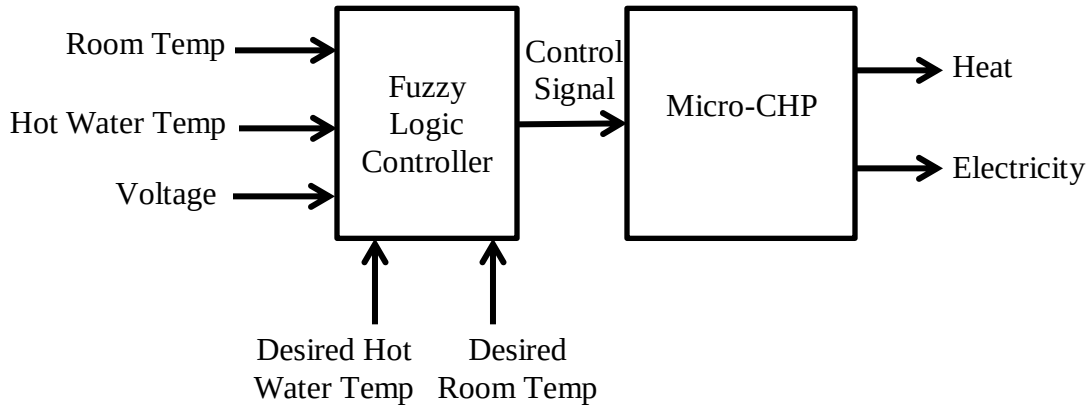

Figure 7.1 Fuzzy controller for micro-CHP

7.3 Design of a Fuzzy Logic Controller

Designing of the fuzzy logic controller includes the development of: input fuzzification; a fuzzy inference system and defuzzification. Building the rules for the fuzzy logic controller has been given particular attention as it plays the main role in the process. As mentioned previously, the controller is designed with three inputs: room temperature (°C), hot water temperature (°C) and the grid voltage (p.u.) and one crisp output as the control signal which varies from 0 to 1. The fuzzy logic controller sends an 'ON' signal to micro-CHP when the output signal reaches value of 0.2 and 'OFF' signal when the output signal reaches 0.8. These thresholds are chosen so that as it keeps the micro-CHP 'on' for longer time keeping hot water and room temperature close to desire temperature and thus decreasing the number of switching. One thing to remember is that the controller is only active when the house is occupied by active occupant(s).

7.3.1 Membership function

An assessment of the membership function of a variable is an important step in applying fuzzy methods. Membership functions are curves which define each element of a variable mapped to a value between 0 and 1. This value is called the degree of membership or membership value and quantifies the grade of membership of the element. This process is called input fuzzification.

Membership functions can take any form as the designer of the system requires. Triangles, trapezoids, bell curves or any other shape as long as those shapes accurately represent the distribution of information within the system and as long as a region of transition exists between adjacent membership functions. However, selections of the shape of the membership functions and break points within the input and output universes affect how the controller works. In this work, trapezoidal membership functions have been chosen for the low, the medium and the high of all the fuzzy inputs due to its simplicity and suitability. Similar fuzzy logic based controller has been used by Shaneb *et al.* [51] for fuel cell based micro-CHP. Figure 7.2, Figure 7.3 and Figure 7.4 show the membership functions of the hot water temperature inside the thermal storage tank, the room temperature and the voltage in per unit system respectively. Per unit system is used in power systems to express values of different power system parameters such as voltage, currents, powers and impedances of the power equipment and grid. For a given parameter, per unit value is a value related to a base quantity.

As the desired hot water temperature and desired room temperature are given to the controller, the difference between the instantaneous and the desired temperatures is given

as the inputs for the controller as shown in Figure 7.2 and Figure 7.3. As the set room temperature and hot water temperature can vary, temperature difference is given as input to the controller. It should be noted that membership functions can overlap while defining its region, which makes the possibility for a certain temperature to be member of two sets at the same time. For example, when the hot water temperature difference is -10°C it has a membership value of the medium and low membership functions. This shows one of the ways in which the fuzzy logic deals with the uncertainty.

Membership functions of different types and of asymmetric nature have been investigated but symmetric sets of trapezoid membership functions have performed slightly more effectively. As a result, the symmetric trapezoid membership functions as shown in Figure 7.2 have been adopted for all the inputs and the output in the present work.

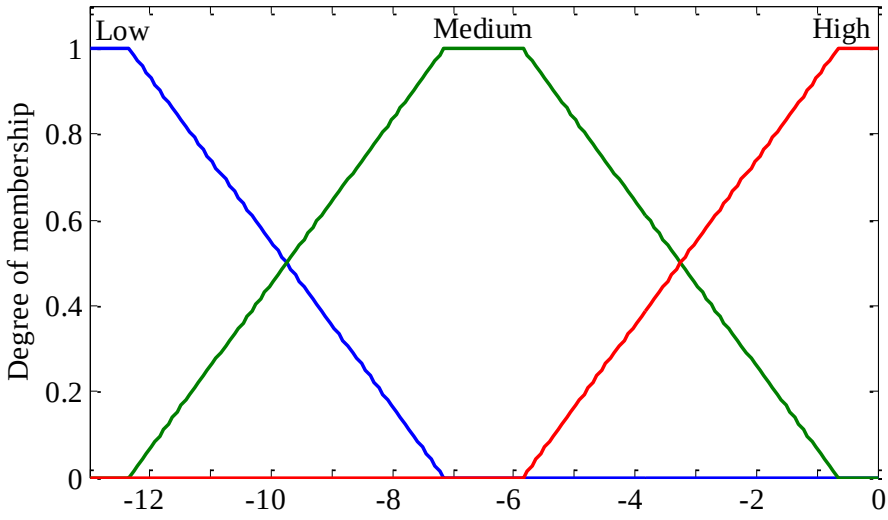

Figure 7.2 Membership function of hot water temperature difference

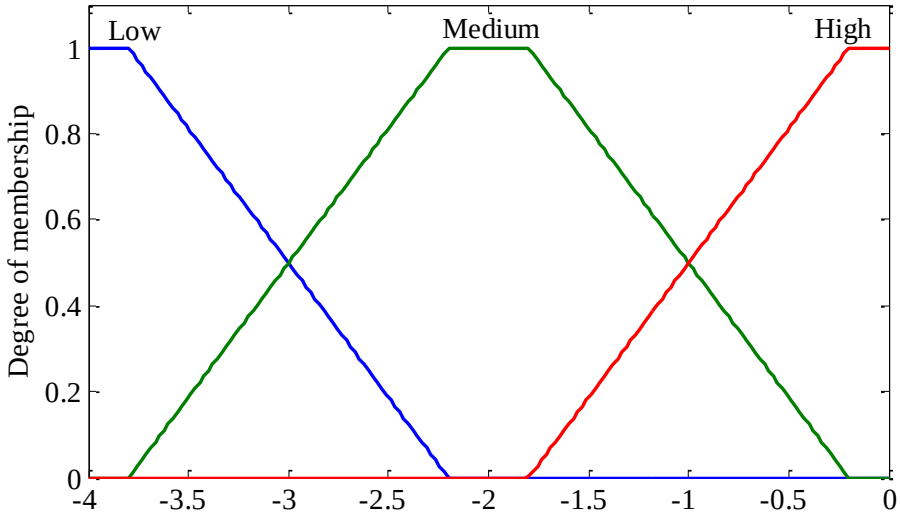

Figure 7.3 Membership function of room temperature difference

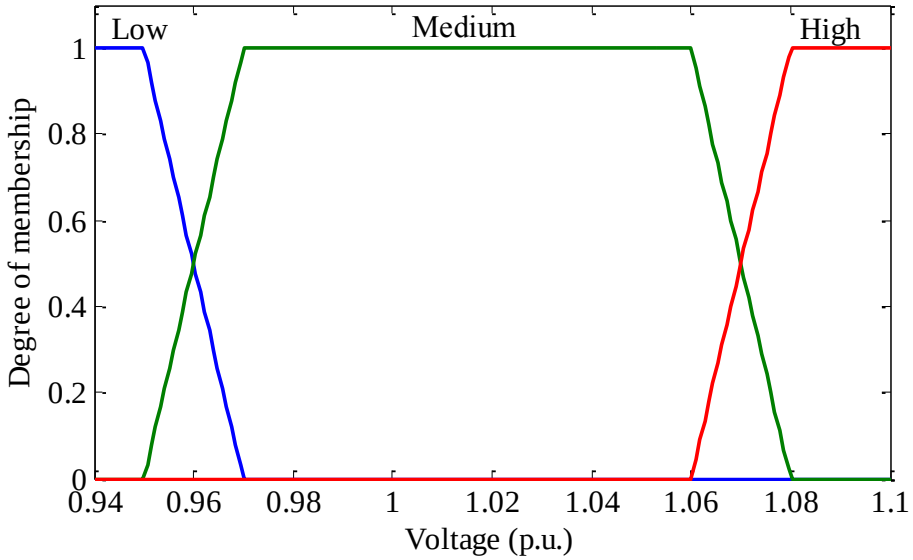

Figure 7.4 Membership function of voltage

In Mamdani type fuzzy inference, the output membership functions are defined in a similar manner to input membership functions. However, in Sugeno type fuzzy inference the output membership functions are either linear or constant. Sugeno type fuzzy inference is

considered with one output having three constant membership functions whose parameters are 1, 0.5 and 0 for high, medium and low respectively.

7.3.2 Rule base

Fuzzy logic controllers are rule-based systems that use fuzzy linguistic variables to model human 'rule-of-thumb' approaches to solve problems. The process state is evaluated and the output of the fuzzy logic is determined at instantaneous time as a function of the inputs and the rules. The rules are in the form of:

IF (process state 1) **AND** (process state 2) **AND** (process state 3) **THEN** (fuzzy logic output); and

IF (process state 1) **OR** (process state 2) **THEN** (fuzzy logic output)

IF and AND/OR parts of the rule (i.e. before THEN) are known as antecedents while the THEN parts are known as consequents.

The selection of the rules is based on the idea of utilising the electrical and thermal energy produced by the micro-CHP and fulfilling the energy demand of the dwelling. As mentioned earlier, three linguistic input variables and one output variable of fuzzy logic (each having three membership functions), have resulted in 8 rules which are presented in Table 7-1. It is to be noted in Table 7-1 that H, M and L denote high, medium and low respectively.

Table 7-1 Rules of the proposed Fuzzy logic controller

		Low Room Temperature			Medium Room Temperature			High Room Temperature		
		Tank Temperature			Tank Temperature			Tank Temperature		
		L	**M**	**H**	**L**	**M**	**H**	**L**	**M**	**H**
Voltage	**L**	H	H	H	H	H	H	H	H	L
	M	H	H	H	H	M	M	H	M	L
	H	H	H	H	H	L	L	H	L	L

7.3.3 Fuzzy inference process

The fuzzy inference process is the process of formulating the mapping from a given input to an output using fuzzy logic. The mapping then provides a basis from which a decision can be made and the process involves the membership functions, fuzzy logic operators and the if-then rules.

A fuzzy inference process comprises of five different process [127]:

- Fuzzification of the input variables
- Application of the fuzzy operator (AND or OR) in the antecedent
- Implication from the antecedent to the consequent
- Aggregation of the consequents across the rules
- Defuzzification

The fuzzy inference process that a fuzzy logic controller uses to convert input values into an output value is shown in Table 7-2. The operator '*Prod*' refers to the product of the input variables, operator '*Probor*' refers to the probability OR which is calculated as:

$$Probor(a, b) = a + b - ab$$

and '*Wtaver*' refers to weighted average.

Table 7-2 Operators for the fuzzy logic controller

Stage	**Operator selected**
AND method	*Prod*
OR method	*Probor*
Defuzzification	*Wtaver*

7.4 Results and Discussion

The fuzzy logic controller has been integrated within the micro-CHP system of the whole integrated simulation model discussed in the Chapter 6. The output of the fuzzy controller varies from 0 to 1 but switching of the micro-CHP is either 'ON' or 'OFF' (i.e. cannot modulate). So, switching of micro-CHP is controlled in such a way that as the output of fuzzy controller reaches 0.8, micro-CHP is switched 'ON' and remains 'ON' until the output drops down to 0.2.

It is assumed that most of the time the grid voltage will be close to 1 p.u. so the fuzzy logic controller was investigated with different grid voltage scenarios: i) grid voltage is close to 1 p.u. and ii) grid voltage close to upper or lower limit. When the grid voltage is close to 1 p.u., two different scenarios associated to costs and its CO_2 emissions were also

investigated and compared to the results obtained without the integration of the controller within the micro-CHP system.

7.4.1 Network operating under healthy voltage condition

Healthy voltage condition refers to the network with voltage within 0.97 p.u. and 1.06 p.u. In this case the input voltage to the fuzzy logic controller is assumed to be completely within the medium membership function i.e. within the voltage of 0.97 p.u. and 1.06 p.u. (refer to Figure 7.4).

Under this scenario, two different scenarios have been investigated to establish how the micro-CHP unit along with other renewable energy sources operate and quantify its associated operating cost and CO_2 emissions. The investigations represent a comparison between with and without the fuzzy logic controller within the micro-CHP including the renewable energy sources and conventional boiler.

7.4.1.1 Feed-in-tariff (FIT) scenario

In 2010, the UK government introduced the feed-in-tariff (FIT), also known as the Clean Energy Cashback scheme. It is a scheme designed to promote the uptake of a range of small-scale renewable and low-carbon electricity generation technologies. The FIT is a price based mechanism where prices are differentiated by technology and size of installation. The FIT guarantees to pay a fixed tariff for each kWh of electricity generated and an additional payment for each kWh of electricity exported to the grid. The FIT is eligible for PV and wind turbines of total installed capacity not exceeding 5 MW and micro-CHP which has a limit of 2 kW. Feed-in-tariff rates are index-linked which means

that they will increase or decrease with inflation. It is a payment guaranteed for 20 or 25 years for PV and wind turbines and 10 years for micro-CHP from the date of installation. Since the introduction of FIT, installation of renewable and low carbon technologies has rapidly increased in the UK [128].

The feed-in-tariff consists of generation and export tariffs which have different rates for different technologies. Tariff rates for different technologies considered are given in Table 7-3 [129].

Table 7-3 Feed-in-tariff for different technologies

	Feed-in-tariff (p/kWh)		
	Generation	**Export**	**Date**
PV	14.9	4.64	01/07/2013 to 01/10/2013
WT	21.65	4.64	01/12/2012 to 31/03/2014
Micro-CHP	12.89	4.64	01/04/2013 to 31/03/2014

The price of electricity imported from the grid is considered at a fixed rate of 12 p/kWh and the price of natural gas is considered on fixed rate of 3.75 p/kWh [130]. According to National Calculation Methodology (NCM) modelling guide [131], CO_2 emission factors for the UK grid supplied electricity, grid displaced electricity and natural gas are 0.517 $kgCO_2/kWh$, 0.529 $kgCO_2/kWh$ and 0.198 $kgCO_2/kWh$ respectively. Maintenance costs considered are to be £50/year for wind turbine [38] and PV [42], for Stirling engine based micro-CHP it is considered to be £0.09/kWh [5] and for conventional boilers, it is considered to be equal to micro-CHP [2]. Using all this information, operating costs for a whole year are calculated with and without the fuzzy logic controller for the both semi-

detached and detached house case studies as described in Chapter 6. The results are summarised in Figure 7.5. The operating cost for semi-detached house is £663 and £647 without and with fuzzy logic controller for micro-CHP and for detached house it is found to be £1295 and £1273 without and with fuzzy logic controller.

Considering a case when there is no micro-CHP and renewable energy sources installed in the dwelling, all its thermal demand is fulfilled by a boiler and all its required electricity is imported from the grid. Assuming a boiler efficiency of 85% [2], total operating cost per year for semi-detached and detached house to fulfil their thermal and electrical demand is £769 and £1625 respectively. Note, cost of electricity consumed by the boiler is not taken into account in the calculation of operating cost. Similarly, the CO_2 emissions due to the use of natural gas and electricity imported for semi-detached and detached houses are 3396 $kgCO_2$ and 7159 $kgCO_2$ respectively.

The operating cost of micro-CHP with controller when compared to the operating cost of conventional boiler-based system and micro-CHP without controller show that there is annual saving of £106 and £16 respectively for the semi-detached house and £330 and £17 respectively for detached house.

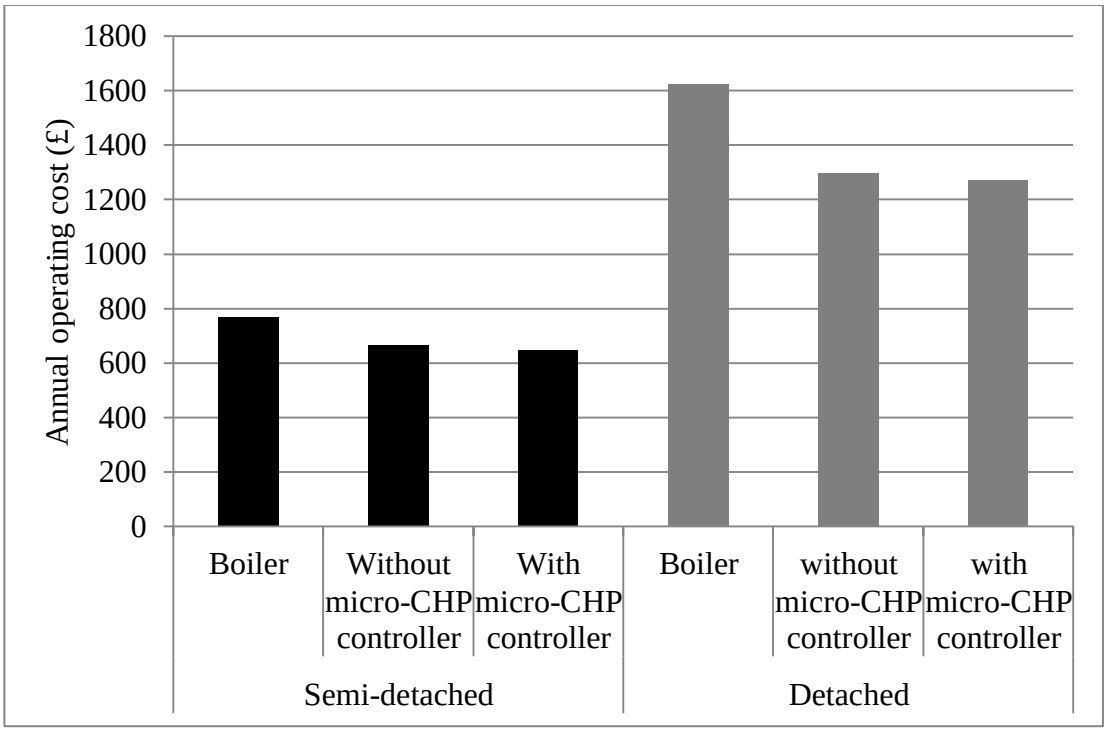

Figure 7.5 Annual operating costs for semi-detached and detached house for different scenario

Similarly, Figure 7.6 shows the annual CO_2 emission for both types of houses based on the use of a boiler and with and without the micro-CHP fuzzy logic controller. For the semi-detached house, with controller for micro-CHP there is saving of 497 $kgCO_2$ and 78 $kgCO_2$ when compared to the conventional boiler and micro-CHP without controller respectively. Similarly for a detached house the respective savings are 1073 $kgCO_2$ and 91 $kgCO_2$.

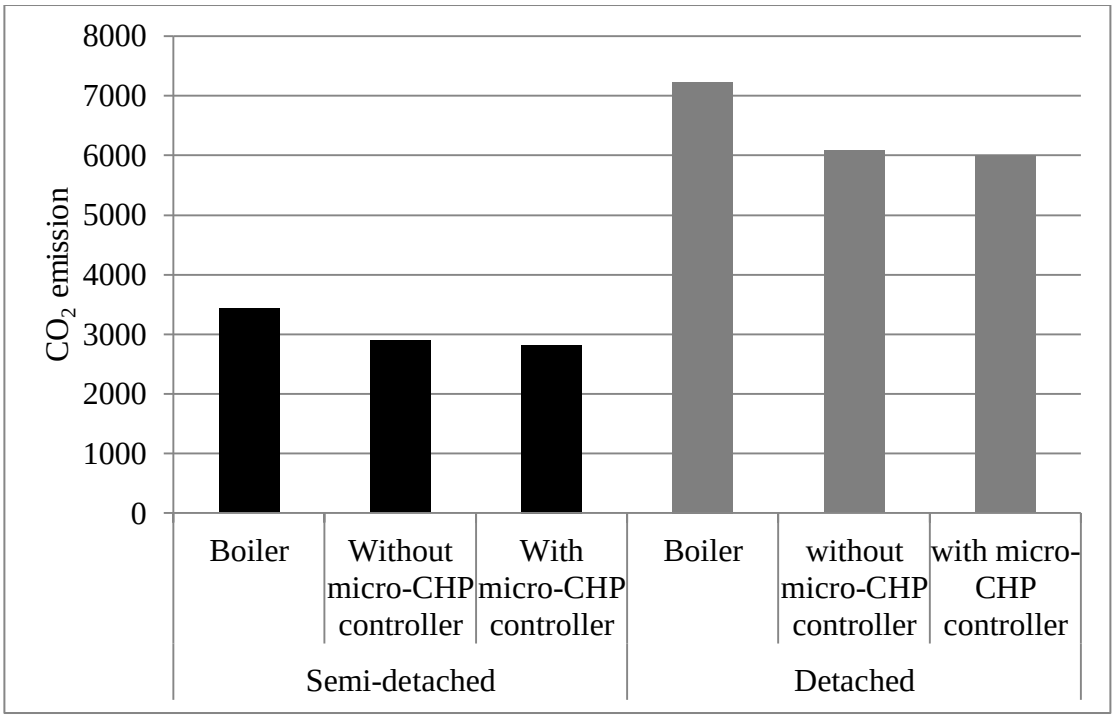

Figure 7.6 Annual CO_2 emission for the semi-detached and detached house for different scenarios.

7.4.1.2 Electricity trading scenario

The feed-in tariff has changed since it was first introduced and is likely to change again in the future. Taking the case of the FIT for a PV system, the tariff has been decreased by more than 50% since it was introduced and the period for which it is paid has also changed from 25 years to 20 years. In the case of micro-CHP, the FIT is only applicable to the first 30,000 units installed and is paid for only 10 years [132], so the electricity trading scenario has been considered. In this scenario any surplus electricity generated by the distributed generators can be sold and exported to the grid and any deficit in electricity can be purchased and imported from the grid.

The values assumed for the maintenance cost of distributed generators and CO_2 emission factors are the same as considered in the FIT scenario. However, the price of natural gas is considered to be on a fixed rate of £0.0228/kWh and the price of electricity met by the micro-grid is considered at a fixed rate of £0.082/kWh [133]. Also, the price of exported electricity is considered to be fixed rate at different percentage value of retail price. Results obtained are summarised in Table 7-4.

The results show that a maximum saving is achieved for the detached housed when the electricity price of exporting is the same as the retail price (i.e. 100%) and micro-CHP with a fuzzy controller is considered. The annual saving of £143 is obtained by exporting electricity when compared to the boiler. Similarly, the maximum saving achieved for the semi-detached house is £40 under the same conditions.

Table 7-4 Annual operating costs and savings when electricity trading scenario is considered for both houses

		operating cost per year (£)		
		50% of retail price	**75% of retail price**	**100% of retail price**
Semi-detached	**Without controller**	536	531	527
	Saving	28	33	38
	With controller	534	529	525
	Saving	31	36	40
Detached	**Without controller**	1,016	1,010	1,004
	Saving	125	131	138
	With controller	1,012	1,005	999
	Saving	131	137	143

From both scenarios, it is seen that the saving obtained is not significant as most of the power generated by the distributed generations are used within the houses even when the house is not occupied since standby loads absorb the available renewable power generated resulting in a lower amount of power export. Another point to note is that, as the economics of micro-CHP unit is strongly driven by the value of the electricity generated and the heat to power ratio of Stirling engine based micro-CHP is high, a small contribution to export power is achieved when it is active. Furthermore, a limitation in modulation of the considered Stirling engine based micro-CHP also limits the saving potential.

In the case of the FIT scenario, as the tariff of exported power to the grid for all considered technologies is much less than the imported power, more saving could be achieved by maximising the proportion of electricity generated within the house rather than exporting. Scheduling the electrical loads such as the washing machine to coincide with heat demand or mid-day when PV generates power is one way to maximise the energy use when generated by micro-generators.

Comparing the saving with the two different scenarios, the FIT scenario seems to be better than the electricity trading scenario with a total annual saving of £209 (when the export electricity price is the same as the retail price in the electricity trading scenario), for detached house. Similarly, for semi-detached house, the total annual saving is £83.

7.4.2 Network operating close to statutory limits

One of the main aims of the fuzzy logic controller is to support the distribution network and in this scenario the operation of the fuzzy logic controller is discussed. Support to the distribution network can be looked upon in two scenarios: i) when the voltage in the

distribution network is close to the upper voltage limit and ii) when the voltage in the distribution network is close to the lower voltage limit.

7.4.2.1 Network operating close to upper voltage limit

As mentioned earlier when there is thermal demand, the micro-CHP is switched on and if there is any excess power generated by micro-CHP, it is exported to the grid. However when the voltage of the network is high at this time, the export of power to the grid will contribute to an increase in the voltage of the distribution network. In such situations, the export of power should be discouraged. Different options could be used to avoid the export of power such as using home energy management system or load scheduling, use of electrical storage or heating water in a tank.

In home energy management system, each appliance is implemented as a task in a priority list based on predefined user instructions and each task can be either non-interruptible or interruptible depending upon the nature of the appliance. However, for home energy management systems to work, all appliances should be connected to a central processor which executes the task on schedule with a two-way communication between them. Adding electrical energy storage (i.e. a battery in the dwelling) is another solution to avoid power export care regarding battery selection is need along with a consideration of the additional cost. Important issues concern limiting the charging and discharging rate of the battery, preventing the battery from getting over-charged or over-discharged, the addition of converters (maintenance and losses), rewiring of the house to fulfil battery and health and safety requirements. In another solution, heating water in the hot water tank using the

immersion heater if the temperature of water is below the maximum set temperature can be considered and is discussed in this section.

The voltage profile shown in Figure 7.7 [18] is obtained for the winter season when 1.1 kW of micro-CHP operating at a 0.97 lagging power factor was connected uniformly through the low voltage distribution network, Figure 5.20. This is used as a reference voltage and as an input to the fuzzy logic controller.

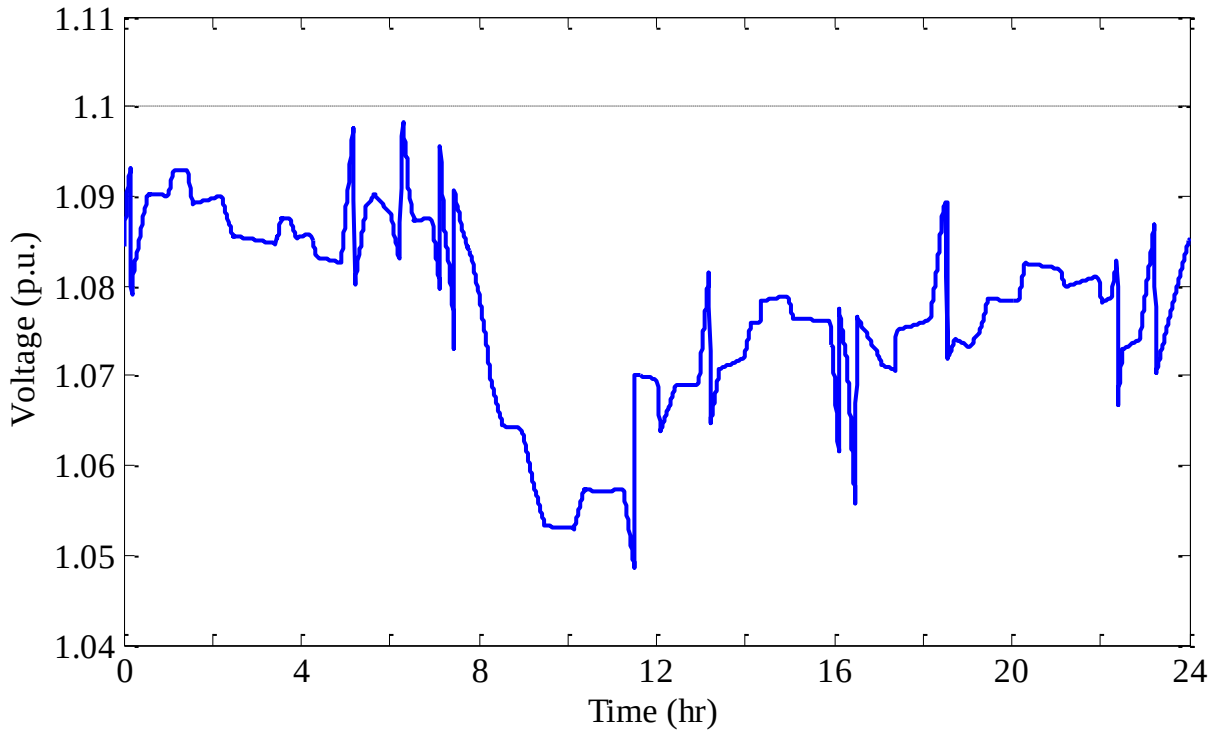

Figure 7.7 Voltage profile when micro-CHP operating at 0.97 lagging was considered.

A simulation of the detached house for a winter weekend (occupancy pattern: 08:00 – 23:00) is carried out with all the inputs same as mentioned in section 6.2 for the detached house and results are shown in Figure 7.8.

It can be seen from the voltage profile, Figure 7.7 that the voltage is close to the upper limit in early morning when the electrical demand is low and generation from micro-CHP is high. At 07:00 hours, the thermal demand (room heating and water heating) starts so micro-CHP is switched 'ON' but at the same time the voltage of the distribution network is close to the upper limit so the electrical power generated by micro-CHP is also used to heat water in the tank instead of exporting to the grid (power graph in Figure 7.8). Similarly, at 22:00 hours when room heating is required and the voltage is close to the upper limit of power generated by the micro-CHP, the power is used to heat water in the tank as it is below the desired set temperature of 62 °C.

Heating water in the tank with power generated by the micro-CHP can be looked on as heating water with much less efficiency than a conventional boiler. However, by limiting the export of power to the grid from many houses in such a way, a possible black out of the grid could be avoided by avoiding further increase in voltage.

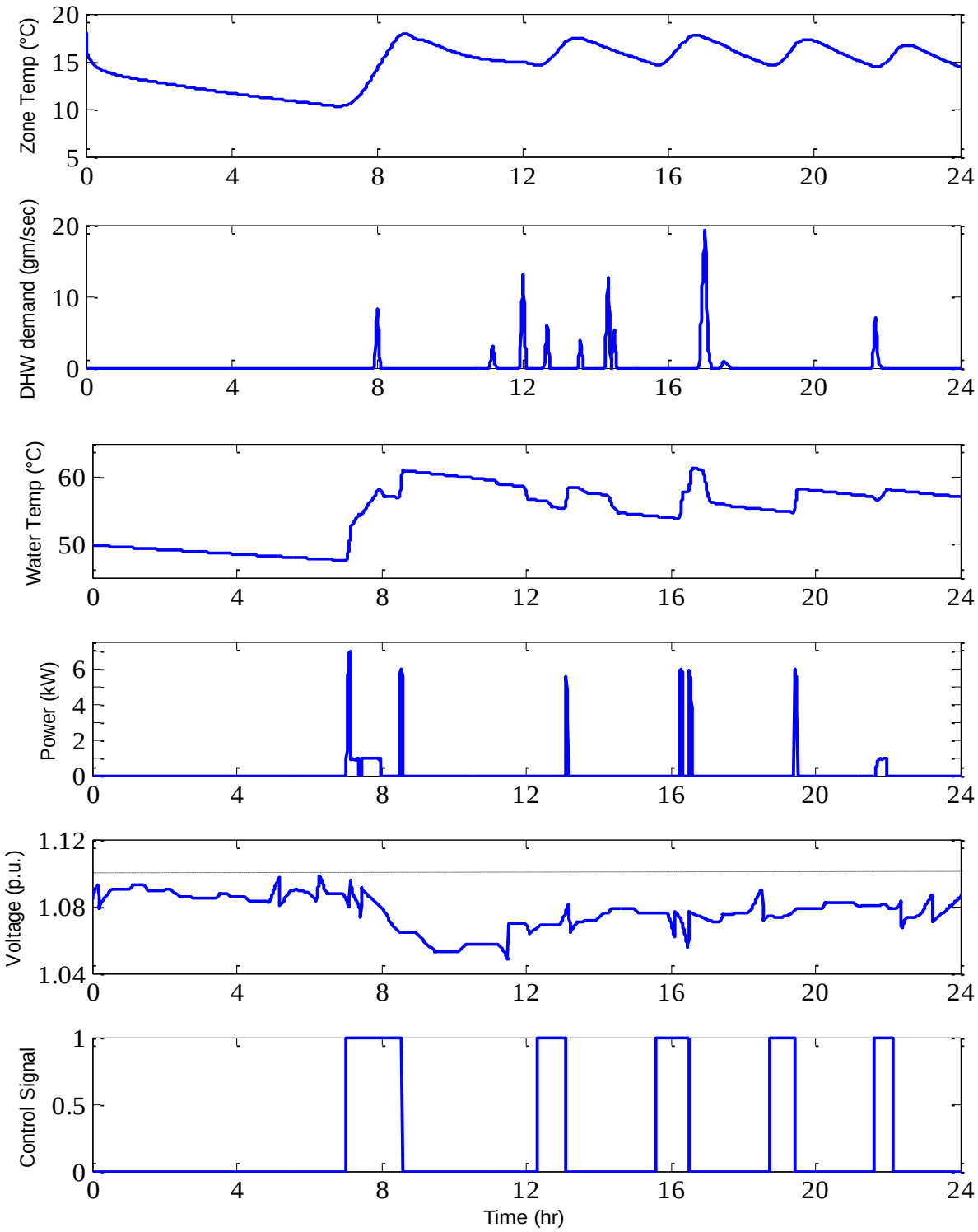

Figure 7.8 Operation of fuzzy logic controller when is voltage close to upper limit

7.4.2.2 Network operating close to lower voltage limit

The voltage of the local LV network tends to decrease when the load connected increases as discussed in section 5.5.2 so in order to avoid a further decrease in network voltage, the load connected should be decreased or power should be generated. Possible solutions as discussed in previous section 7.4.2.1 could be applied for this scenario as well by using home energy management system to decrease the load demand or use of electrical storage as a power generation source. This scenario looks into the situation how micro-CHP contributes to the distribution network through fuzzy logic control when the voltage of is close to lower limit. The voltage profile obtained when simulating the typical winter load profile in the distribution network from section 5.5.3 is used as the reference voltage for the fuzzy logic controller. A simulation of the detached house for a winter weekend is performed with same inputs as in section 6.2 and results are shown in Figure 7.9. When the house is occupied and there is thermal demand, the micro-CHP is switched 'ON'. It is to be noted at 18:00 hours that the voltage is close to the lower limit. At this time, to support the distribution network, the micro-CHP is switched 'ON' and heats the house radiators. This can be seen from zone temperature graph in Figure 7.9 where internal space heating is earlier than at other times. In this scenario, the micro-CHP heats the radiators or water in the tank which ever has higher demand. This option would only be permitted for limited time periods on occasions when the heat may not be in demand but can be accumulated for later benefit.

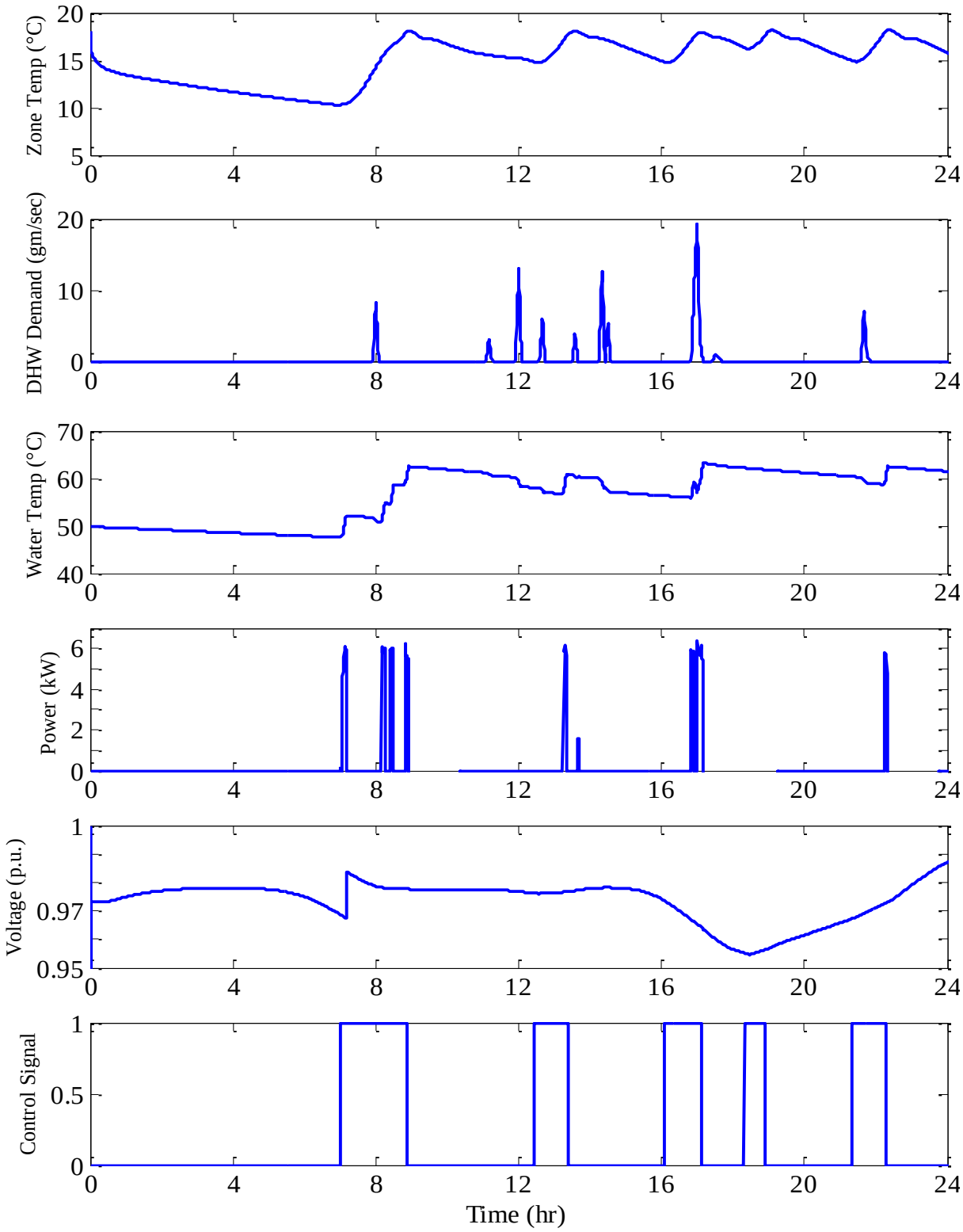

Figure 7.9 Operation of fuzzy logic controller when is voltage close to lower limit

Chapter 8 Conclusions and Further Work

It has been recognised that the current energy demand, (including heating and power demands in buildings) and the amount of energy consumed worldwide are not sustainable. In the efforts to prevent energy crises and environmental damage, a combination of improved energy efficient technologies and renewable energy sources such as PV, wind turbines and micro-CHP are being continually developed and connected to the grid. However, large deployment of these technologies may create new problems in the power distribution network such as voltage instability, rise in fault current, reverse power flow and voltage unbalance.

In order to optimise the energy generated by the micro-CHP and prevent potential problems for the distribution network (i.e. maintain the stability of the power distribution network), a controller based on fuzzy logic for micro-CHP has been proposed in this research. The research focused on the energy flow to and from a building in the presence of possible alternative energy sources (in the building) and a consideration of the stability of the electricity grid (which can be monitored via the smart meter).

8.1Energy Flow within a Building

In this research, a new transfer function based model for Stirling engine based micro-CHP (based on experimental data), which has the advantage of both simplicity and yet high accuracy has been developed. The developed micro-CHP model can accurately simulate the start-up and shut down characteristics of a domestic scale micro-CHP system and is able to

respond at very small time intervals, allowing analysis of high frequency behaviour of electrical and hot water demands.

The proposed model is the first modelling work which involves a micro-CHP module coupled to a house heating system that is fully dynamic in nature (previous models suggested in the literature allow steady-state based analysis only). The proposed building integrated energy model is uniquely capable of dealing with spikes in load demands (i.e. hot water and electrical demands) as well as being able to interact with energy storage dynamic models, such as hot water tanks and batteries, potentially in electric vehicles.

An integrated dynamic simulation model of a building with its heating system for analysing micro-CHP systems and optional renewable energy sources such as PV and wind turbines in domestic application has been developed and presented in this thesis. A detailed dynamic treatment of the plant, equipment and building elements has been considered.

There are few limitations of the models presented.

- The solar irradiation model does not consider any blinds, curtains or internal shading devices. All radiant sources are assumed to be distributed uniformly to all opaque room surfaces with the exception of the direct component of solar radiation which is assumed to be absorbed by the floor surface only.
- The modelled micro-CHP model representing Whispergen MKV does not include the auxiliary burner.
- Constant inverter efficiency is assumed in PV modelling, assumption of ambient temperature for the PV modules.
- Simplified wind turbine model with MPPT was used.

The model has been applied to two typical UK houses: a semi-detached and a detached houses consisting of 3 and 4 bedrooms respectively. Energy use in each house was simulated for analysing typical winter and summer operating weeks as well as for the whole year using hourly weather data of rural area with optimum wind direction. Renewable energy sources and micro-CHP were considered to be installed in both houses. Results show that the electrical contribution by the micro-CHP heavily depends on the thermal demand of the building, especially the space heating, as time taken to warm the rooms up to the desired temperature is longer as compared to water heating demand patterns. Results also show that the power exported from the micro-CHP and renewable energy sources mainly depends on the electrical demand of the house. Electricity generated by these sources can contribute to around 20% of the overall electrical demand of both types of house considered in this work. However the increased number of micro-CHP module starts in the case of the detached house was found to result in a reduction in the electrical efficiency and overall fuel utilisation of the micro-CHP as compared with the semi-detached house type where the number of micro-CHP starts was lower.

8.2Proposed Fuzzy Logic Controller

A fuzzy logic controller which is capable of minimising the annual operation cost and CO_2 emission of a micro-CHP module has been developed and evaluated. The developed fuzzy logic controller is also capable to control depending upon the stability of the local electrical distribution network. This controller has been designed for a Stirling engine based micro-CHP module arranged in heat-led mode to allow for demand profiles and a wide range of desired room and hot water temperatures. Different scenarios were considered for the

evaluation of the fuzzy based controller, depending upon the state of health of the power distribution network.

Based on the results obtained for the annual operating cost, the feed-in-tariff scenario was found to be more favourable compared to an electricity trading scenario (even when the export tariff was the same as the import tariff for the electricity trading scenario) and an annual saving of up to £208 could be achieved. Micro-CHP unit with the fuzzy logic controller when compared to conventional boiler based system and micro-CHP without the fuzzy logic controller shows there is annual operating cost savings of £156 and £16 respectively for the semi-detached house and £380 and £17 respectively for detached house. Similarly, an annual carbon saving of just under 17% was achieved for both types of houses when compared to conventional boiler-based heating systems.

Even though thermal demand of typical domestic houses in the UK has been modelled based on the weather conditions, the result presented does not to give a definitive answer in regard to the economic viability of micro-generation systems as the electrical demand of the houses has been created by only typical weekday and weekend pattern which is repeated for whole year and due to the limitation of the models as mentioned above. Government supports have proven to be extremely important in the penetration of micro-generation technologies in domestic sector. However, a broad conclusion regarding with economic viability of micro-generation systems could be made. The micro-generation system is not economically viable under current conditions due to the large capital cost. Payback period were estimated to be longer than the working life time of the micro-generation systems. In case of micro-CHP, the difference in capital cost between a micro-

CHP system and an equivalent condensing boiler is one of the key drivers of its cost effectiveness along with its lower electrical efficiency. Increasing the electrical efficiency of micro-CHP systems would significantly improve their economics, as the value of a unit of electricity generated is much higher than a unit of heat. Utilisation of the electricity generated within the house could improve the economics rather than exporting, as the export tariff is much less than the retail price of electricity, by scheduling electrical loads such as a washing machine to coincide with periods of heat demand.

The response of the fuzzy logic controller with respect to supporting the grid is also shown either by switching the micro-CHP 'ON' when the voltage of the grid decreases (and is close to the lower statutory voltage limit), or by switching the micro-CHP 'OFF' when the voltage increases and is close to the upper statutory limit. In this research, the voltage of the LV network via a smart meter is taken as a reference signal; however other signals such as frequency and dynamic pricing can also be taken as a reference.

When considering the practical implementation of the proposed fuzzy logic controller, it provides a number of attractive features such as fast execution time, flexibility for implementation in a control unit such as microprocessor, have fast execution time, and updating as experiential data on system response and tariffs (etc.) become available.

8.3 Suggested Further Work

In this research, a simulation model of a typical UK power distribution network which includes voltage levels between 11 kV and 400V was developed. In this network model, only one out of six 11 kV feeders with its connected loads was modelled in detail and the

other five were modelled as a lumped load. Similarly, only one of the eight 11 kV/400 V substations (including the connected feeders and loads) was modelled in detail whilst other seven were represented as a lumped load. Results have shown that the electrical contribution from the micro-CHP is heavily dependent on the thermal demand of the house. So, analysis of the impact of large deployment of micro-CHP on the 11 kV power network taking into account thermal demand requires to be investigated. Though some previous work of this kind has been done, it has not taken into account the thermal demand of the building.

Further investigation may also be conducted on the analysis of the energy flow in buildings based on the new (and prospective) building regulations, advanced (e.g. phase-change) thermal storage and electrical storage for alternative occupancy patterns and social groups.

Further work may also be conducted to develop a practical implementation of the proposed fuzzy logic controller in a real system or through the use of an emulator of a real system in order to demonstrate the effectiveness of the proposed controller.

References

[1] J. Klemeš and S. Pierucci, "Emission reduction by process intensification, integration, P-Graphs, micro CHP, heat pumps and advanced case studies," *Applied Thermal Engineering*, vol. 28, pp. 2005-2010, 2008.

[2] Carbon Trust, "Micro-CHP Accelerator, Final report," March 2011.

[3] A. Alexakis, G. Gounis, K. Mahkamov, and J. Davis, "Experimental and theoretical evaluation of the performance of a Whispergen Mk Vb micro CHP unit in typical UK house conditions " in *World Renewable Energy Congress*, Linköping, Sweden, 2011, pp. 8-11.

[4] A. D. Hawkes and M. A. Leach, "Cost-effective operating strategy for residential micro-combined heat and power," *Energy*, vol. 32, pp. 711-723, 2007.

[5] E. S. Barbieri, P. R. Spina, and M. Venturini, "Analysis of innovative micro-CHP systems to meet household energy demands," *Applied Energy*, vol. 97, pp. 723-733, 2012.

[6] O. A. Shaneb, G. Coates, and P. C. Taylor, "Sizing of residential μCHP systems," *Energy and Buildings*, vol. 43, pp. 1991-2001, 2011.

[7] M. Dentice d'Accadia, M. Sasso, S. Sibilio, and L. Vanoli, "Micro-combined heat and power in residential and light commercial applications," *Applied Thermal Engineering*, vol. 23, pp. 1247-1259, 2003.

[8] M. Newborough, "Assessing the benefits of implementing micro-CHP systems in the UK " *Proceedings of the Institution of Mechanical Engineers, Part A: Journal of Power and Energy*, vol. 218, pp. 203-218, 2004.

[9] B. Fox, D. Flynn, L. Bryans, N. Jenkins, D. Milborrow, M. O'Malley, *et al.*, *Wind Power Integration: Connection and system operational aspects*: Institution of Engineering and Technology, 2007.

[10] N. Jenkins, R. Allan, P. Crossley, D. Kirschen, and G. Strbac, *Embedded generation*. London, UK: The Institution of Engineering and Technology, 2000.

[11] O. C. Onar, M. Uzunoglu, and M. S. Alam, "Modeling, control and simulation of an autonomous wind turbine/photovoltaic/fuel cell/ultra-capacitor hybrid power system," *Journal of Power Sources*, vol. 185, pp. 1273-1283, 2008.

[12] Department of Energy & Climate Change, "Energy Consumption in the UK Available at: https://www.gov.uk/government/publications/energy-consumption-in-the-uk," 2012.

[13] A. D. Peacock and M. Newborough, "Effect of heat-saving measures on the CO2 savings attributable to micro-combined heat and power (μCHP) systems in UK dwellings," *Energy*, vol. 33, pp. 601-612, 2008.

[14] D. C. G. Veitch and K. Mahkamov, "Assessment of economical and ecological benefits from deployment of a domestic combined heat and power unit based on its experimental performance," *Proceedings of the Institution of Mechanical Engineers, Part A: Journal of Power and Energy,* vol. 223, pp. 783-798, November 1, 2009 2009.

[15] R. Yao and K. Steemers, "A method of formulating energy load profile for domestic buildings in the UK," *Energy and Buildings,* vol. 37, pp. 663-671, 2005.

[16] A. D. Hawkes, D. J. L. Brett, and N. P. Brandon, "Fuel cell micro-CHP techno-economics: Part 2 – Model application to consider the economic and environmental impact of stack degradation," *International Journal of Hydrogen Energy,* vol. 34, pp. 9558-9569, 12// 2009.

[17] N. Mohan, T. M. Undeland, and W. P. Robbins, "Power Electronics - Converters, Applications, and Design (3rd Edition)," ed: John Wiley & Sons, 2003.

[18] C. Barbier, A. Maloyd, and G. Putrus, "Embedded controller for LV network with distributed generation," Econnect Ventures Ltd., Department of Trade and IndustryMay 2007.

[19] M. MacDonald, "System Integration of Additional Micro-generation (SIAM)," Department of Trade and Industry DG/CG/00028/REP, 2004.

[20] S. Karmacharya, G. Putrus, C. Underwood, and K. Mahkamov, "Thermal modelling of the building and its HVAC system using Matlab/Simulink," in *Environment Friendly Energies and Applications (EFEA), 2012 2nd International Symposium on*, 2012, pp. 202-206.

[21] I. Richardson and M. Thomson, "One-Minute Resolution Domestic Electricity Use Data, 2008-2009," ed. Colchester, Essex: UK Data Archive October 2010.

[22] A. W. Al-Dabbagh, L. Lu, and A. Mazza, "Modelling, simulation and control of a proton exchange membrane fuel cell (PEMFC) power system," *International Journal of Hydrogen Energy,* vol. 35, pp. 5061-5069, 5// 2010.

[23] A. Wright and S. Firth, "The nature of domestic electricity-loads and effects of time averaging on statistics and on-site generation calculations," *Applied Energy,* vol. 84, pp. 389-403, 2007.

[24] J. Widén and E. Wäckelgård, "A high-resolution stochastic model of domestic activity patterns and electricity demand," *Applied Energy,* vol. 87, pp. 1880-1892, 2010.

[25] I. Richardson, M. Thomson, D. Infield, and C. Clifford, "Domestic electricity use: A high-resolution energy demand model," *Energy and Buildings,* vol. In Press, Corrected Proof, 2010.

[26] H. Ren and W. Gao, "Economic and environmental evaluation of micro CHP systems with different operating modes for residential buildings in Japan," *Energy and Buildings,* vol. 42, pp. 853-861, 2010.

[27] Carbon Trust, "Micro-CHP Accelerator, Interim Report," November 2007.

[28] A. D. Peacock and M. Newborough, "Impact of micro-combined heat-and-power systems on energy flows in the UK electricity supply industry," *Energy,* vol. 31, pp. 1804-1818, 2006.

[29] H. I. Onovwiona and V. I. Ugursal, "Residential cogeneration systems: review of the current technology," *Renewable and Sustainable Energy Reviews,* vol. 10, pp. 389-431, 2006.

[30] J. Cockroft and N. Kelly, "A Comparative Assessment of Future Heat and Power Sources for the UK Domestic Sector," *Energy Conversion and Management,* vol. 47, pp. 2349-2360, 2006.

[31] V. Kuhn, J. Klemes, and I. Bulatov, "MicroCHP: Overview of selected technologies, products and field test results," *Applied Thermal Engineering,* vol. 28, pp. 2039-2048, 2008.

[32] M. A. Smith and P. C. Few, "Domestic-scale combined heat-and-power system incorporating a heat pump: analysis of a prototype plant," *Applied Energy,* vol. 70, pp. 215-232, 2001.

[33] M. De Paepe, P. D'Herdt, and D. Mertens, "Micro-CHP systems for residential applications," *Energy Conversion and Management,* vol. 47, pp. 3435-3446, 2006.

[34] F. TeymouriHamzehkolaei and S. Sattari, "Technical and economic feasibility study of using Micro CHP in the different climate zones of Iran," *Energy,* vol. 36, pp. 4790-4798, 2011.

[35] G. Conroy, A. Duffy, and L. M. Ayompe, "Economic, energy and GHG emissions performance evaluation of a WhisperGen Mk IV Stirling engine μ-CHP unit in a domestic dwelling," *Energy Conversion and Management,* vol. 81, pp. 465-474, 2014.

[36] S. L. Walker, "Building mounted wind turbines and their suitability for the urban scale—A review of methods of estimating urban wind resource," *Energy and Buildings,* vol. 43, pp. 1852-1862, 2011.

[37] A. D. Peacock, D. Jenkins, M. Ahadzi, A. Berry, and S. Turan, "Micro wind turbines in the UK domestic sector," *Energy and Buildings,* vol. 40, pp. 1324-1333, 2008.

[38] Z. Li, F. Boyle, and A. Reynolds, "Domestic application of micro wind turbines in Ireland: Investigation of their economic viability," *Renewable Energy,* vol. 41, pp. 64-74, 2012.

[39] B. Greening and A. Azapagic, "Environmental impacts of micro-wind turbines and their potential to contribute to UK climate change targets," *Energy,* vol. 59, pp. 454-466, 9/15/ 2013.

[40] P. A. B. James, M. F. Sissons, J. Bradford, L. E. Myers, A. S. Bahaj, A. Anwar, *et al.*, "Implications of the UK field trial of building mounted horizontal axis micro-wind turbines," *Energy Policy,* vol. 38, pp. 6130-6144, 2010.

[41] G. G. Pillai, G. A. Putrus, T. Georgitsioti, and N. M. Pearsall, "Near-term economic benefits from grid-connected residential PV (photovoltaic) systems," *Energy,* vol. 68, pp. 832-843, 4/15/ 2014.

[42] Z. Li, F. Boyle, and A. Reynolds, "Domestic application of solar PV systems in Ireland: The reality of their economic viability," *Energy,* vol. 36, pp. 5865-5876, 2011.

[43] A. Arsalis, M. P. Nielsen, and S. K. Kær, "Application of an improved operational strategy on a PBI fuel cell-based residential system for Danish single-family households," *Applied Thermal Engineering,* vol. 50, pp. 704-713, 2013.

[44] L. Barelli, G. Bidini, F. Gallorini, and A. Ottaviano, "Dynamic analysis of PEMFC-based CHP systems for domestic application," *Applied Energy,* vol. 91, pp. 13-28, 2012.

[45] H. Xu, Z. Dang, and B.-F. Bai, "Analysis of a 1 kW residential combined heating and power system based on solid oxide fuel cell," *Applied Thermal Engineering,* vol. 50, pp. 1101-1110, 2013.

[46] R. Possidente, C. Roselli, M. Sasso, and S. Sibilio, "Experimental analysis of micro-cogeneration units based on reciprocating internal combustion engine," *Energy and Buildings,* vol. 38, pp. 1417-1422, 2006.

[47] C. Roselli, M. Sasso, S. Sibilio, and P. Tzscheutschler, "Experimental analysis of microcogenerators based on different prime movers," *Energy and Buildings,* vol. 43, pp. 796-804, 2011.

[48] K. Lombardi, V. I. Ugursal, and I. Beausoleil-Morrison, "Proposed improvements to a model for characterizing the electrical and thermal energy performance of Stirling engine micro-cogeneration devices based upon experimental observations," *Applied Energy,* vol. 87, pp. 3271-3282, 2010.

[49] V. Dorer and A. Weber, "Energy and CO2 emissions performance assessment of residential micro-cogeneration systems with dynamic whole-building simulation programs," *Energy Conversion and Management,* vol. 50, pp. 648-657, 2009.

[50] H. I. Onovwiona, V. Ismet Ugursal, and A. S. Fung, "Modeling of internal combustion engine based cogeneration systems for residential applications," *Applied Thermal Engineering,* vol. 27, pp. 848-861, 2007.

[51] O. A. Shaneb, P. C. Taylor, and G. Coates, "Real time operation of μCHP systems using fuzzy logic," *Energy and Buildings,* vol. 55, pp. 141-150, 2012.

[52] A. D. Peacock and M. Newborough, "Controlling micro-CHP systems to modulate electrical load profiles," *Energy,* vol. 32, pp. 1093-1103, 2007.

[53] O. A. Shaneb, P. C. Taylor, and G. Coates, "Optimal online operation of residential μCHP systems using linear programming," *Energy and Buildings*, vol. 44, pp. 17-25, 2012.

[54] C.-C. T and J. G., " The potential market for micro-CHP in the UK," Energy Saving Trust, London2002.

[55] S. Ingram, S. Probert, and K. Jackson, "The impact of small scale embedded generation on the operating parameters of distribution networks," Department of Trade and Industry (DTI), 2003.

[56] Department of Energy & Climate Change, "Planning our electric future: a White Paper for secure, affordable and low-carbon electricity," 2011.

[57] WADE, "Guide to decentralized energy technologies," World Alliance for Decentralized Energy, Edinburgh,September 2003.

[58] M. Pehnt, M. Cames, C. Fischer, B. Praetorius, L. Schneider, K. Schumacher, *et al.*, *Micro Cogeneration: Towards Decentralized Energy Systems*. Berlin, Germany: Springer, 2006.

[59] EU, "Directive 2004/8/EC of the European Parliament and fo the Council of 11 Febraury 2004 on the promotion of cogeneration based on a useful heat demand in the internal energy market and amending Directive 92/42/EE," European Union, Bruxelles,2004.

[60] B. Thomas, "Benchmark testing of Micro-CHP units," *Applied Thermal Engineering*, vol. 28, pp. 2049-2054, 2008.

[61] I. Staffell, "Fuel cell for domestic heat and power: are they worth it?," PhD, The University of Birmingham 2009.

[62] A. R. Korsgaard, M. P. Nielsen, and S. K. Kær, "Part one: A novel model of HTPEM-based micro-combined heat and power fuel cell system," *International Journal of Hydrogen Energy*, vol. 33, pp. 1909-1920, 2008.

[63] Institute of Physics. *Available at: http://www.physics.org/articlequestions.asp?id=51 Access date: 08/07/2013*.

[64] T. Burton, D. Sharpe, N. Jenkins, and E. Bossanyi, *Wind energy handbook*. West sussex, England: John Wiley & Sons, Ltd, 2002.

[65] M. Gaunaa and J. Johansen, "Determination of the maximum aerodynamic efficiency of wind turbine rotors with winglets," *Journal of Physics: Conference Series*, vol. 75, p. 012006, 2007.

[66] M. Narayana, "Optimal control strategies for small scale wind energy conversion systems," PhD Thesis, Northumbria University, 2011.

[67] B. Fox, D. Flynn, L. Bryans, N. Jenkins, D. Milborrow, M. O'Malley, *et al.*, *Wind Power Integration: Connection and system operational aspects*. London: The Institution of Engineering and Technology, 2007.

[68] Energy Saving Trust, "Location location location - The Energy Saving Trust's field trial report on domestic wind turbines.," Energy Saving Trust, London2009.

[69] S. L. Walker, "Building mounted wind turbines and their suitability for the urban scale - A review of methods of estimating urban wind resource," *Energy and Buildings,* vol. 43, pp. 1852-1862, 2011.

[70] Encraft, "Warwick wind trials final report," Encraft, Leamington Spa2009.

[71] E. García-Bustamante, J. F. González-Rouco, P. A. Jiménez, J. Navarro, and J. P. Montávez, "A comparison of methodologies for monthly wind energy estimation," *Wind Energy,* vol. 12, pp. 640-659, 2009.

[72] Z. Simic, J. G. Havelka, and M. Bozicevic Vrhovcak, "Small wind turbines – A unique segment of the wind power market," *Renewable Energy,* vol. 50, pp. 1027-1036, 2013.

[73] W. El-Khattam and M. M. A. Salama, "Distributed generation technologies, definitions and benefits," *Electric Power Systems Research,* vol. 71, pp. 119-128, 2004.

[74] U. S. Department of Energy, "The Potential Benefits of Distributed Generation and Rate-Related Issues that May Impede Their Expansion: A Study Pursuant to Section 1817 of the Energy Policy Act of 2005," Washington, DC2007.

[75] D. Haeseldonckx, L. Peeters, L. Helsen, and W. D'haeseleer, "The impact of thermal storage on the operational behaviour of residential CHP facilities and the overall CO2 emissions," *Renewable and Sustainable Energy Reviews,* vol. 11, pp. 1227-1243, 2007.

[76] K. H. Khan, M. G. Rasul, and M. M. K. Khan, "Energy conservation in buildings: cogeneration and cogeneration coupled with thermal energy storage," *Applied Energy,* vol. 77, pp. 15-34, 2004.

[77] S. Martínez-Lera, J. Ballester, and J. Martínez-Lera, "Analysis and sizing of thermal energy storage in combined heating, cooling and power plants for buildings," *Applied Energy,* vol. 106, pp. 127-142, 2013.

[78] N. Nallusamy, S. Sampath, and R. Velraj, "Experimental investigation on a combined sensible and latent heat storage system integrated with constant/varying (solar) heat sources," *Renewable Energy,* vol. 32, pp. 1206-1227, 2007.

[79] A. Sharma, S. D. Sharma, D. Buddhi, and L. D. Won, "Effect of thermo physical properties of heat exchanger material on the performance of latent heat storage system using an enthalpy method," *International Journal of Energy Research,* vol. 30, pp. 191-201, 2006.

[80] H. L. Ferreira, R. Garde, G. Fulli, W. Kling, and J. P. Lopes, "Characterisation of electrical energy storage technologies," *Energy,* vol. 53, pp. 288-298, 5/1/ 2013.

[81] D. P. Jenkins, J. Fletcher, and D. Kane, "Model for evaluating impact of battery storage on microgeneration systems in dwellings," *Energy Conversion and Management,* vol. 49, pp. 2413-2424, 2008.

[82] U. S. Department of Energy. *Building Technologies office: Building Energy Software Tools Directory. Available at: http://apps1.eere.energy.gov/buildings/tools_directory/. Accessed date:10/11/2010*. Available: http://apps1.eere.energy.gov/buildings/tools_directory/

[83] A. S. Kalagasidis, P. Weitzmann, T. R. Nielsen, R. Peuhkuri, C.-E. Hagentoft, and C. Rode, "The International Building Physics Toolbox in Simulink," *Energy and Buildings,* vol. 39, pp. 665-674, 2007.

[84] "TRNSYS—A Transient system simulation program, Solar Energy Laboratory, Available at: http://www.trnsys.com/, Access data: 11/06/2013."

[85] R.K. Strand, R.J. Liesen, D.E. Fisher, and C. O. Pedersen, "Modular HVAC simulation and the future integration of alternative cooling systems in a new building energy simulation program," *ASHRAE Transactions,* vol. 108, pp. 1107-1118, 2002.

[86] ISO 13790, "Thermal performance of buildings — Calculation of energy use for space heating and cooling."

[87] M. M. Gouda, S. Danaher, and C. P. Underwood, "Building thermal model reduction using nonlinear constrained optimization," *Building and Environment,* vol. 37, pp. 1255-1265, 2002.

[88] C. P. Underwood and F. W. H. Yik, *Modelling Methods for Energy in Buildings*: Wiley-Blackwell, 2004.

[89] G. Henze and C. Neumann, "Building simulation in building automation systems," in *Building Performance Simulation for Design and Operation*, J. L. M. Hensen and R. Lamberts, Eds., ed London: Spon Press, 2011, pp. 436-440.

[90] A. Skartveit and J. A. Olseth, "A model for the diffuse fraction of hourly global radiation," *Solar Energy,* vol. 38, pp. 271-274, 1987.

[91] B. Y. H. Liu and R. C. Jordan, "The interrelationship and characteristic distribution of direct, diffuse and total solar radiation," *Solar Energy,* vol. 4, pp. 1-19, 1960.

[92] A. D. Jones, " Computer modelling of the power supply and demand of a photovoltaic clad building " PhD Thesis, University of Northumbria at Newcastle, Newcastle upon Tyne, UK, 1999.

[93] C. P. Underwood and J. S. Edge, "Flow characteristics in circuits using three-port modulating control valves," *Building Services Engineering Research and Technology,* vol. 16, pp. 127-132, August 1, 1995.

[94] M. M. Gouda, S. Danaher, and C. P. Underwood, "Low-order model for the simulation of a building and its heating system," *Building Services Engineering Research and Technology,* vol. 21, pp. 199-208, 2000.

[95] Department for Communities and Local Government, "English Housing Survey Housing Stock Report 2009," 2011.

[96] B R Anderson, P F Chapman, N G Cutland, C M Dickson, G Henderson, J H Henderson, *et al.*, "BREDEM-12 model description: 2001 update," Watford 2002.

[97] National Calculation Method. *NMC: National Calculation Method - Introduction to SBEM. Available at: http://www.ncm.bre.co.uk/ Accessed date: 08/08/2012*. Available: http://www.ncm.bre.co.uk/

[98] U. S. Department of Energy. *EnergyPlus Energy Simulation Software: Weather Data. Available at: http://apps1.eere.energy.gov/buildings/energyplus/cfm/weather_data3.cfm/region=6_europe_wmo_region_6/country=GBR/cname=United%20Kingdom. Accessed date: 08/08/2012.*

[99] R. Judkoff and J. Neymark, "IEA Building energy simulation test (BESTEST) and diagnostic method," in *IEA ECBSC Annex 21 Subtask C and IEA SHC Task 12 Subtask B*, ed, 1995.

[100] ANSI/ASHRAE, "ANSI/ASHRAE Standard 140-2001Standard Method of Test for the Evaluation of Building Energy Analysis Computer Programs," ed, 2004.

[101] N. T. Bowman and K. J. Lomas, "Empirical validation of dynamic thermal computer models of buildings," *Building Services Engineering Research and Technology*, vol. 6, pp. 153-162, November 1, 1985.

[102] J. Davis, "Experimental and theoretical analysis of the performance of a Whispergen MkVb micro-CHP in a UK 4 bed detached house," Masters Thesis, Durham University, 2011.

[103] M. Wolf and H. H. Rauschenbach, "Series resistance effects on solar cell measurements," *Advanced Energy Conversion*, vol. 3, pp. 455-479, 1963.

[104] T. J. McMahon, T. S. Basso, and S. R. Rummel, "Cell shunt resistance and photovoltaic module performance," in *Photovoltaic Specialists Conference, 1996., Conference Record of the Twenty Fifth IEEE*, 1996, pp. 1291-1294.

[105] R. L. Y. Sah, R. N. Noyce, and W. Shockley, "Carrier generation and recombination in P-N junctions and P-N junction characteristics," *Proceedings of the IRE*, vol. 45, pp. 1228-1243, 1957.

[106] K. Ishaque, Z. Salam, and H. Taheri, "Simple, fast and accurate two-diode model for photovoltaic modules," *Solar Energy Materials and Solar Cells*, vol. 95, pp. 586-594, 2011.

[107] D. Sera, R. Teodorescu, and P. Rodriguez, "PV panel model based on datasheet values," in *Industrial Electronics, 2007. ISIE 2007. IEEE International Symposium on*, 2007, pp. 2392-2396.

[108] M. G. Villalva, J. R. Gazoli, and E. R. Filho, "Comprehensive approach to modeling and simulation of photovoltaic arrays," *Power Electronics, IEEE Transactions on,* vol. 24, pp. 1198-1208, 2009.

[109] Solarcentury '185W Solar module'. *Availble at: http://www.solarcentury.co.uk/media_manager/public/79/installers-and-roofers/products/modules/SC-M185-H18-DS0212.pdf, Access date: 10/07/2013*.

[110] B. Subudhi and R. Pradhan, "A Comparative Study on maximum power point tracking techniques for photovoltaic power systems," *Sustainable Energy, IEEE Transactions on,* vol. 4, pp. 89-98, 2013.

[111] T. Jiang, G. Putrus, S. McDonald, M. Conti, B. Li, and D. Johnston, "Generic Photovoltaic System Emulator Based on Lambert omega Function," *Universities' Power Engineering Conference (UPEC), Proceedings of 2011 46th International,* pp. 1-5, 2011.

[112] S. M. Raza Kazmi, H. Goto, G. Hai-Jiao, and O. Ichinokura, "Review and critical analysis of the research papers published till date on maximum power point tracking in wind energy conversion system," in *Energy Conversion Congress and Exposition (ECCE), 2010 IEEE*, 2010, pp. 4075-4082.

[113] Ned Mohan, Tore M. Undeland, and W. P. Robbins, *Power Electronics Converters – Applications and Design. 3rd ed.* New York: John Wiley, 2003.

[114] M. Arifujjaman, M. T. Iqbal, and J. E. Quaicoe, "Energy capture by a small wind-energy conversion system," *Applied Energy,* vol. 85, pp. 41-51, 2008.

[115] R. Wardle, C. Barteczko-Hibbert, D. Miller, and E. Sidebotham, "Initial Load Profiles from CLNR Intervention Trials," Customer-Led Network Revolution 2013.

[116] M. Dürr, A. Cruden, S. Gair, and J. R. McDonald, "Dynamic model of a lead acid battery for use in a domestic fuel cell system," *Journal of Power Sources,* vol. 161, pp. 1400-1411, 2006.

[117] H. Zhang, A. Davigny, F. Colas, Y. Poste, and B. Robyns, "Fuzzy logic based energy management strategy for commercial buildings integrating photovoltaic and storage systems," *Energy and Buildings,* vol. 54, pp. 196-206, 2012.

[118] L. A. Zadeh, "Fuzzy sets," *Information and Control,* vol. 8, pp. 338-353, 1965.

[119] L. A. Zadeh, "A Fuzzy-Set-Theoretic Interpretation of Linguistic Hedges," *Journal of Cybernetics,* vol. 2, pp. 4-34, 1972/01/01 1972.

[120] Y. Bai and D. Wang, "Fundamentals of Fuzzy Logic Control — Fuzzy Sets, Fuzzy Rules and Defuzzifications," in *Advanced Fuzzy Logic Technologies in Industrial Applications*, Y. Bai, H. Zhuang, and D. Wang, Eds., ed: Springer London, 2006, pp. 17-36.

[121] G. Chen and T. T. Pham, *Introduction to Fuzzy Sets, Fuzzy Logic and Fuzzy Control Systems*. Boca Raton, Florida: CRC Press, 2001.

[122] M. Tekin, D. Hissel, M. C. Pera, and J. M. Kauffmann, "Energy-Management Strategy for Embedded Fuel-Cell Systems Using Fuzzy Logic," *Industrial Electronics, IEEE Transactions on,* vol. 54, pp. 595-603, 2007.

[123] A. Mellit, S. A. Kalogirou, L. Hontoria, and S. Shaari, "Artificial intelligence techniques for sizing photovoltaic systems: A review," *Renewable and Sustainable Energy Reviews,* vol. 13, pp. 406-419, 2009.

[124] Z. Qun and H. Juhua, "The Design and Simulation of Fuzzy Logic Controller for Parallel Hybrid Electric Vehicles," in *Automation and Logistics, 2007 IEEE International Conference on,* 2007, pp. 908-912.

[125] X. Bin, L. Ming, Y. Shichun, G. Bin, and C. Haigang, "Design and Simulation of Fuzzy Control Strategy for Parallel Hybrid Electric Vehicle," in *Intelligent System Design and Engineering Application (ISDEA), 2010 International Conference on,* 2010, pp. 539-543.

[126] A. Sakhare, A. Davari, and A. Feliachi, "Fuzzy logic control of fuel cell for stand-alone and grid connection," *Journal of Power Sources,* vol. 135, pp. 165-176, 2004.

[127] Mathworks. *Fuzzy Inference Process - MATLAB & SIMULINK, Available at: http://www.mathworks.co.uk/help/fuzzy/fuzzy-inference-process.html#FP346, Access date: 20/08/2013*.

[128] S. L. Walker, "Can the GB feed-in tariff deliver the expected 2% of electricity from renewable sources?," *Renewable Energy,* vol. 43, pp. 383-388, 2012.

[129] Office of Gas and Electricity Markets (OFGEM). *Feed-in Tariff Scheme Tariff Tables , http://www.ofgem.gov.uk/Sustainability/Environment/fits/tariff-tables/Pages/index.aspx, Access date: 01/02/2013*.

[130] Department of Energy & Climate Change. *Domestic energy price statistics, Available at: https://www.gov.uk/government/organisations/department-of-energy-climate-change/series/domestic-energy-prices, Access date: 02/07/2013*.

[131] Department for Communities and Local Government, "National Calculation Methodology (NCM) modelling guide," 2011.

[132] Office of Gas and Electricity Markets (OFGEM). *Applying for the Feed-in-Tariff (FIT) Scheme, Available at: https://www.ofgem.gov.uk/environmental-programmes/feed-tariff-fit-scheme/applying-feed-tariff-fit-scheme, Access date: 02/08/2013*.

[133] A. D. Hawkes and M. A. Leach, "On policy instruments for support of micro combined heat and power," *Energy Policy,* vol. 36, pp. 2973-2982, 2008.

Appendix A: Specification of 'Whispergen' Stirling engine based micro-CHP

General:

Engine - 4 cylinders double acting Stirling cycle

Generator - 4 pole single phase induction machine

Electrical output:

Electricity supply - 230 Vac, 50 Hz

Nominal mode - up to 1 kW

Thermal output:

Nominal mode - up to 7 kW

Maximum - up to 12 kW (including auxiliary burner)

Fuel:

Type - 2H-2nd family natural gas

Supply pressure - 17-25 mbar (20 mbar nominal)

Fuel consumption:

Maximum burner firing rate - 1.55 m^3/hour

Appendix B: Specification of 185 W Solar Module

Photovoltaic cell technology	Monocrystalline
Number of cells	72
Module efficiency	14.71%
Peak power *(P_{max})	185 W
Maximum power voltage **(V_{mp})	36.80 V
Maximum power current **(I_{mp})	5.03 A
Open circuit voltage **(V_{oc})	44.4 V
Short circuit current **(I_{sc})	5.69 A
Temperature coefficient of the power	-0.46%/°C
Temperature coefficient of the open-circuit voltage (K_V)	-0.384%/°C
Temperature coefficient of the short-circuit current (K_I)	0.031%/°C
* Measured under STC of 1kW/m^2 irradiance, AM 1.5 spectrum, 25 °C cell temperature. ** Values of current, voltage and power +/- 5%	

Appendix C: Specification of the Wind Turbine

Wind rotor characteristics

Radius of the wind rotor	2.25 m
Number of blades	2
Moment of inertia of the wind rotor and rotating parts of the generator (J)	9.77 $kg.m^2$
Permanent Magnet Generator	
No of pole pairs (p)	6
Stator phase resistance (R_{ph})	1.25 ohm
k' (= $p\Phi_m$)	1.5

Value of power coefficient with respect to tip speed ratio

Tip speed ratio (λ)	C_p
0	0
1	0.04
2	0.12
3	0.21
4	0.3
5	0.37
6	0.4
7	0.39
8	0.34
9	0.25
10	0.13
11	0

Appendix D: Parameters of the LV network

Details of 11kV feeder				
Type	**Conductor**	**Resistance, R (Ω/km)**	**Inductance, X_L (Ω/km)**	**Remark**
185mm XLPE	CU	1.28000E-01	9.10000E-02	From Busbar 2-6, 500m each
95mm XLPE	CU	2.47000E-01	1.00000E-01	From Busbar 6-10, 500m each
Details of 400V feeder				
Type	**Conductor**	**Resistance, R (Ω/km)**	**Inductance, X_L (Ω/km)**	**Remark**
240 CNE	AL	1.25800E-01	6.85000E-02	Line 1 (7.45m)
120 CNE	AL	2.53300E-01	6.85000E-02	Line 2 (95m) Line3 (133.75m)
70 CONSAC	AL	4.43000E-01	7.05000E-02	Line 4 (34m) Line 5 (37.5m) Line 6 (65m) Line 7 (100m)

Appendix E: Publications

Journal Paper

- S. Karmacharya (60%), G. Putrus, C. Underwood, K. Mahkamov, S. McDonald and T. Alexakis, 'Simulation of energy use in buildings with multiple micro-generators', Applied Thermal Engineering, Volume 62, Issue 2, 25 January 2014, Pages 581-592.
- S. Karmacharya, G. Putrus, C. Underwood, and K. Mahkamov, "Development of a Controller for Micro Combined Heat and Power (CHP) System to Optimise Energy conversion and Support Power Distribution Networks" (prepared for submission).

Conference Paper

- S. Karmacharya, G. Putrus, C. Underwood, and K. Mahkamov, "Evaluation of domestic electrical demand and its effect on low voltage network," in Universities Power Engineering Conference (UPEC), 2012 47th International, 2012, pp. 1-4.
- S. Karmacharya, G. Putrus, C. Underwood, and K. Mahkamov, "Thermal modelling of the building and its HVAC system using Matlab/Simulink," in Environment Friendly Energies and Applications (EFEA), 2012 2nd International Symposium on, 2012, pp. 202-206.